Epistasis in wheat breeding

by

Augusto Tessele

B.S., Federal University of Paraná, 2015
M.S., Federal University of Viçosa, 2017

AN ABSTRACT OF A DISSERTATION

submitted in partial fulfillment of the requirements for the degree

DOCTOR OF PHILOSOPHY

Interdepartmental Genetics Program
College of Agriculture

KANSAS STATE UNIVERSITY
Manhattan, Kansas

2024

Abstract

The core objective of wheat breeding is to develop superior varieties to the target population of environments. As most agronomic traits are quantitative, the underlying genetic architecture is assumed to be additive, implying that the superiority of parental lines is transmitted to the offspring. However, often rather than rarely, wide crosses between elite genotypes yield poor breeding populations, indicating that additive might not be the major type of gene action. The inbreeding nature of wheat suggests that epistasis could be the underlying genetic architecture. The work presented here describes conventional and innovative methods to test the existence and extent of epistasis in wheat breeding. The first chapter presents a comprehensive literature review that discusses the theoretical framework for the creation of epistasis from gene duplication events and the expansion of this construct to the population levels. Then, the history of wheat is utilized to discuss the evolution of epistasis into a complex genetic system and the strategies utilized by breeding programs to manage this complexity and attain satisfactory levels of genetic gain. The second chapter utilizes an innovative approach to test the existence of sign epistasis in wheat breeding. Sign epistasis occurs when the effect of an allele can be beneficial or detrimental upon variation in the genetic background. Through the coupling of interchromosomal linkage disequilibrium analysis with the calculation of allele frequencies, 19 candidate interactions of sign epistasis were identified. Although the validation analyses attributed to random genetic drift the sign epistasis patterns observed in 11 candidate interactions, eight interactions presented strong evidence for sign epistasis and the main hypothesis could not be refuted. These findings imply that the effect of alleles can vary from positive to negative depending on the genetic background and explain the often poor combining ability of high performing lines. The third chapter explores the genetic architecture of wheat grain yield by modeling additive and additive-by-additive epistatic effects, using data from 3740 experimental lines. Modeling epistasis in whole genome or sub genome models marginally improved prediction accuracy in genomic selection models and resulted in non-orthogonal partition of genetic variance components. The estimation of sub genome additive effects showed that the best lines did not have the greatest additive effects in more than one sub genome, suggesting the possibility of making targeted crosses that combine genotypes with the highest additive effects in each subgenome.

Epistasis in wheat breeding

by

Augusto Tessele

B.S., Federal University of Paraná, 2015
M.S., Federal University of Viçosa, 2017

A DISSERTATION

submitted in partial fulfillment of the requirements for the degree

DOCTOR OF PHILOSOPHY

Interdepartmental Genetics Program
College of Agriculture

KANSAS STATE UNIVERSITY
Manhattan, Kansas

2024

Approved by:

Major Professor
Dr. Allan K. Fritz

Copyright

Abstract

The core objective of wheat breeding is to develop superior varieties to the target population of environments. As most agronomic traits are quantitative, the underlying genetic architecture is assumed to be additive, implying that the superiority of parental lines is transmitted to the offspring. However, often rather than rarely, wide crosses between elite genotypes yield poor breeding populations, indicating that additive might not be the major type of gene action. The inbreeding nature of wheat suggests that epistasis could be the underlying genetic architecture. The work presented here describes conventional and innovative methods to test the existence and extent of epistasis in wheat breeding. The first chapter presents a comprehensive literature review that discusses the theoretical framework for the creation of epistasis from gene duplication events and the expansion of this construct to the population levels. Then, the history of wheat is utilized to discuss the evolution of epistasis into a complex genetic system and the strategies utilized by breeding programs to manage this complexity and attain satisfactory levels of genetic gain. The second chapter utilizes an innovative approach to test the existence of sign epistasis in wheat breeding. Sign epistasis occurs when the effect of an allele can be beneficial or detrimental upon variation in the genetic background. Through the coupling of interchromosomal linkage disequilibrium analysis with the calculation of allele frequencies, 19 candidate interactions of sign epistasis were identified. Although the validation analyses attributed to random genetic drift the sign epistasis patterns observed in 11 candidate interactions, eight interactions presented strong evidence for sign epistasis and the main hypothesis could not be refuted. These findings imply that the effect of alleles can vary from positive to negative depending on the genetic background and explain the often poor combining ability of high performing lines. The third chapter explores the genetic architecture of wheat grain yield by modeling additive and additive-by-additive epistatic effects, using data from 3740 experimental lines. Modeling epistasis in whole genome or sub genome models marginally improved prediction accuracy in genomic selection models and resulted in non-orthogonal partition of genetic variance components. The estimation of sub genome additive effects showed that the best lines did not have the greatest additive effects in more than one sub genome, suggesting the possibility of making targeted crosses that combine genotypes with the highest additive effects in each subgenome.

Table of Contents

List of Figures

List of Tables

Acknowledgements

I would like to express my gratitude to Dr. Allan Fritz for his unwavering guidance and support throughout this journey. The countless days we spent in the field walking populations or on harvest trips across Kansas or the numerous times I knocked on his office door for lengthy conversations, were invaluable learning experiences about wheat and breeding.

I extend my sincere thanks to my committee members: Dr. Morris, Dr. Akhunov, and Dr. Johnson. The rigorous scientific discussions and knowledge in quantitative genetics that I gained from our committee meetings will undoubtedly serve as a strong foundation for my future pursuits.

I wish to express my appreciation to Dr. Clinesmith for his friendship, contributions to my analyses, and the countless conversations we've had, and continue to have, about wheat breeding and epistasis. I am also grateful to Addison Hope for her friendship, constructive feedback on my project, and engaging discussions on wheat breeding.

Special thanks go to Shaun Winne and Andy Auld for their support in my project, particularly through supporting the generation of phenotypic data. I also want to acknowledge Anggie Matthews for her assistance in assisting with the generation of the genotypic data used in my research. I would like to express my appreciation to everyone involved in the K-State Hard Red Winter Wheat program that somehow contributed to this project.

I am indebted to Dr. Crossa and Dr. Gonzales for hosting me at CIMMYT and sharing their invaluable knowledge of statistical and quantitative genetics. The experience and expertise I gained during my time there will undoubtedly play a pivotal role in my career.

I want to express my deepest gratitude to my wife, Priscila, for her unconditional support in pursuing my dreams. She has been my foundation and lifelong companion. I also extend my thanks to my family, particularly my parents, for supporting my decision to study abroad and for instilling in me the values of hard work and dedication. I wouldn’t be here without them.

I want to thank God for blessing me with health and for surrounding me with innumerous good people throughout my life.

Dedication

This dissertation is dedicated to every person that has influenced and supported my decision to pursue a career in plant breeding. Particularly to my wife Priscila, my parents Antonio and Tania, and my grandfather Antonio.

Chapter 1 - Epistasis: from gene interactions to breeding programs

Abstract

In this review, we discuss the theoretical grounds of genetic novelty in the context of evolution, emphasizing its close association with gene duplications and how it leads to the emergence of epistatic gene interactions. Subsequently, we extend these theoretical constructs to the population level, exploring the influence of random genetic drift on the fate and dispersion of gene duplications. Later, we discuss how epistatic variance can be created from gene duplications, and we delve into how epistasis can be magnified or constrained under the structure of subpopulations. This concept is later expanded to numerous gene interactions, and we establish a connection with the shifting balance theory. In the latter part of this review, we draw a parallel between these theoretical foundations and the evolutionary trajectory of wheat. We propose that current wheat breeding programs operate under assumptions remarkably similar to the shifting balance theory. Furthermore, we dissect the pivotal role of epistasis, hypothesized here to be the foundational genetic architecture of wheat, in shaping the structure of breeding programs. We examined the implications of operating a closed or open breeding program and strategies to cope with epistasis in order to introduce genetic diversity. Finally, we discuss the potential implication of epistasis to the successful utilization of genomic selection in wheat breeding programs.

Epistasis in the genome level

Mutations and gene duplications

Mutation is the single source of molecular novelty. The constant occurrence of mutations associated with recombination, which shuffles the genome and amplifies variation, creates genetic variability in populations that, under the effect of natural selection and genetic drift, drives the evolution of species.

On a molecular level, the vast majority of mutations have neutral effects on the fitness of individuals because of the degenerative nature of the genetic code. As the neutral theory of molecular evolution asserts, most evolutionary changes are the result of the continued mutation pressure that under the influence of random genetic drift leads to the fixation of selectively neutral mutations (Kimura, 1991). Among the relatively few mutations that have a phenotypic effect, the

majority are likely deleterious to the fitness of an individual (Fisher, 1930). Thus, just a very small portion of mutations affecting the phenotype are responsible for the evolution of species.

Sniegowski et al (2000) pointed out that natural selection does not conserve mutations in a population because of their future adaptative utility, but because of the current functionality. Ohno (1970) argued that a single locus controlling a specific function in a species cannot undergo mutation if that mutation will affect the functionality of the protein expressed. Since mutation is the driving force of genetic variation but the massive majority are seemingly useless or even deleterious, how could a species adequately explore the benefits of mutations without adaptation penalties? The answer is gene duplications. Only through the creation of a redundant gene copy can a highly conserved gene have its function altered to a novel function (Ohno 1970). Kimura and Ohta (1974) stated that the neofunctionalization of a gene must follow a duplication event. In theory, gene duplications promote a reduced selective constraint for one or both copies to evolve (Panchy et al., 2016), which causes negligible, if any, disruption on the adaptation of individuals carrying the duplicated genes.

Different mechanisms can lead to gene duplication events, as tandem duplication (Zhang, 2003), segmental duplication (Bailey et al., 2002), retroduplication (Drouin and Dover, 1990; Brosius, 1991), and duplication mediated by transposable elements (Jiang et al., 2004) (reviewed by Panchy et al., 2016). However, the most drastic mechanism is whole genome duplication or increase in ploidy through interspecific crossing of related species, which is responsible for most duplicate genes in plant species (Panchy et al. 2016). While most whole genome duplication events lead to extinction (Reams and Roth, 2005), a few persist. And although many of the duplicated genes are lost, some are conserved or acquire new functions (Wallace et al., 2018). Whole genome duplication events are an important source of functional diversity in the evolution of species (Musso et al., 2008) and can expand the functional diversity of genes to develop new epistatic interactions (Jiang et al., 2011). Studies in yeast have demonstrated that duplicated genes extend their functional diversity by evolving substantially more epistatic interactions than single-copy genes (Jiang et al., 2011). Sanjuán and Elena (2006) showed that complex genomes, those with high number of genes, alternative metabolic pathways, or multiple regulatory elements, tended to present higher levels of epistasis than simpler genomes.

The fate of duplicated genes

Once genes undergo one of the possible duplication pathways, there are several potential outcomes for the duplicated copies. When genes encoding a protein with a single function are duplicated, it can lead to negative epistasis (Qian et al., 2010). In this scenario, both gene products compete for the same metabolic pathway or perform similar functions, potentially resulting in suboptimal or detrimental effects on the fitness of an individual. This competition between duplicated genes may limit their adaptive potential and could lead to the eventual loss of one of the duplicate copies if it does not acquire a new, beneficial function. Thus, one common fate is non-functionalization, where one of the copies becomes non-functional through degenerative mutations, while the other retains the wildtype function of the ancestral allele (Lynch and Conery, 2000). Deleting one copy of two identical genes is not expected to impose significant penalties (Panchy et al., 2016), and this outcome has minimal direct influence on adaptive evolution (Lynch, 2002 – Figure 1.1A).

Another possible fate of gene duplication is subfunctionalization, where the duplicated genes are retained, but there is a division of the original ancestral function between both paralogs. This division occurs as a result of complementary loss-of-function alleles (Lynch and Force, 2000). In cases of subfunctionalization, selection must retain both copies of the duplicated genes if the ancestral function still plays a direct role in adaptation. However, the subdivision of ancestral functions will lead to a dependency on both genes for the proper maintenance of the ancestral function (Musso et al., 2008). This interdependence ensures that both copies are preserved because the loss of either one would result in a loss of the overall ancestral function (Figure 1.1B).

Additionally, duplicate genes can undergo neofunctionalization, a process where one copy acquires a novel, non-redundant function while the other maintains its ancestral function (Ohno, 1970; Lynch and Conery, 2000). If the newly acquired function is beneficial for fitness, then both genes are likely to be retained by natural selection (Panchy et al., 2016). In cases where pleiotropic genes encode proteins involved in different gene networks, they may experience "adaptive conflict" (Hittinger and Carroll, 2007), where a mutation that optimizes one metabolic pathway might negatively affect another. Gene duplications can resolve this adaptive conflict by allowing each copy to specialize and optimize a specific metabolic pathway, effectively reducing the

conflict and enhancing the adaptation of the organism (Hughes, 1994; Hittinger and Carroll, 2007 – Figure 1.1C). This process contributes to the diversification of gene functions in a genome.

Figure 1.1 Three possible fates of gene duplications after reaching fixation in a population. (A) Non-functionalization of a gene copy. (B) Sub-functionalization of gene functions. (C) Specialization of gene functions if ancestral gene was pleiotropic.

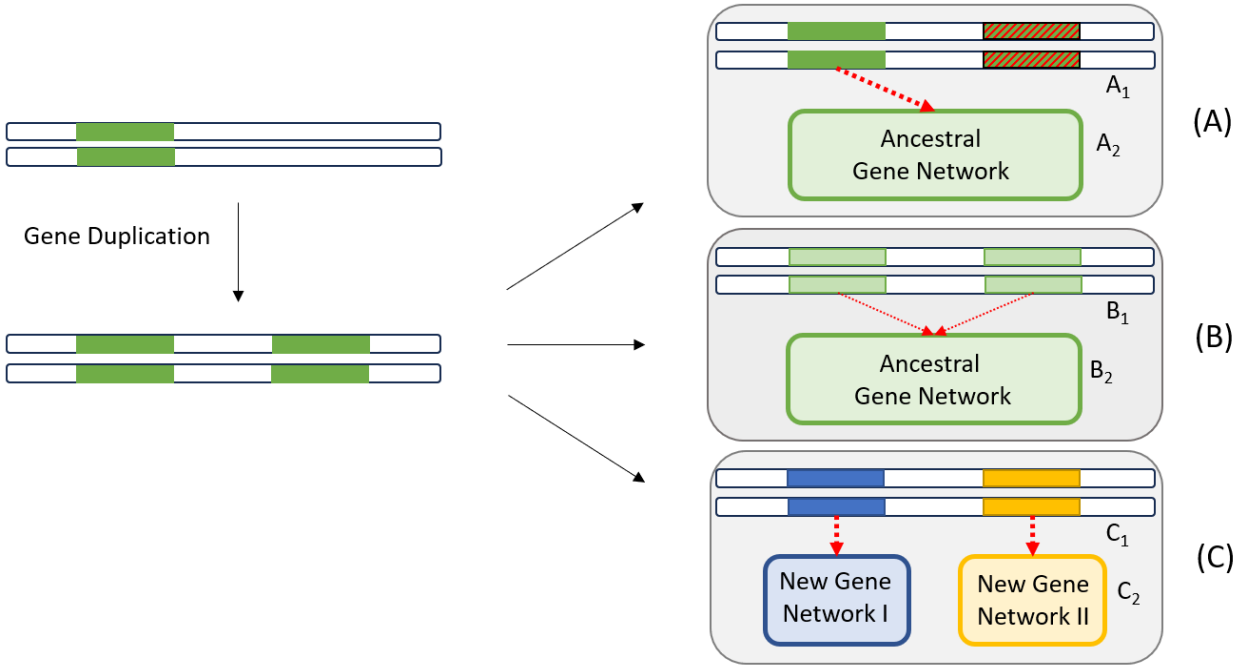

Epistasis in the population level

The fate of duplicated genes in the population level

Like point mutations, the chance of fixation of duplicated genes in a diploid population is equal to $1/2n$, where n is the number of individuals in the population (Nei and Rooney, 2005). Unless the duplication results in an outstanding improvement in fitness, the process towards fixation is lengthy in large populations. The fastest way for a new gene duplication event to reach fixation in a population is through genetic drift, whose effect is much more pronounced in smaller populations (Ohta, 1973; Lynch et al., 2008).

As highlighted by Hastings and Harrison (1994) and supported by studies across various species (Igarashi et al., 2018; Beesley et al., 2021; Orozco-Ruiz et al., 2023), true panmictic populations are rare. Most species are subdivided into distinct subpopulations, and within these

subpopulations, gene duplication events may occur and become fixed at varying frequencies mostly due to genetic drift, especially if there is no immediate selective advantages or disadvantages associated with the duplicated genes. Subsequent migration can spread the newly duplicated genes to other subpopulations, where the persistence of the duplicated genes is once again contingent upon genetic drift and/or selective advantages/disadvantages (Figure 1.2). Once in different subpopulations, the fate of the gene duplication could differ.

Figure 1.2 Possible form of spreading gene duplications in a species. Genetic drift leads to the fixation of the newly duplicated gene in subpopulation A. Upon migration of individuals from subpopulation A to subpopulations B and C, the duplicated gene is spread to those subpopulations. Genetic drift causes the duplicated gene to persist in subpopulation B, but it eliminates the duplicated gene from subpopulation C. Dashed arrows indicate the level of migration.

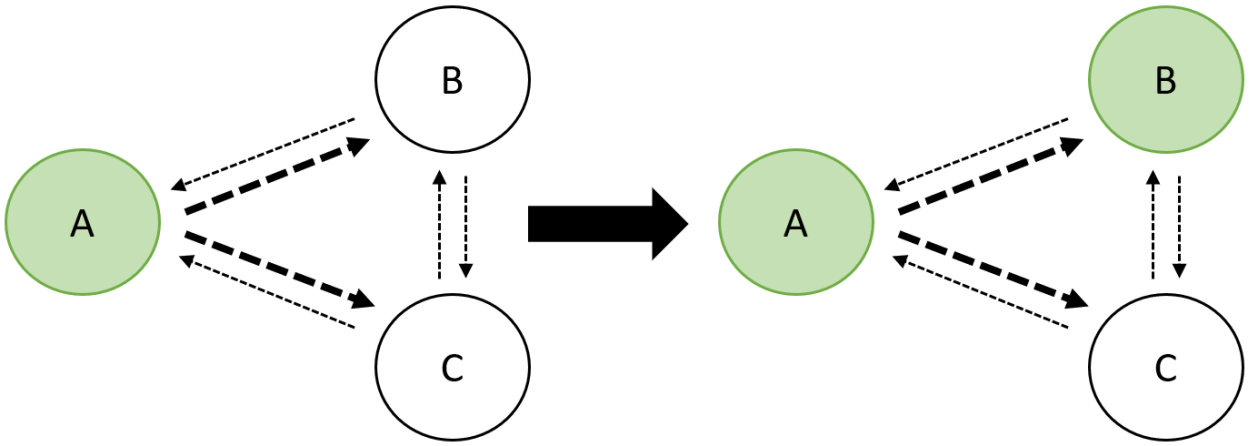

Duplicated genes that maintain the original fitness of the subpopulation have a relaxed selection pressure to have one of the copies "knocked-out ". Knockout mutations can independently occur on each copy of the duplicated genes in two different subpopulations, and since both copies still act on the same metabolic pathway, fitness is maintained. However, if migration brings these two populations together, both knocked-out genes can be combined in the same genetic background, creating a duplicate factor model of epistatic interaction (see Figure 1.3 - Hill et al., 2008; Holland, 2001).

Figure 1.3 Exemplification of a duplicate factor model of epistatic interaction. (A) shows the pairing of two duplicated genes from subpopulations A and B, respectively, where different copies of the duplicated gene were "knocked out". (B) shows how recombination can combine the

two “knocked out” alleles in the same genetic background, leading to decreased fitness ($A_2A_2B_1B_1$).

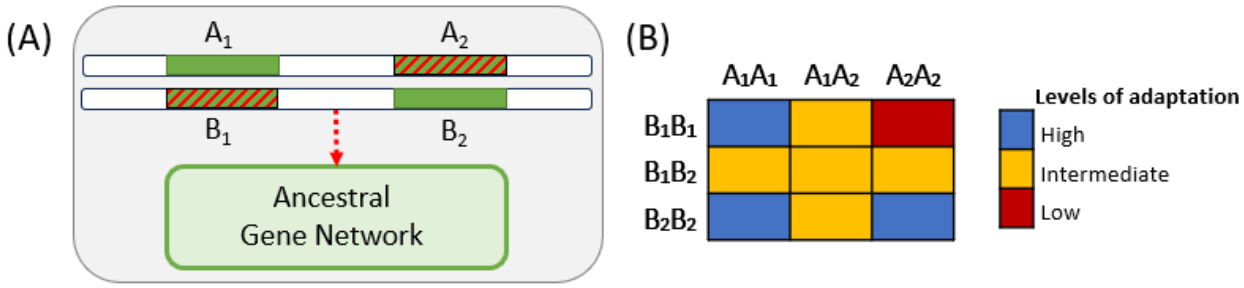

The coevolution of duplicated pleiotropic genes and their respective metabolic pathways can lead to specialization and increased adaptation. Upon migration, the combination of these specialized genes and coevolved metabolic pathways can potentially bring the carrier subpopulation closer to the adaptive peak. This concept can be visualized using the wildtype and mutant allelic combinations of genes and metabolic pathways (Figure 1.4), where the interaction between wildtype gene A_1A_1 and wildtype metabolic pathway B_1B_1 leads to improved adaptation. Similarly, the mutant duplicated gene A_2A_2 and coevolved metabolic pathway B_2B_2 are also favorable for adaptation. However, a mismatch between gene product and metabolic pathway occurs when A_1 is combined with B_2 or A_2 with B_1, resulting in a penalty to overall fitness. This concept gives rise to sign epistasis.

Although the concept of sign epistasis was exemplified using gene duplications and gene networks, it could very well be described as involving only genes themselves. If A_1 and B_1 are interacting genes, a mutation can create an alternative allele, A_2, which could have an altered protein folding that results in decreased fitness. A complementary mutation in B_1 creates B_2, which complements the protein folding changes in A_2 and creates an alternative allelic interaction with similar adaptive effects, as shown in Figure 1.4B. Alternatively, sign epistasis could also arise from gene knockouts as described in Figure 1.3 if negative epistasis (Qian et al., 2010) occurs between the duplicated genes. In this case, the A_1 and B_1 in Figure 1.3 would rather result in low adaptation.

In summary, duplication events are likely to happen randomly in different subpopulations of a species during its evolution. Even if these gene duplications are not spread to other subpopulations, it can still create genetic variation within a species. For instance, in maize,

presence-absence variation linked to phenotypic traits has been reported (Chia et al., 2012; Lu et al., 2015; Wallace et al., 2014). Additionally, when gene duplications that have evolved separately in different populations are brought together in the same genetic background, it can lead to the emergence of epistatic variance.

Figure 1.4 Graphic representation of how the evolution of gene duplications and metabolic pathways can lead to sign epistasis. (A) shows the pairing of duplicated genes from population A, which maintained the original gene function (either through subfunctionalization or non-functionalization) and gene network (A_1 and B_1), with the duplicated genes from population B, which evolved to acquired specialized function and gene networks (A_2 and B_2). (B) depicts how recombination can create a mismatch between gene function and gene networks, leading to inferior adaptation.

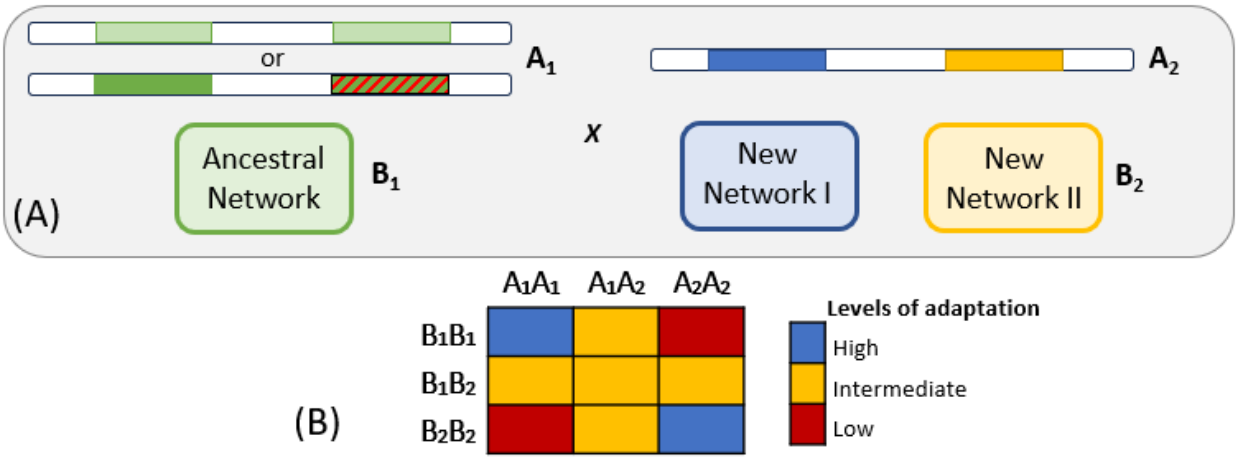

Epistasis and the Shifting Balance Theory (SBT)

The Shifting Balance Theory, proposed by Wright (1932), suggests that the genetic architecture underlying adaptive traits is epistatic and pleiotropic. In this context, the effect of allelic combinations, instead of individual alleles, is responsible for increasing the adaptation of populations. Epistasis occurs when the effect of an allele depends on the genetic background in which it occurs, suggesting that different combinations of alleles may lead to similar levels of adaptation, as depicted in Figure 1.4. This scenario indicates that individuals can adapt to environmental pressures in various combinations of alleles, often leading to similar fitness outcomes (Wright, 1988). In this context, Frank (1999) utilized the NK model, which simulates n genes with k interactions per gene, and observed that highly connected networks could render

certain alleles advantageous in one genetic background but disadvantageous in another. Gibson (1996) investigated the role of a gene and its transcriptional activator in the embryogenesis of Drosophila and showed that epistasis arises naturally from the physical interaction between the gene promoter and the activator protein. It was also reported that different genotypic combinations can produce the same genetic output.

Another fundamental premise of this theory is that the subdivided structure of populations increases the power of random genetic drift, sometimes counteracting the forces of natural selection and leading to the fixation of alleles that are not the most adapted (Ohta, 1973; Dobzhansky et al., 1977; Lynch et al., 2008). Additionally, natural selection is not a static force; it can favor different combinations of alleles depending on changing environmental conditions. For example, in a study by Taylor et al. (2019), large-effect flowering time genes in Arabidopsis thaliana were mutated, and the fitness of these mutants was measured in various environments. The results showed that some mutations improved adaptation in specific environments but not in others. Casal (2000) investigated the interactions between phytochromes and cryptochromes in plants and found that phytochromes *phyA* and *phyB* exhibited both synergistic and antagonistic behaviors under different light conditions.

Although epistatic gene action is assumed to be the foundational genetic architecture under this theory, the visualization of epistasis in populations is very complex because epistatic variance is a function of allele frequencies (Whitlock et al., 1995; Neiman and Linksvayer, 2006). For instance, in a population where A_1 and B_1 alleles are equal ($p_{A1} = p_{B1} = 0.5$), all nine allelic combinations are observed at similar frequencies, resulting in maximum epistatic variation. In the event of a genetic bottleneck, the frequency of the A_1 allele can decay, leading to a decrease in allelic combinations involving A_1 and a reduction in epistatic variance (Whitlock et al., 1995; Cheverud and Routman, 1996; Cheverud, 2000; Holland, 2001), which is then converted into additive variance. In an extreme scenario, A_2 allele is fixed while gene B still segregates, results in no variance in locus A while locus B is completely additive (Bernardo, 2020; Technow et al., 2021; Cheverud and Routman, 1996; Neiman and Linksvayer, 2006) (Figure 1.5). Therefore, the presence of epistatic gene effects does not translate into epistatic variance, and any disruption of balanced allele frequencies ($p_{A1} = p_{B1} = 0.5$) leads to a reduction in epistatic variance and an increase in additive variance.

Intermediate allele frequencies for both alleles involved in a coadapted epistatic interaction establish an unstable equilibrium in the population. Even a slight increase in the frequency of one allele, such as B_2, can trigger a corresponding increase in the frequency of the other allele, A_2, due to direct selection pressure acting on the gene combination (Wade and Goodnight, 1998; Holland, 2001). This phenomenon is known as "the tipping point" in epidemiology and illustrates how a small change can lead to substantial shifts in a system. Throughout the process of fixation of the $A_2A_2B_2B_2$ combination, epistatic variance is converted to additive variance, and any remaining variance is further eliminated from the population upon the fixation of alleles A_2 and B_2. Although genetic variance is zero for this epistatic interaction, fitness is at its peak.

Figure 1.5 A simple two-locus epistatic gene action model that produces only additive variance from the fixation of the A_2 allele.

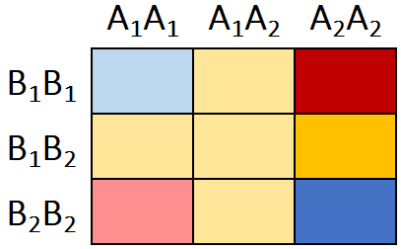

Epistasis and fitness landscapes

In the preceding sections, we presented the effects of two-way epistatic interactions involving two similarly fit allelic combinations and applied it to the context of populations. However, in natural settings, the occurrence of sign epistasis is anticipated to involve more than just two genes interacting with each other. Numerous gene networks with varying levels of complexity may underpin diverse adaptive traits, collectively influencing the fitness of genotypes and populations. This greatly increases the potential number of allelic combinations within a species, making it impractical to visualize the entire array of allelic combinations, as it would necessitate numerous dimensions (Wright, 1932). The concept of the fitness landscape metaphor devised by Wright (1932) serves as a valuable tool for conceptualizing the genetic complexity in high-dimensional spaces (Svensson and Calsbeek, 2013). This metaphor employs a simplified graphical representation with two dimensions representing allelic combinations and a third dimension indicating their corresponding adaptive value, as illustrated in Figure 1.6. As a

metaphor, it shouldn't be interpreted literally, but it offers an intuitive understanding of the complexity and ruggedness associated with increasing gene interactions (Kauffman 1993; Technow et al., 2021).

Figure 1.6 Graphical representation of a hypothetical fitness landscape. X and y-axis represent gene combinations and the z-axis represents adaptation. Black squares, blue circles and white stars represent subpopulations exploring different parts of the fitness landscape. The pressure of selection tends to push the populations to the top of the adaptive peaks (dotted arrow).

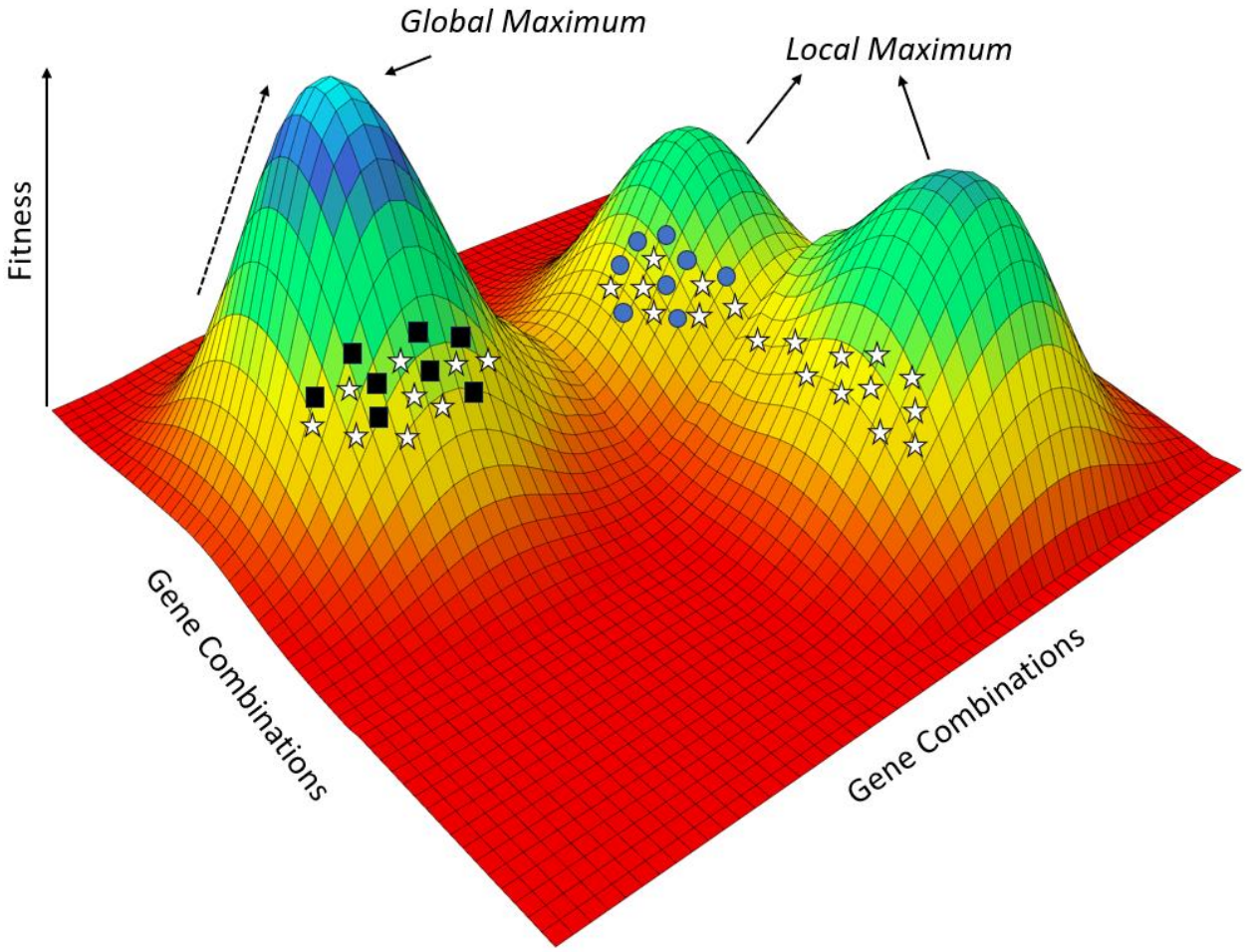

The potential for multiple allelic combinations to confer comparable levels of adaptation coupled with the vast number of potential gene combinations, results in a fitness landscape characterized by rugged terrain of hills and valleys representing high and low levels of adaptation, respectively (Wright, 1932). Such adaptive landscapes represent dynamic systems that can exhibit

multiple stable equilibria (Whitlock et al., 1995), whereby distinct subpopulations may possess unique allelic combinations that confer equal adaptation to a given local environment.

The rugged landscape, as depicted in Figure 1.6, is assumed to contain local regions of maximum adaptation and one global optimum. When a hypothetical base population is navigating across various adaptive peaks on this fitness landscape (illustrated as "star" shapes in Figure 1.6), subdividing into smaller subpopulations can potentially expedite adaptation. In smaller populations, the impact of genetic drift becomes more pronounced, leading to the fixation of random allelic combinations. The reduced number of segregating allelic combinations narrows the maximum number of potential combinations in each subpopulation. This implies that subpopulations are constrained to exploring a smaller portion of the fitness landscape, as illustrated by the "squares" and "circles" shapes (Figure 1.6). As mentioned earlier, the random fixation of alleles involved in epistatic interactions has the potential to convert epistatic variance into additive variance (Neiman and Linksvayer, 2006). This conversion can increase additive variance and heritability, thereby enhancing the response to selection pressures. Bryant and Meffert (1995) observed that a bottlenecked population of houseflies exhibited higher additive variance and heritability compared to non-bottlenecked populations when selecting for increased morphometric shape.

However, the random nature of genetic drift can constrain the genetic diversity in a way to strand the subpopulation on a local maximum peak, where selection gains quickly reach a plateau (as illustrated by the "circle" shapes). To move to the global optimum, migration from other subpopulations is necessary to bring in diversity, but it may require passing through a less fit state first (valley), which works against the pressure of selection (Holland, 2001; Lande, 1976). In this scenario, once again genetic drift could enable this subpopulation to traverse valleys of adaptation before reaching new peaks (Wright, 1982) through the rapid fixation of better fit allelic combinations. Alternatively, the variable nature of environmental pressures may alter the landscape by flattening hills or creating ridges, allowing populations to transition to different stable equilibria.

Gene and genome duplication in wheat

The evolutionary history of common wheat demonstrates how this species evolved under the influence of whole genome duplication events and how it took advantage of the different outcomes of gene duplications.

First, the interspecific hybridization between the allotetraploid wheat *Triticum turgidum* (2n = 4x = 28, genome AABB), originated from *Triticum urartu* (A genome) and a species most similar to *Aegilops speltoides* (B genome), with *Aegilops tauschii* (D genome) gave rise to common wheat (2n = 6x = 42, genome AABBDD) (Peng et al., 2011; Nesbitt and Samuel, 1998). The two hybridization events presented numerous opportunities for duplicate genes to develop novel genetic pathways that could specialize, create biological novelties, and provide adaptative benefits (Blanc and Wolfe, 2004), potentially broadening the environments of adaptation of the species (Madlung, 2013).

Second, the three genomes comprising common wheat underwent different evolutionary pathways and genes under weak selection pressure eventually specialized into new functions that could have been fixed due to fitness advantages or genetic drift. Hence, the two interspecific polyploidization events created a possibility to assemble different evolutionary adaptations into the same genetic background. Santantonio et al (2019a) suggests that homeologs may have evolved to express or function at different optimal conditions but when present in the same genome, through allopolyploidization events, confer greater phenotypic plasticity. This phenomena could explain the broader adaptability and enhanced resistance to biotic and abiotic stresses of hexaploid wheat compared to its progenitors (Yang et al., 2014; Eckardt, 2014).

Besides the possible parallel expression of homeologous and neofunctionalization of genes, a hallmark of polyploidization is an extensive change in gene expression (Leach et al., 2014) due to homoeologous interaction. Zhang et al (2014) compared gene expression patterns of *Triticum turgidum* subs *durum* with extracted tetraploid wheat (reversed from hexaploid AABBDD to tetraploid AABB) and observed anomalous phenotypic traits in the reversed wheat and differential expression of genes between the two tetraploid genomes. Leach et al (2014) analyzed the patterns of gene expression in hexaploid wheat and found that at least 45% of homoeologous genes are expressed in the three distinct homoeoloci, but the majority of homeologous presented biased expression patterns in which one gene controlled most of the expression. They also found that 55% of genes were expressed in only one or two homoeoloci.

Other studies also reported differential gene expression in homoeologous genes in wheat (He et al., 2003; Chagué et al., 2010; Wang et al., 2016; Zhao et al., 2020).

Important and well-known genes in wheat domestication and breeding also evolved to develop complex gene interaction with their homoeologous pairs. The *Q* genes, located in homeologous group 5 chromosomes, influence free threshing character and are amongst the most important domestication genes in wheat. Zhang et al (2011) showed that evolution led to hyperfunctionalization, pseudogenization and subfunctionalization of *5AQ*, *5Bq* and *5Dq*, respectively, and that the functionality of *5Bq* and *5Dq* depended upon the allelic state of *5AQ*/*q*. They also pointed to reduced functionality of *5Dq* when *5Bq* was deleted. Santantonio et al (2019a) found evidence of subfunctionalization epistasis in the reduced height genes (*Rht*) in wheat. The authors observed a deviation from additivity when the *Rht1* and *Rht2* were present in the same genetic background, indicating redundant gene function.

The recent hybridization events that led to the creation of hexaploid wheat made it somewhat intuitive to think of epistasis as involving mostly homeologous genes, especially because major orthogonal genes act on the same metabolic pathway and result in a clear distortion of additive gene activity. However, it is plausible to speculate that homeologous interactions comprise only one small portion of the total epistatic interactions (Santantonio et al., 2019b). During the evolution of the three diploid genomes that comprise hexaploid wheat, gene duplications could have occurred and led to the development of new gene interactions within each subgenome, which were later combined into one single species. Studies have reported epistatic gene effects in diploid wheat, *Triticum monococcum* (Tranquilli and Dubcovsky, 2000), and also within sub genomes in hexaploid wheat (Reif et al., 2011; Sehgal et al., 2020).

The subpopulation structure of the wheat germplasm in North America

The origin of hexaploid wheat is thought to have occurred approximately 9,000 years ago, spreading eastward from the Fertile Crescent region, potentially south and west of the Caspian Sea (Braidwood, 1969; Salamini et al., 2002; Giles and Brown, 2006). Over time, early local farmers dispersed bread wheat, both eastward towards Asia and westward toward Europe, between 8,500 and 2,300 years before present (William et al., 2011). As the germplasm was introduced to new regions, it underwent natural and unconscious selection by farmers, ultimately adapting to the local environments. Landraces of wheat from Europe, Asia, and Africa, which are believed to have been

part of the initial wave of wheat dispersal, displayed a significant positive correlation between their genetic and geographic distances from the Fertile Crescent (Balfourier et al 2019). Hence, isolation by distance played a key role in driving the differentiation of African-Asian wheat germplasm, a phenomenon previously reported by Bonman et al. (2015). The dispersion of the core wheat germplasm pool and subsequent adaptation of subpopulations to new environmental optima could have led to the fixation of coadapted gene complexes.

In the 16th century, wheat was globally dispersed with the discovery of the New World, and Spaniards introduced superior wheat cultivars to the East coast of Latin and Northern America (Ball, 1930; William et al., 2011; Balfourier et al., 2019). Specifically in the United States, an important introduction of Mediterranean germplasm in the 19th century became widely grown and served as progenitors of better adapted cultivars (Ball, 1930; Balfourier et al., 2019). However, these introductions were not well-adapted to the harsh environments of the Great Plains (Ball, 1930). In 1873, the hard-red winter wheat landraces introduced in Kansas, primarily Turkey Red, plant selections out of Turkey, and closely related cultivars Crimean and Kharkof from Russia and Ukraine, were specifically adapted to the continental climate and dominated production in the Great Plains, becoming the core of early improved varieties and the founder lines of breeding programs in the Great Plains (Ball, 1930; Quisenberry, 1974; Quisenberry and Reitz, 1974; Schmidt, 1974; Cox et al., 1986; Paulsen and Shroyer, 2008). Although genetic diversity was introduced in the 1940s and ‘50s, it was later eliminated, and the hard-red winter wheat gene pool returned to be centered on Turkey-type wheats, which comprise nearly half of the genes of cultivars from the end of the 20th century (Cox et al., 1986; Cox, 1991)

Balfourier et al. (2019) conducted a comprehensive phylogeographic analysis of 4403 wheat landraces, traditional and modern cultivars, which represent the worldwide genetic diversity of wheat. The analysis showed that North American soft red wheat cultivars clustered with French and Spanish accessions, as well as landraces from the Mediterranean and Iberian Peninsula region. Meanwhile, North American hard red winter wheat cultivars grouped with Russian, Ukrainian, Hungarian, and Romanian accessions, as well as landraces from Southeastern Europe. These findings support the historical origin and introduction of wheat germplasm in the United States.

The genetic diversity of North American winter wheat is based on geographic origin, with consistent differentiation between hard and soft winter wheat classes (Zhang et al., 2010; Sthapit et al,. 2022). However, the hard and soft traits in wheat are controlled by the genes Pin-a and Pin-

b on chromosome 5D (Hogg et al, 2004), suggesting that the grain hardness genes are unlikely the major drivers of differentiation between these market classes (Zhang et al. 2010).

The current differentiation between the soft and hard red wheat market classes in the US can be attributed to the initial germplasm introductions. Breeding efforts to improve the soft and hard wheat classes mostly involve elite-by-elite crosses within these gene pools (Sthapit et al., 2022). Balfourier et al (2019) showed that while soft wheat has maintained constant high levels of founder lines, the genetic contribution of the founder genotypes in the hard-red wheat pool has increased in modern cultivars when compared to traditional varieties. Zhang et al. (2010) analyzed hard and soft wheat genotypes and observed that 29 out of 75 hard wheat accessions that clustered in the southern and central Great Plains had Jagger, Ogallala, and Trego in their pedigree, underscoring the high utilization of regional genotypes in the improvement of wheat in the Great Plains.

The hard red winter wheat (HWW) variety Jagger was registered as having originated from a single cross between a Kansas State's experimental line (KS84W85) and the soft winter wheat (SWW) variety Stephens, from the Pacific Northwest. Theoretically, the single cross between HWW and SWW lines implies that Jagger carries a significant portion of SWW in its genetic background, which might have dispersed throughout the Great Plain's germplasm over time, as Jagger was in the pedigree of numerous varieties. However, the accuracy of Jagger's pedigree is questionable, as unpublished evidence suggests that it originates from a three-way cross. Another line of evidence supporting the hypothesis that Jagger carries HWW background comes from studies about the genetic diversity of wheat in the great plains. In the study conducted by Balfourier et al (2019), Jagger was found within the great plains cluster, which also contained founder lines Kharkov and Crimean.

To summarize, the two primary subpopulations of wheat introduced in the United States have predominantly relied on crosses within their respective gene pools due to local adaptation and market class. While genetic diversity has been incorporated into these pools, it has not been retained over time.

Epistasis and the structure of breeding programs

The structure of public wheat breeding programs in the Great Plains is similar to the structure and assumptions of the Shifting Balance Theory. Breeding programs perform crosses

mostly within their breeding pool (within subpopulation), but also bring in germplasm from other programs (migration). As the germplasm that is exchanged is usually top performing elite lines, superior allelic combinations can be brought into the breeding pools. Technow et al (2021) illustrated a similar scenario in private corn breeding programs, where inbred lines from top performing breeding programs are incorporated into the breeding pool of other breeding programs and promote an overall improvement in hybrid performance.

In most closed breeding programs with frequent crossing of related genotypes, the process of inbreeding constrains the complexity of epistatic interactions. Most of the variance is additive (Technow et al, 2021) and the response to selection has predictable changes in allele frequency (Holland 2001), giving rise to the Fisher model (Coyne et al., 1997 – Table 2). The Fisher model is based on additive gene action and considers the influence of dominance and epistasis to be nil. Each allele is assumed to have an independent and fixed effect on adaptation, such that individuals that accumulate more favorable alleles are better adapted. Under this model, the fitness landscape is comprised of a single adaptive peak. However, the Fisher model still fits the dynamics of the fitness landscape under the restricted region of a single adaptive peak (Holland, 2001). This concept relates to the philosophy of wheat breeder Warren Kronstad, and probably many other breeders, which said: "*find a good parental line and build your program around it*" (Rollie Sears, personal communication to Allan Fritz). The Colorado State wheat breeding program has been employing that approach to an extent. The HWW variety Byrd, released in 2011, has been frequently used as a parental line, which proved to be successful. The 2023 Wheat variety Guide from Plains Gold had 13 HWW varieties available, nine of which had Byrd in their pedigree. This portion of the Colorado program could be conceptualized as either the "squares" or "circle" shapes in the fitness landscape (Figure 1.6). A similar situation occurred with the Kansas State University wheat breeding program after the release of HWW variety Jagger in 1994. In following breeding cycles, Jagger was heavily used as a parent in crossing blocks, mostly because of presenting the align chromosomal segment 2NS from *Aegilops ventricosa* that carries the leaf rust resistance gene *Lr37* (Fang et al. 2011). Jagger is found in the pedigree several K-State varieties, as Everest, Danby, Fuller, Joe, Overley.

A breeding program that operates within a closed framework restrains genetic diversity and mitigates the adverse impacts of epistasis. During the initial stages of establishing such a program around a strong combiner, parental lines that exhibit poor compatibility with the core

combiner are systematically eliminated. From a practical perspective, breeders will recycle genotypes that are frequently successful in developing superior offspring with the good combiner and discontinue the utilization of parental lines not as promising. From a fitness landscape viewpoint, genotypes that are not on the same adaptive peak as the good combiner are excluded. Breeders adopting this strategy may disregard the existence of epistasis, as, over time, all of the epistatic variance is converted into additive variance.

However, it is necessary to acknowledge potential drawbacks of this approach. If the initial genetic base is narrow and expanding the genetic base is necessary, introducing diversity in a closed program may yield results that fall short of expectations. The introduction of foreign germplasm is expected to bring new allelic combinations. If both foreign and local genotypes are high performing (elite), it is possible that they carry distinct, highly adaptive allelic combinations, say $A_1A_1B_1B_1$ and $A_2A_2B_2B_2$ (Figure 1.4B). Crossing these two genotypes results in an F_2 generation that segregates to allelic combinations previously fixed in each parental line, leading to a phenomenon called F_2 breakdown (Whitlock et al., 1995), where the mean performance of the population is lower than the midparent value. Epistatic variance, which was non-existent within each parental pool for this hypothetical interaction, is unleashed in the breeding population. Depending on the number of allelic combinations differing in the parental lines, the reduction in performance might be so significant that it causes the whole population to be discarded – which can be exemplified in a cross involving "square" and "circle" shapes in Figure 1.6, where the offspring fall into a valley of performance. In such cases, a single generation of crosses is not enough to recover all favorable allelic combinations of either parental line, as the rapid nature of inbreeding prevents recombination to assemble better-than-parental allelic combinations.

Another theoretical concern arises from the concept of local optimum adaptive peaks within the fitness landscape. If a breeding program opts for a closed approach, there is the risk of becoming stranded in a local fitness peak, analogous to the "circle" shapes in Figure 1.6, where it becomes nearly impossible to reach the global fitness peak (Holland, 2001). In nature, transitioning from a local to the global adaptation peak entails passing through a stage of less adaptation (valley). This transition can be facilitated by genetic drift and variations in selection pressures, which may give rise to ridges connecting the peaks. In the context of breeding programs, such transition might involve discontinuing breeding efforts at the local adaptive peak and initiating anew towards the global adaptive peak, though the likelihood of existing breeding programs adhering strictly to this

strategy is null. However, a scenario resembling a continuous shift between adaptive peaks may be exemplified by the case of Chinese wheat germplasm. According to Balfourier et al (2019), Chinese landraces significantly contributed to the genetic background of traditional wheat varieties. However, in the latter half of the 20th century, Chinese breeding programs increasingly incorporated Italian germplasm (Salvi et al., 2013; Hao et al., 2017), resulting in the creation of numerous traditional cultivars during the 1960s and 1970s. At present, Italian genetics constitute a substantial proportion of the genetic background of elite wheat cultivars in China, surpassing the contribution of Chinese landraces in certain germplasm pools. The prevalence of Italian genetic heritage in Chinese breeding programs suggests that it may provide superior performance compared to local landraces and traditional varieties.

The process of shifting adaptive peaks does not guarantee that the newly targeted peak represents the global maximum of adaptation for the given target population of environments. In the Chinese scenario, the utilization of Italian germplasm may represent a transition to a higher peak, but it does not imply that this represents the global optimum for Chinese environments. In fact, determining the true global adaptive peak is impossible. In practical terms, breeding programs can only assess whether the adaptive peak they are currently pursuing leads to satisfactory improvements. This evaluation is grounded in the present performance of the germplasm and genetic gains. Chinese breeders possibly recognized the enhanced performance potential and the prospect of achieving greater genetic gains with the Italian pool and redirected their focus toward a more frequent utilizing this genetic source.

While the decision to either persist with a current adaptive peak or shift to a new one is complex and has many implications, the time required for a breeding program to ascend to the summit of a local adaptive peak is uncertain, and possibly requires several generations of breeding efforts (Holland, 2001). This suggests that the need to shift adaptive peaks due to diminishing or exhausted genetic gains might not be necessary for several generations, although it remains a possibility to transition peaks if the aim is to achieve faster rates of genetic gain.

On the other hand, some breeders prefer to construct their program around two or three good combiners, particularly if they aim to establish a large genetic base. This approach suggests that their breeding pool could be exploring different adaptive peaks on the fitness landscape, analogous to the “star” shapes in Figure 1.6. In such cases, epistatic variance is expected to be observed even in breeding populations developed with parental lines from within the breeding

program, provided that these parental lines occupy different adaptive peaks. Similar to closed program bring in foreign germplasm, crossing genotypes with different epistatic frameworks ultimately leads to F_2 breakdown. Given the recurrent nature of this phenomenon, the number of populations developed per breeding cycle and/or the size of the breeding populations may be augmented in such breeding programs, compared to closed programs, to compensate for the suboptimal performance in early generations. In addition, top-crosses are preferred and more common than single-crosses, as the former permits better management of the genetic complexity and often yields superior populations.

In breeding programs with a large genetic base, the relatively frequent occurrence of crosses between genotypes with different epistatic frameworks increases the likelihood that, at some point, the epistatic framework of either parental line will be recovered in the offspring. This process may lead to the unexpected assembling of new and superior allelic combinations, even from initially undesirable allelic combinations (as exemplified in Figure 1.7). This phenomenon is analogous to crossing "square" and "circle" shapes, as depicted in Figure 1.6. If the epistatic framework characteristic of the "square" shapes is recaptured in the offspring, for instance, it opens the door for the creation of novel allelic combinations and the introgression of superior allelic combinations found in the “circle” shaped adaptive peak. The downside of this potential advantage is the overall inefficiency of the breeding program, as the number of breeding populations developed must be much higher for a reasonable probability of successfully recovering a parental epistatic framework.

Figure 1.7 Hypothetical di-genic epistatic interaction scenarios. Blue and yellow represents high adaptation and red indicates low adaptation.

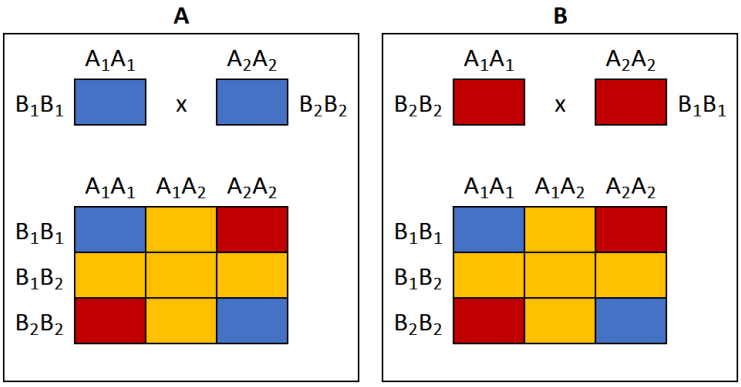

One potential advantage of breeding programs with large genetic base may be the introduction of external germplasm into their breeding pool. The different epistatic frameworks in the breeding pool increase the probability of finding a matching epistatic framework between foreign and local germplasm and to successfully introduce allelic diversity through conventional crossing approaches (single or top-crosses).

The way breeding programs with large genetic base navigate the fitness landscape differs from closed programs. As such programs are exploring multiple adaptive peaks, the chance of getting stranded in a region of local adaptation is null. The practicality of this hypothetical framework comes from the fact that breeders recycle more frequently genotypes that are successful at developing superior germplasm than genotypes that are average. From a fitness landscape perspective, this observation suggests that breeders successfully abandon low adaptation peaks to focus on higher ones. In the long run, broad genetic base breeding programs may operate like closed programs, as breeders are expected to recycle more constantly the best germplasm.

Another potential advantage of running a breeding program with a large genetic base arises when the target population of environments is vast. A program exploring multiple adaptive peaks might find allelic combinations that are better suited to a subset of the TPE. In such cases, recycling the better adapted lines within different parts of the TPE increases the overall genetic gain of the program. For instance, the Kansas State wheat breeding program has the germplasm divided into western and eastern Kansas adapted pools. Crosses between these pools are rarely performed, as the introduction of western germplasm in the eastern pool will increase plant height, extend the cycle, and diminish the resistance to rusts. The opposite is true, where introducing eastern germplasm into the western pool decreases the plant height and cycle length, and reduced resistance to viruses. One shortcoming of this approach is the increased complexity of managing a subdivided germplasm pool.

Epistasis and the introduction of genetic diversity

Wide crosses have the opportunity to bring in new allelic combinations at the expense of disrupting already existing ones (Figure 1.7). On average, the potential gains under this balance tend to be minimal under the conventional approaches to develop breeding populations for two reasons. First, the distribution of factors fixed during the evolution of a species via mutation or standing genetic variation is expected to be exponential, that is, large effect variants are fixed first

(Barret & Schluter, 2008; Hedrick, 2013), followed by smaller effect variants (Orr 2005). Although wide crosses could bring in favorable, small effect allelic combinations, it comes at the expense of disrupting large effect combinations. Second, the segregation of allelic combinations in Figure 1.7A and B creates epistatic variance which slow down genetic advances in such populations (Wang et al., 2004: Technow et al., 2021). As highlighted by Holland (2001), based on the studies of Upadhyaya and Nigam (1998) and Humphrey et al (1969), there is a low correlation between early and late generations when epistasis is significant, implying limited response to early generation selection. In addition, the quick pace of inbreeding, associated with small effective population size, prevents recombination to assemble the optimal set of allelic combinations, as allelic combinations become quickly fixed for either favorable or unfavorable combinations.

As the immediate, single cross approach to introduce genetic diversity may be challenging under the influence of epistasis, gradual approaches could be successful. Backcrossing has been widely known and used in plant breeding as a strategy to introduce a few alleles of interest from a donor line in the background of a recurrent line (Hospital, 2005). However, it has not been widely discussed as a strategy to constrain the genetic complexity (segregation of epistatic loci) of complex traits when crossing parental lines from two different peaks in the fitness landscape. For instance, a breeder that is not successful at introducing diversity from an external, elite source may be failing to constrain the genetic complexity in the breeding populations. That becomes even more important when local adaptation alleles are not observed in the external germplasm. Hence, the constraint of epistatic variance leads to increased additive variance and increases the response to selection in the breeding population, potentially permitting to cross a valley of adaptation in the fitness landscape.

Another similar approach could be the utilization of pseudo-backcrosses. These are comprised of three-way crosses (top crosses) with recurrent lines having a similar pedigree. The similar genetic background of the recurrent lines suggests that these could share the same epistatic framework and yet provide diversity to the population. This approach could be less useful if the amount of epistatic variance in the initial cross is very large.

The lengthiest approach is recurrent selection. With recurrent selection, the speed of inbreeding is counteracted with the recurrent rounds of recombination, which permits assembling new sets of allelic combinations. With recurrent selection, one can navigate the population in the fitness landscape and climb the hill that best fits the environmental pressures of target population

of environments. One major concern with recurrent selection is the possibility that the population is comprised of genotypes exploring different adaptive peaks. This implies that the selection and recombination of the best performing lines creates epistatic variance and slows down genetic gain, as selected lines presented alternative epistatic frameworks.

The goal of making wide crosses in wheat breeding is to introduce new, superior alleles to the local germplasm. The utilization of one or even two (pseudo)backcrosses may be considered too lengthy for the fast pace of breeding programs. However, it is much faster than utilizing conventional crossing approaches that lead to the early discarding of breeding populations and could impede the introduction of any new alleles in the breeding pool.

Effects of epistasis on genomic selection

The successful implementation of genomic selection in wheat breeding is based on the improvement in selection accuracy tied to expediting breeding cycles, which can only be accomplished with adequate levels of prediction accuracy. In that regard, studies have reported prediction accuracies ranging from zero to around 0.5 for grain yield (Juliana et al., 2018; Watson et al., 2019; Belamkar et al., 2018; Lozada et al., 2019). This wide range of prediction accuracy compromises the reliability of genomic selection for ample adoption in breeding programs. There are several potential reasons for the poor prediction accuracies, including the lack of genome-assembly data for multiple wheat lines (Walkowiak et al., 2020) to capture structural variations in the genome of elite germplasm; the influence of genotype-by-environment interactions (Juliana et al., 2018), especially in low heritability traits; or the small relatedness between training and validation populations (Bernardo, 2020). Bernardo (2020) synthesized the results of Jacobson et al. (2015) and Brandariz and Bernardo (2019) in corn to demonstrate that a training population consisting of individuals with varying degrees of relatedness to the validation population exhibited comparable selection gains to a training population of half-siblings that was ten times smaller. In wheat, reduced prediction accuracies were also observed with reduced relatedness between training and validation populations (Liu et al., 2016; Kristensen et al. 2018; Kristensen et al., 2019a; Kristensen et al., 2019b). One potential factor contributing to the significance of relatedness in prediction accuracy may lie in the linkage phase between quantitative trait loci (QTLs) and markers, initially assumed to remain consistent across training and validation populations, particularly at high marker densities (Meuwissen et al., 2001; Haile et al., 2017). However,

disentangling the effects of linkage phase and relatedness on the prediction accuracy of genomic selection is not possible due to the inherent entanglement between these two factors. (Wientjes et al., 2013). Epistasis could also be a potential explanation for this phenomenon. One possibility is that training and selection populations with small relatedness might not share the same allele fixed that converts epistatic variance into additive variance. For instance, if the training population is fixed for the A_2 allele (Figure 1.4 B) but the validation population is fixed for the A_1 allele, the estimated effects of the B alleles in the training population will present opposite effects in the validation population, diminishing the prediction accuracy. This situation is expected to become more frequent the more distant training and validation populations are, which could be contributing to the importance of relatedness for prediction accuracy. Another potential way epistasis could influence prediction accuracy relates to segregating epistatic loci, especially at intermediate allele frequencies ($p_{A1} = p_{A2} = 0.5$). Under this scenarios, no marginal additive effect or variance heterogeneity is associated with each locus (Forsberg and Carlborg, 2017), as neither additive nor epistatic models can capture this type of epistasis. The incapability of models to estimate marginal effects for this type of interaction prevents genomic selection from estimating more accurate GEBV, as distinguishing genotypes with favorable and unfavorable combinations is not possible. It is worth noting that this is not a challenge affecting only genomic selection, but all models that attempt to estimate effects of sign epistatic interactions.

Conclusions

The theoretical aspects discussed in this literature review point towards the fundamental importance of epistatic gene action as the main genetic architecture in wheat. However, empirical studies are required to further support this theoretical framework. Specifically, the existence of sign epistasis has to be proven in wheat. If sign epistasis is absent, it implies a fitness landscape characterized by a single adaptive peak with alleles having constant effects. This could suggest that the lack of success introducing foreign germplasm would be attributed to the segregation of local adaptation alleles. Similarly, the limitations in the predictive accuracy of genomic selection models could be attributed to factors like linkage phase, relatedness, and genotype-by-environment interactions. Conversely, if sign epistasis is proven to exist in wheat, breeding programs would face the decision to operate an open or closed breeding program with known consequences to the germplasm pool and breeding efficiency. Breeders would be able to employ targeted crossing

strategies to specific combinations of parental lines. In addition, hybrid wheat breeding programs could build heterotic pools based on this framework, as epistasis plays a more prominent role than dominance in hybrid wheat heterosis (Jiang er al., 2017). Finally, the imminent necessity to model sign epistasis could provide the spark for quantitative geneticists and statisticians to develop models that account for this foundational type of gene action, which could improve the prediction accuracy in genomic selection models. Alternatively, the responsibility to deal with sign epistasis could be attributed to breeders by better managing epistasis in the breeding program and suing their knowledge on the germplasm to determine the most appropriate training datasets for specific selection populations.

References

Bailey, J. A., Gu, Z., Clark, R. A., Reinert, K., Samonte, R. V., Schwartz, S., ... & Eichler, E. E. (2002). Recent segmental duplications in the human genome. Science, 297(5583), 1003-1007.

Balfourier, F., Bouchet, S., Robert, S., De Oliveira, R., Rimbert, H., Kitt, J., ... & Paux, E. (2019). Worldwide phylogeography and history of wheat genetic diversity. Science advances, 5(5), eaav0536.

Ball, C. R. (1930). The history of American wheat improvement. Agricultural history, 4(2), 48-71.

Barrett, R. D., & Schluter, D. (2008). Adaptation from standing genetic variation. Trends in ecology & evolution, 23(1), 38-44.

Beesley, N. J., Attree, E., Vázquez-Prieto, S., Vilas, R., Paniagua, E., Ubeira, F. M., ... & Hodgkinson, J. E. (2021). Evidence of population structuring following population genetic analyses of Fasciola hepatica from Argentina. International journal for parasitology, 51(6), 471-480.

Belamkar, V., Guttieri, M. J., Hussain, W., Jarquín, D., El-Basyoni, I., Poland, J., ... & Baenziger, P. S. (2018). Genomic selection in preliminary yield trials in a winter wheat breeding program. G3: Genes, Genomes, Genetics, 8(8), 2735-2747.

Bernardo, R. (2020). Breeding for quantitative traits in plants (Vol. 3, p. 369). Woodbury: Stemma press.

Blanc, G., & Wolfe, K. H. (2004). Functional divergence of duplicated genes formed by polyploidy during Arabidopsis evolution. The Plant Cell, 16(7), 1679-1691.

Bonman, J. M., Babiker, E. M., Cuesta-Marcos, A., Esvelt-Klos, K., Brown-Guedira, G., Chao, S., ... & Gordon, T. C. (2015). Genetic diversity among wheat accessions from the USDA National Small Grains Collection. Crop Science, 55(3), 1243-1253.

Braidwood, R. J., Çambel, H., & Watson, P. J. (1969). Prehistoric investigations in southeastern Turkey. Science, 164(3885), 1275-1276.

Brandariz, S. P., & Bernardo, R. (2019). Predicted genetic gains from targeted recombination in elite biparental maize populations. The plant genome, 12(1), 180062.

Brosius J. (1991) Retroposons: seeds of evolution. Science 251: 753.

Bryant EH, Meffert LM (1995). An analysis of selectional response in relation to a population bottleneck. Evolution 49: 626–634.

Casal, J. J. (2000). Phytochromes, cryptochromes, phototropin: photoreceptor interactions in plants. Photochemistry and Photobiology, 71(1), 1-11.

Chagué, V., Just, J., Mestiri, I., Balzergue, S., Tanguy, A. M., Huneau, C., ... & Chalhoub, B. (2010). Genome-wide gene expression changes in genetically stable synthetic and natural wheat allohexaploids. New Phytologist, 187(4), 1181-1194.

Cheverud, J. M. (2000). Detecting epistasis among quantitative trait loci. Epistasis and the evolutionary process, 58-81.

Cheverud, J. M., & Routman, E. J. (1996). Epistasis as a source of increased additive genetic variance at population bottlenecks. Evolution, 50(3), 1042-1051.

Chia, J. M., Song, C., Bradbury, P. J., Costich, D., De Leon, N., Doebley, J., ... & Ware, D. (2012). Maize HapMap2 identifies extant variation from a genome in flux. Nature genetics, 44(7), 803-807.

Cox, T. S. (1991). The contribution of introduced germplasm to the development of US wheat cultivars. Use of Plant Introductions in Cultivar Development Part 1, 17, 25-47.

Cox, T. S., Murphy, J. P., & Rodgers, D. (1986). Changes in genetic diversity in the red winter wheat regions of the United States. Proceedings of the National Academy of Sciences, 83(15), 5583-5586.

Coyne, J. A., Barton, N. H., & Turelli, M. (1997). Perspective: a critique of Sewall Wright's shifting balance theory of evolution. Evolution, 51(3), 643-671.

Dobzhansky, T., Ayala, F. J., Stebbins, G. L., & Valentine, J. W. (1977). Evolution. San Francisco: Freeman. 572 p.

Drouin G, Dover GA (1990) Independent gene evolution in the potato actin gene family demonstrated by phylogenetic procedures for resolving gene conversions and the phylogeny of angiosperm actin genes. J Mol Evol 31: 132–150

Eckardt, N. A. (2014). Genome dominance and interaction at the gene expression level in allohexaploid wheat.

Fang, T., Campbell, K. G., Liu, Z., Chen, X., Wan, A., Li, S., ... & Yan, L. (2011). Stripe rust resistance in the wheat cultivar Jagger is due to Yr17 and a novel resistance gene. Crop Science, 51(6), 2455-2465.

Fisher, R. A. (1930). The genetical theory of natural selection. Oxford: Clarendon Press. 272 p.

Forsberg, S. K., & Carlborg, Ö. (2017). On the relationship between epistasis and genetic variance heterogeneity. Journal of experimental botany, 68(20), 5431-5438.

Frank, S. A. (1999). Population and quantitative genetics of regulatory networks. Journal of theoretical biology, 197(3), 281-294.

Gibson, G. (1996). Epistasis and pleiotropy as natural properties of transcriptional regulation. Theoretical population biology, 49(1), 58-89.

Giles, R. J., & Brown, T. A. (2006). GluDy allele variations in Aegilops tauschii and Triticum aestivum: implications for the origins of hexaploid wheats. Theoretical and applied genetics, 112, 1563-1572.

Haile, J. K., N'Diaye, A., Clarke, F., Clarke, J., Knox, R., Rutkoski, J., ... & Pozniak, C. J. (2018). Genomic selection for grain yield and quality traits in durum wheat. Molecular breeding, 38, 1-18.

Hao, C., Wang, Y., Chao, S., Li, T., Liu, H., Wang, L., & Zhang, X. (2017). The iSelect 9 K SNP analysis revealed polyploidization induced revolutionary changes and intense human selection causing strong haplotype blocks in wheat. Scientific Reports, 7(1), 41247.

Hastings, A., & Harrison, S. (1994). Metapopulation dynamics and genetics. Annual review of Ecology and Systematics, 25(1), 167-188.

He, P., Friebe, B. R., Gill, B. S., & Zhou, J. M. (2003). Allopolyploidy alters gene expression in the highly stable hexaploid wheat. Plant molecular biology, 52, 401-414.

Hedrick, P. W. (2013). Adaptive introgression in animals: examples and comparison to new mutation and standing variation as sources of adaptive variation. Molecular ecology, 22(18), 4606-4618.

Hill, W. G., Goddard, M. E., & Visscher, P. M. (2008). Data and theory point to mainly additive genetic variance for complex traits. PLoS genetics, 4(2), e1000008.

Hittinger, C. T., & Carroll, S. B. (2007). Gene duplication and the adaptive evolution of a classic genetic switch. Nature, 449(7163), 677-681.

Hogg, A. C., Sripo, T., Beecher, B., Martin, J. M., & Giroux, M. J. (2004). Wheat puroindolines interact to form friabilin and control wheat grain hardness. Theoretical and Applied Genetics, 108, 1089-1097.

Holland, J. B. (2001). Epistasis and plant breeding. Plant breeding reviews, 21, 27-92.

Hospital, F. (2005). Selection in backcross programmes. Philosophical Transactions of the Royal Society B: Biological Sciences, 360(1459), 1503-1511.

Hughes, A. L. (1994). The evolution of functionally novel proteins after gene duplication. Proceedings of the Royal Society of London. Series B: Biological Sciences, 256(1346), 119-124.

Humphrey, A. B., Matzinger, D. F., & Cockerham, C. C. (1969). Effects of Random Intercrossing in a Naturally Self-Fertilizing Species, Nicotiana tabacum L. 1. Crop Science, 9(4), 495-497.

Igarashi, Y., Zhang, H., Tan, E., Sekino, M., Yoshitake, K., Kinoshita, S., ... & Asakawa, S. (2018). Whole-genome sequencing of 84 Japanese eels reveals evidence against panmixia and support for sympatric speciation. Genes, 9(10), 474.

Jacobson, A., Lian, L., Zhong, S., & Bernardo, R. (2015). Marker imputation before genomewide selection in biparental maize populations. The Plant Genome, 8(2), plantgenome2014-10.

Jiang N, Bao Z, Zhang X, Eddy SR, Wessler SR (2004) Pack-MULE transposable elements mediate gene evolution in plants. Nature 431: 569–573

Jiang, H., Xu, L., & Gu, Z. (2011). Growth of novel epistatic interactions by gene duplication. Genome Biology and Evolution, 3, 295-301.

Jiang, Y., Schmidt, R. H., Zhao, Y., & Reif, J. C. (2017). A quantitative genetic framework highlights the role of epistatic effects for grain-yield heterosis in bread wheat. Nature genetics, 49(12), 1741-1746.

Juliana, P., Singh, R. P., Poland, J., Mondal, S., Crossa, J., Montesinos-López, O. A., ... & Govindan, V. (2018). Prospects and challenges of applied genomic selection—a new paradigm in breeding for grain yield in bread wheat. The plant genome, 11(3), 180017.

Kauffman, S. A. (1993). The origins of order: Self-organization and selection in evolution. Oxford University Press, USA.

Kimura, M. (1991). The neutral theory of molecular evolution: a review of recent evidence. The Japanese Journal of Genetics, 66(4), 367-386.

Kimura, M., & Ohta, T. (1974). On some principles governing molecular evolution. Proceedings of the National Academy of Sciences, 71(7), 2848-2852.

Kristensen, P. S., ed Jahoor, A., Andersen, J. R., ad Orabi, J., Janss, L., & Jensen, J. (2019a). Multi-trait and trait-assisted genomic prediction of winter wheat quality traits using advanced lines from four breeding cycles. Crop Breeding, Genetics and Genomics, 1(2).

Kristensen, P. S., Jahoor, A., Andersen, J. R., Cericola, F., Orabi, J., Janss, L. L., & Jensen, J. (2018). Genome-wide association studies and comparison of models and cross-validation strategies for genomic prediction of quality traits in advanced winter wheat breeding lines. Frontiers in plant science, 9, 69.

Kristensen, P. S., Jensen, J., Andersen, J. R., Guzmán, C., Orabi, J., & Jahoor, A. (2019b). Genomic prediction and genome-wide association studies of flour yield and alveograph quality traits using advanced winter wheat breeding material. Genes, 10(9), 669.

Lande, R. (1976). Natural selection and random genetic drift in phenotypic evolution. Evolution, 314-334.

Leach, L. J., Belfield, E. J., Jiang, C., Brown, C., Mithani, A., & Harberd, N. P. (2014). Patterns of homoeologous gene expression shown by RNA sequencing in hexaploid bread wheat. BMC genomics, 15(1), 1-19.

Liu, G., Zhao, Y., Gowda, M., Longin, C. F. H., Reif, J. C., & Mette, M. F. (2016). Predicting hybrid performances for quality traits through genomic-assisted approaches in Central European wheat. PLoS One, 11(7), e0158635.

Lozada, D. N., Mason, R. E., Sarinelli, J. M., & Brown-Guedira, G. (2019). Accuracy of genomic selection for grain yield and agronomic traits in soft red winter wheat. BMC genetics, 20, 1-12.

Lu, F., Romay, M. C., Glaubitz, J. C., Bradbury, P. J., Elshire, R. J., Wang, T., ... & Buckler, E. S. (2015). High-resolution genetic mapping of maize pan-genome sequence anchors. Nature communications, 6(1), 1-8.

Lynch, M. (2002). Gene duplication and evolution. Science, 297(5583), 945-947.

Lynch, M., & Force, A. (2000). The probability of duplicate gene preservation by subfunctionalization. Genetics, 154(1), 459-473.

Lynch, M., and Conery, J.S. (2000). The evolutionary fate and consequences of duplicate genes. Science, 290(5494), 1151–1155.

Lynch, M., O'Hely, M., Walsh, B., and Force, A. (2008). The probability of preservation of a newly arisen gene duplicate. Genetics, 181(1), 33–45. doi: 10.1534/genetics.107.074963

Madlung, A. (2013). Polyploidy and its effect on evolutionary success: old questions revisited with new tools. Heredity, 110(2), 99-104.

Meuwissen, T. H., Hayes, B. J., & Goddard, M. (2001). Prediction of total genetic value using genome-wide dense marker maps. genetics, 157(4), 1819-1829.

Musso, G., Costanzo, M., Huangfu, M., Smith, A. M., Paw, J., San Luis, B. J., ... & Zhang, Z. (2008). The extensive and condition-dependent nature of epistasis among whole-genome duplicates in yeast. Genome research, 18(7), 1092-1099.

Nei, M., Rooney, A.P. (2005). Concerted and birth-and-death evolution of multigene families. Annual Review of Genetics, 39(1), 121–152.

Nesbitt, M., & Samuel, D. (1998). Wheat domestication: archaeobotanical evidence. Science, 279(5356), 1431-1431.

Neiman, M., & Linksvayer, T. A. (2006). The conversion of variance and the evolutionary potential of restricted recombination. Heredity, 96(2), 111-121.

Ohno, S. (1970). Evolution by gene duplication. Springer Science & Business Media.

Ohta, T. (1973). Slightly deleterious mutant substitutions in evolution. Nature, 246(5428), 96-98.

Orozco-Ruiz, A. M., Galvan-Tirado, C., Orlov, A. M., Orlova, S. Y., & García-De León, F. J. (2023). Genetic analyses reveal a non-panmictic genetic structure in the sablefish Anoplopoma fimbria in the northern Pacific. ICES Journal of Marine Science, fsad058.

Orr, H. A. (2005). Theories of adaptation: what they do and don't say. Genetica, 123, 3-13.

Panchy, N., Lehti-Shiu, M., & Shiu, S. H. (2016). Evolution of gene duplication in plants. Plant physiology, 171(4), 2294-2316.

Paulsen, G. M., & Shroyer, J. P. (2008). The early history of wheat improvement in the Great Plains. Agronomy Journal, 100, S-70.

Peng, J. H., Sun, D., & Nevo, E. (2011). Domestication evolution, genetics and genomics in wheat. Molecular Breeding, 28, 281-301.

Qian, W., Liao, B. Y., Chang, A. Y. F., & Zhang, J. (2010). Maintenance of duplicate genes and their functional redundancy by reduced expression. Trends in Genetics, 26(10), 425-430.

Quisenberry, K. S. (1974). Let's talk Turkey. Transactions of the Kansas Academy of Science (1903), 77(3), 135-144.

Quisenberry, K. S., & Reitz, L. P. (1974). Turkey wheat: The cornerstone of an empire. Agricultural History, 48(1), 98-110.

Reams, A. B., & Roth, J. R. (2015). Mechanisms of gene duplication and amplification. Cold Spring Harbor perspectives in biology, 7(2), a016592.

Reif, J. C., Maurer, H. P., Korzun, V., Ebmeyer, E., Miedaner, T., & Würschum, T. (2011). Mapping QTLs with main and epistatic effects underlying grain yield and heading time in soft winter wheat. Theoretical and Applied genetics, 123, 283-292.

Salamini, F., Özkan, H., Brandolini, A., Schäfer-Pregl, R., & Martin, W. (2002). Genetics and geography of wild cereal domestication in the near east. Nature Reviews Genetics, 3(6), 429-441.

Salvi, S., Porfiri, O., & Ceccarelli, S. (2013). Nazareno Strampelli, the 'Prophet'of the green revolution. The Journal of Agricultural Science, 151(1), 1-5.

Sanjuán, R., & Elena, S. F. (2006). Epistasis correlates to genomic complexity. Proceedings of the National Academy of Sciences, 103(39), 14402-14405.

Santantonio, N., Jannink, J. L., & Sorrells, M. (2019a). Homeologous epistasis in wheat: the search for an immortal hybrid. Genetics, 211(3), 1105-1122.

Santantonio, N., Jannink, J. L., & Sorrells, M. (2019b). Prediction of subgenome additive and interaction effects in allohexaploid wheat. G3: Genes, Genomes, Genetics, 9(3), 685-698.

Schmidt, J. W. (1974). Turkey wheat: A Mennonite contribution to Great Plains agriculture. Mennonite Life, 30, 67-69.

Sehgal, D., Rosyara, U., Mondal, S., Singh, R., Poland, J., & Dreisigacker, S. (2020). Incorporating genome-wide association mapping results into genomic prediction models for grain yield and yield stability in CIMMYT spring bread wheat. Frontiers in plant science, 11, 197.

Sniegowski, P. D., Gerrish, P. J., Johnson, T., & Shaver, A. (2000). The evolution of mutation rates: separating causes from consequences. Bioessays, 22(12), 1057-1066.

Sthapit, S. R., Ruff, T. M., Hooker, M. A., & See, D. R. (2022). Population structure and genetic diversity of US wheat varieties. The Plant Genome, 15(2), e20196.

Svensson, E., & Calsbeek, R. (Eds.). (2012). The adaptive landscape in evolutionary biology. OUP Oxford.

Taylor, M. A., Wilczek, A. M., Roe, J. L., Welch, S. M., Runcie, D. E., Cooper, M. D., & Schmitt, J. (2019). Large-effect flowering time mutations reveal conditionally adaptive paths

through fitness landscapes in Arabidopsis thaliana. Proceedings of the National Academy of Sciences, 116(36), 17890-17899.

Technow, F., Podlich, D., & Cooper, M. (2021). Back to the future: implications of genetic complexity for the structure of hybrid breeding programs. G3, 11(7), jkab153.

Tranquilli, G., & Dubcovsky, J. (2000). Epistatic interaction between vernalization genes Vrn-Am1 and Vrn-Am2 in diploid wheat. Journal of Heredity, 91(4), 304-306.

Upadhyaya, H. D., & Nigam, S. (1998). Epistasis for vegetative and reproductive traits in peanut. Crop science, 38(1), 44-49.

Wade, M. J., & Goodnight, C. J. (1998). Perspective: the theories of Fisher and Wright in the context of metapopulations: when nature does many small experiments. Evolution, 52(6), 1537-1553.

Walkowiak, S., Gao, L., Monat, C., Haberer, G., Kassa, M. T., Brinton, J., ... & Pozniak, C. J. (2020). Multiple wheat genomes reveal global variation in modern breeding. Nature, 588(7837), 277-283.

Wallace, J. G., Bradbury, P. J., Zhang, N., Gibon, Y., Stitt, M., & Buckler, E. S. (2014). Association mapping across numerous traits reveals patterns of functional variation in maize. PLoS genetics, 10(12), e1004845.

Wallace, J. G., Rodgers-Melnick, E., & Buckler, E. S. (2018). On the road to breeding 4.0: unraveling the good, the bad, and the boring of crop quantitative genomics. Annual review of genetics, 52, 421-444.

Wang, J., van Ginkel, M., Trethowan, R., Ye, G., DeLacy, I., Podlich, D., & Cooper, M. (2004). Simulating the effects of dominance and epistasis on selection response in the CIMMYT Wheat Breeding Program using QuCim. Crop Science, 44(6), 2006-2018.

Wang, X., Zhang, H., Li, Y., Zhang, Z., Li, L., & Liu, B. (2016). Transcriptome asymmetry in synthetic and natural allotetraploid wheats, revealed by RNA-sequencing. New Phytologist, 209(3), 1264-1277.

Watson, A., Hickey, L. T., Christopher, J., Rutkoski, J., Poland, J., & Hayes, B. J. (2019). Multivariate genomic selection and potential of rapid indirect selection with speed breeding in spring wheat. Crop Science, 59(5), 1945-1959.

Whitlock, M. C., Phillips, P. C., Moore, F. B. G., & Tonsor, S. J. (1995). Multiple fitness peaks and epistasis. Annual review of ecology and systematics, 26(1), 601-629.

Wientjes, Y. C., Veerkamp, R. F., & Calus, M. P. (2013). The effect of linkage disequilibrium and family relationships on the reliability of genomic prediction. Genetics, 193(2), 621-631.

William, A. N. G. U. S., Alain, B. O. N. J. E. A. N., & Maarten, V. G. (2011). The world wheat book: a history of wheat breeding (Vol. 2). Lavoisier.

Wright, S. (1932). The roles of mutation, inbreeding, crossbreeding, and selection in evolution.

Wright, S. (1982). Character change, speciation, and the higher taxa. Evolution, 427-443.

Wright, S. (1988). Surfaces of selective value revisited. The American Naturalist, 131(1), 115-123.

Yang, C., Zhao, L., Zhang, H., Yang, Z., Wang, H., Wen, S., ... & Liu, B. (2014). Evolution of physiological responses to salt stress in hexaploid wheat. Proceedings of the National Academy of Sciences, 111(32), 11882-11887.

Zhang, D., Bai, G., Zhu, C., Yu, J., & Carver, B. F. (2010). Genetic diversity, population structure, and linkage disequilibrium in US elite winter wheat. The Plant Genome, 3(2).

Zhang, H., Zhu, B., Qi, B., Gou, X., Dong, Y., Xu, C., ... & Liu, B. (2014). Evolution of the BBAA component of bread wheat during its history at the allohexaploid level. The Plant Cell, 26(7), 2761-2776.

Zhang, L., Ma, B., Wang, L., & Xu, Y. (2003). Greedy method for inferring tandem duplication history. Bioinformatics, 19(12), 1497-1504.

Zhang, Z., Belcram, H., Gornicki, P., Charles, M., Just, J., Huneau, C., ... & Chalhoub, B. (2011). Duplication and partitioning in evolution and function of homoeologous Q loci governing domestication characters in polyploid wheat. Proceedings of the National Academy of Sciences, 108(46), 18737-18742.

Zhao, N., Dong, Q., Nadon, B. D., Ding, X., Wang, X., Dong, Y., ... & Xu, C. (2020). Evolution of homeologous gene expression in polyploid wheat. Genes, 11(12), 1401.

Chapter 2 - Selection signatures of epistasis in breeding families

Abstract

In order to design optimal breeding strategies, knowledge on the genetic architecture underlying traits of interest is critical. The breeder's equation forms the foundation of quantitative genetics and drives important breeding decisions. Oftentimes, however, field observations contradict the expectation that additive gene action underpins quantitative traits and suggest that epistasis could be an important type of gene action. Epistasis is classified into magnitude epistasis, whose effect of alleles varies in scale depending on the genetic background, and sign epistasis, when the effect alleles can be beneficial or detrimental upon variation in the genetic background. Hence, the objective of this study was to expand our understanding of the role of magnitude and sign epistasis in wheat. In the first part of this study, we utilized data from 1376 $F_{5:6}$ experimental lines tested for grain yield in the K-State wheat breeding program in 2017, which were genotyped using genotype-by-sequencing. Relationship matrices based on whole genome maker data were used to estimate additive and epistatic effects. Using a natural and orthogonal interaction approach parameterization, we observed a higher contribution of epistatic than additive effects. The epistatic effects were not statistically independent from the additive effects, though, which was affected by linkage disequilibrium (LD). However, the LD observed could have been partially created from selection of epistatic interactions. Then, we tested the existence of selection signatures of sign epistasis through the analysis of interchromosomal LD in breeding families. A methodology that accounts for population structure and minimizes genetic drift was used to detect interchromosomal regions with abnormally strong LD and contrasting allelic combinations. In total, 19 candidate epistatic interactions were identified, of which 11 were later discarded for presenting allele frequencies that could be attributed to genetic drift. We could not, however, provide sufficient evidence to reject the sign epistasis hypothesis of eight interactions with the current dataset and analysis. The potential existence of sign epistasis in the wheat has important implications to breeding programs, such as a decrease in the effective population size when off-combinations are deleterious, reduction in overall performance of breeding populations when parental lines have contrasting allelic combinations, poorer prediction accuracy in genomic selection models, among others.

Introduction

The primary objective of breeding is to enhance the genetic potential of cultivars, making them better suited and more resilient to a targeted population of environments (Cooper et al., 2002). A comprehensive understanding of the genetic framework governing key agronomic traits enables the formulation of optimal breeding strategies that maximize the likelihood of success. The cornerstone of quantitative genetics lies in the infinitesimal model (Fisher, 1918), which posits that the phenotypic variation of quantitative traits arises from a multitude of segregating Mendelian loci, each exerting minor effects, in combination with environmental influences (Turelli, 2017). The predominant genetic action is additive, with dominance and epistasis generally regarded as having limited significance. While the infinitesimal model has played a pivotal role in advancing plant breeding and facilitating continuous genetic improvements in various crop species, breeding observations contradict the underlying additive hypothesis. In wheat, it is not rare that elite lines are not good parents in breeding crosses despite the accumulation of small-effect positive alleles, suggesting that an alternative gene action may underlie agronomic traits. Given that the effect of dominance is expected to be irrelevant in inbreeding species, epistasis is the potential genetic architecture.

Magnitude epistasis occurs when the effect of an allele varies in magnitude depending on the specific allele or genetic background it interacts with (Weinreich et al., 2005; Poelwijk et al., 2007). As this type of epistasis is a function of the statistical effects of alleles and their interactions, genetic variance components for additive and epistasis can be estimated (Holland, 2001), which have been reported in wheat for different agronomic traits under classical quantitative genetics (Goldringer et al., 1997; Ketata et al., 1976a; Ketata et al., 1976b; Sun et al., 1972; Chapman and McNeal, 1971; Singh and Singh, 1976) or through genome-wide frameworks (Zhang et al., 2008; Sannemann et al., 2018; Santantonio et al., 2019; Kippes et al., 2014; Boeven et al., 2020; Jiang et al., 2017). However, obtaining the true epistatic effects of agronomic traits is challenging. First, additive-by-additive epistasis is converted into additive variance as a function of allele frequencies (Whitlock et al. 1995; Cheverud and Routman, 1996; Wade and Goodnight, 1998; Bernardo, 2020), rendering underestimated epistatic variance components. In addition, linkage disequilibrium (LD) introduces genetic covariation among additive, dominance, and epistatic effects (Zeng et al, 2005), hindering the orthogonal partitioning of genetic effects (Hill and Mäki-Tanila, 2015). These genetic components do not reflect the biological effect of genes (Huang and

Mackay, 2016) and can lead to erroneous conclusions concerning the most suitable breeding strategies (Vitezica et al., 2017). Although LD increases the complexity of obtaining true estimates of epistatic effects, LD may be partially created from natural and artificial selection of epistatic interactions, of which sign epistasis is the easiest to detect.

Sign epistasis occurs when the effect of an allele depends on the allelic state of the interacting gene, exhibiting either a beneficial or deleterious effect (Weinreich et al., 2005; Poelwijk et al., 2007). Allelic combinations, instead of the individual alleles, are under selection. In cases where the interacting genes segregate in a sign epistatic interaction, the alleles are concurrently under positive and negative selection. Hence, the influence of sign epistasis on the genome closely resembles the effects of balancing selection. Balancing selection maintains genetic diversity at the sites under selection and can augment diversity at linked loci (Lewontin and Hubby, 1966; Hudson and Kaplan, 1988; Charlesworth et al., 1997; Takahata and Satta, 1998). The polymorphism flanking the loci under balancing selection can span over large or short regions, depending on the local recombination frequency and the strength of linkage with the alleles under selection (Charlesworth et al., 1997; Wiuf et al. 2004; Charlesworth, 2006). This linkage disequilibrium can be leveraged to detect selection signatures of sign epistasis.

Linkage disequilibrium between closely-linked sites primarily arises due to the effects of random genetic drift or the common ancestry of chromosomal blocks (Koch et al., 2013), and are maintained due to low recombination. Long-range linkage disequilibrium, however, suggests that a countervailing force to recombination maintain strong linkage between distant sites, which could be due to population admixture (Maccaferri et al., 2005; Chao et al., 2010), genetic drift (Koch et al., 2013), artificial selection (Flint-Garcia et al., 2003; Joukhadar et al., 2019), structural variation in chromosomes (Zhao et al., 2022), or epistasis (Lewontin et al., 1960). The situation is expected to be even more pronounced when analyzing interchromosomal linkage disequilibrium, where the independent assortment of chromosomes ensures the recombination of unlinked loci in disequilibrium in every meiotic event. Thus, maintaining disequilibrium between loci in different chromosomes requires a very strong force, which, in breeding programs, can be aided in the face of non-random mating and artificial selection. And artificial selection could be driven by epistatic interactions.

The main hypothesis in this research is that epistasis constitutes an important component of the genetic architecture underlying agronomic traits in wheat. The first objective consisted of

estimating the contribution of magnitude epistatic effects to the overall genetic variation in grain yield in the K-State breeding program. The second objective comprised of testing the existence of loci in abnormally strong interchromosomal linkage disequilibrium. The final objective consisted of testing the hypothesis that selection for sign epistatic interactions created the strong LD between interchromosomal loci while disentangling confounding genetic artifacts.

Material and Methods

Statistical Analysis of Magnitude Epistasis

Plant Material and Genomic Data

The data utilized comprised of 1376 $F_{5:6}$ wheat lines tested for grain yield in 2017. These lines comprise the IPSR (Individual Plant Selection Row) stage of the breeding program, which is the first stage of the breeding pipeline where genotypes are yield tested. Before reaching the IPSR stage, these genotypes were under single plant selection within populations from F_2 to F_5, where the seed of the selected plants was bulked to form the next generation. The selected plants in the F_5 were harvested individually and planted as small plots in the IPSR stage. Hence, this stage comprises the core of the genetic diversity in each breeding cycle, as only visual selection was applied in previous generations.

The $F_{5:6}$ lines were genotyped using the genotype-by-sequencing (GBS) method (Poland et al. 2012). As part of the pipeline of the K-State wheat breeding program, markers with a MAF <0.01, more than 20% missing values and more than 20% of heterozygotes were filtered out, as described in Jarquin et al (2017). The R package 'rrBLUP' (Endelman, 2011) was used for marker imputation, where missing markers were imputed with the mean value among all lines for that marker and resulted in a total of 55,148 SNPs.

Phenotypic Analysis

The experiment was set up in a modified augmented design (Federer and Raghavarao, 1975) with one replication of each experimental line. In this experimental design, whole-plot checks are systematically allocated to every seven columns across all rows, and sub-plot checks are randomly assigned within blocks. As part of the data analysis pipeline of the breeding program,

yield data was adjusted using the row-column design following Lin and Poushinsky (1985) as follows:

$$Y'_{ij(k)} = Y_{ij(k)} - R_i - C_j$$

where $Y_{ij(k)}$ denotes the observed yield value for the *k*th experimental line in the whole-plot of the *i*th row (*i*= 1, …, r) and the *j*th column (*j*= 1, …, c) and $Y'_{ij(k)}$ is the adjusted mean. R_i and C_j were calculated as:

$$R_i = \frac{\sum_{j=1}^{c} X_{ij(A)}}{c} - \bar{X}_A$$

$$C_j = \frac{\sum_{i=1}^{r} X_{ij(A)}}{r} - \bar{X}_A$$

and

$$\bar{X}_A = \frac{\sum_i \sum_j X_{ij(A)}}{rc}$$

where $X_{ij(A)}$ is the observed value of the control plot in the *ij*th whole-plot. The software Agrobase Generation II [Agrobase Generation II 2014, Agronomix, Winnipeg, MB, Canada; https://www.agronomix.com/ (accessed 21 March 2023)] was used to analyze the modified augmented design and obtain best linear unbiased estimates of the experimental lines.

Statistical Models

To test the contribution of epistatic variance relative to the whole genetic variance, two models were compared in this study. The first model consisted of a purely additive model, while the second was extended to accommodate both an additive and additive-by-additive epistatic terms. In both models, the variance was estimated according to the natural and orthogonal interactions approach (NOIA) parametrization (Alvarez-Castro and Carlborg 2007; Vitezica et al. 2017).

Additive Model

The linear model for grain yield performance that includes an additive term is given by:

$$\boldsymbol{y} = \mathbf{1}\mu + \boldsymbol{Zg} + \boldsymbol{\varepsilon}$$

where $\boldsymbol{y}$ is the response vector (adjusted phenotypic data), $\mathbf{1}$ is a vector of ones, μ is the intercept, $\boldsymbol{\varepsilon}$ is a vector of random residuals with $\boldsymbol{\varepsilon} \sim N(0, \boldsymbol{I}\sigma_e^2)$, where σ_e^2 is the residual variance,

$\boldsymbol{Z}$ is a design matrix of random effects, $\boldsymbol{I}$ is an identity matrix, and $\boldsymbol{g}$ is the vector of additive genomic breeding values distributed as $\boldsymbol{g} \sim N(\boldsymbol{0}, \sigma_A^2 \boldsymbol{A})$, where σ_A^2 is the genomic additive genetic variance and the **A** is an additive genomic relationship matrix constructed according to Vitezica et al. (2017) (see Raffo et al. 2022 and Joshi et al. 2020) as:

$$A = \frac{WW'}{tr(WW')/n}$$

where $\boldsymbol{W}$ is the centered and standardized matrix of markers calculated as $w_{ij} = (x_{ij} - 2p_j)$**,** where i (i =1,…,n) denotes the genotypes and j (j=1,…,m) the markers, and p_j is the allele frequency of the reference allele in the population, and the term $tr(\boldsymbol{WW'})/n$ is the trace for the $\boldsymbol{WW'}$ matrix, which standardizes the **A** to a variance equal to one. Note that the additive coefficients are identical to Method 1 of VanRaden (2008), but the scaling is different to relax the assumption of HWE, as demonstrated by Joshi et al. (2020).

Additive and Epistatic Model

The second model, which extends the first by including an additive-by-additive epistatic term was defined as:

$$\boldsymbol{y} = \boldsymbol{1}\mu + \boldsymbol{Zg} + \boldsymbol{Zh} + \boldsymbol{\varepsilon}$$

where $\boldsymbol{h}$ is a vector of additive-by-additive epistatic genomic values with $\boldsymbol{h} \sim N(0, \sigma_H^2 \boldsymbol{H})$, where σ_H^2 is the epistatic variance and $\boldsymbol{H}$ is the additive-by-additive relationship matrix given by:

$$H = \frac{\boldsymbol{A}_G \odot \boldsymbol{A}_G}{tr(\boldsymbol{A}_G \odot \boldsymbol{A}_G)/n}$$

where $tr(\boldsymbol{A}_G \odot \boldsymbol{A}_G)/n$ is the trace for the $\boldsymbol{A}_G \odot \boldsymbol{A}_G$ matrix, which standardizes the additive-by-additive relationship matrix to a variance of 1, and $\odot$ is the Hadamard product between the two matrices.

Variance Components

The estimation of variance components was performed with a Bayesian approach using the BGLR R-package (Perez and de los Campos 2014). The eigenvalue decomposition of the variance-covariance matrices was performed according to Acosta-Pech et al (2017) to speed up computational time and modeled as Bayesian Ridge Regression (BRR). For each model, we used

a total of 50,000 iterations where the first 5,000 were discarded as burn-in. The samples were thinned using one of every 10, resulting in a total of 4,500 samples used to estimate the variance components. In a Bayesian MCMC setting, the estimation of the genetic variance components was calculated using the genetic values of each MCMC sample, as proposed by Sorensen, Fernando, and Gianola (2001) to account for linkage disequilibrium explicitly (see Lehermeier et al., 2017).

Selection Signatures of Sign epistasis

Plant Material and Genomic Data

We utilized historical data from the Kansas State hard red wheat breeding program from 2011 to 2021. The data comprised of experimental lines from the last four stages of yield trials of the breeding pipeline, namely: IPSR (individual plant selection row), PYN (preliminary yield nursery), AYN (advanced yield nursery), and EYN (elite yield nursery, which is the elite yield trial). In the previous four generations in the breeding pipeline, from F_2 to F_5, populations were selected based on their overall merit and single plant selection was imposed within populations. All the lines were genotyped at the $F_{5:6}$ generation (IPSR stage) using genotype-by-sequencing (GBS) (Poland et al. 2012). As part of the genotyping pipeline of the K-State wheat breeding program, markers with a MAF <0.01, more than 20% missing values and more than 20% of heterozygotes were filtered out, as described in Jarquin et al (2017). The R package 'rrBLUP' (Endelman, 2011) was used for marker imputation, where missing markers were imputed with the mean value among all lines for that marker and resulted in a total of 55,148 SNPs. For this study, however, a MAF>0.3 was utilized for the discovery of candidate interactions. The objective was to reduce the number of candidate interactions for screening and to increase the probability of detecting interactions with sign epistasis-like allelic frequencies (intermediate allele frequencies).

Generating Hypothesis on Selection Signatures of Sign Epistasis

The objective of this stage was to explore the potential existence of strong interchromosomal linkage disequilibrium in the breeding program, which could indicate the existence of selection signatures of sign epistasis. To test this hypothesis, experimental lines from the elite yield trial stage of the breeding program were analyzed. These were the best performing lines in the breeding pipeline from 2010 to 2021. A linkage disequilibrium analysis (r^2) was

conducted, and only interchromosomal interactions were considered. The results (data not shown) identified strong interchromosomal LD in the dataset and permitted us to continue testing for the sign epistasis hypothesis.

Minimizing the Influence of Population Structure and Genetic Drift

We selected 40 breeding families for discovering and validating candidate selection signatures indicative of sign epistasis. These were the largest families tested in the first-year yield trial stage of the breeding pipeline, with sizes ranging from 20 to 45 genotypes. To prevent circularity, we designated 25 families as the discovery set and the remaining 15 as the validation set. In the initial phase of our analysis, we conducted a principal component analysis (PCA) for each of the 40 families to identify and exclude any outlier genotypes detected in the two-dimensional plot defined by the first two principal components. This precautionary measure was taken to mitigate the potential introduction of population structure resulting from genotyping or data handling errors.

The balancing selection nature of sign epistasis suggests that segregating alleles might be at intermediate frequencies. Thus, to increase the likelihood of selecting sign epistatic loci, we set the MAF to 0.3. To circumvent the population structure issue, we ran an interchromosomal LD analysis in each families individually and retained all interactions presenting $r^2>0.9$. Although this approach controls population structure, it was highly influenced by genetic drift within families. To address this issue, we combined the marker data of the 25 families, ran another interchromosomal linkage disequilibrium analysis (Figure 2.1), and selected all interchromosomal interactions presenting $r^2>0.8$. Finally, interactions that were selected in both analyses and observed in a minimum of two families were deemed worthy of further investigation.

In parallel, a control interaction was utilized to serve as a null hypothesis. The control interaction consisted of two random single nucleotide polymorphisms (SNPs) with MAF greater than 0.3, randomly selected from chromosomes 1D and 2B. The analytical procedures applied to assess the candidate interactions were also applied in the evaluation of the control interaction.

Figure 2.1 Schematic representation of the interchromosomal linkage disequilibrium analysis. The circles represent the individual analysis of interchromosomal linkage disequilibrium within each population, which controls for the confounding effect of population structure. The square represents the combined dataset of the 25 families used to run the second interchromosomal

linkage disequilibrium analysis, which diminishes the effect of genetic drift in the analysis by averaging out the effect of genetic drift in a single or few populations.

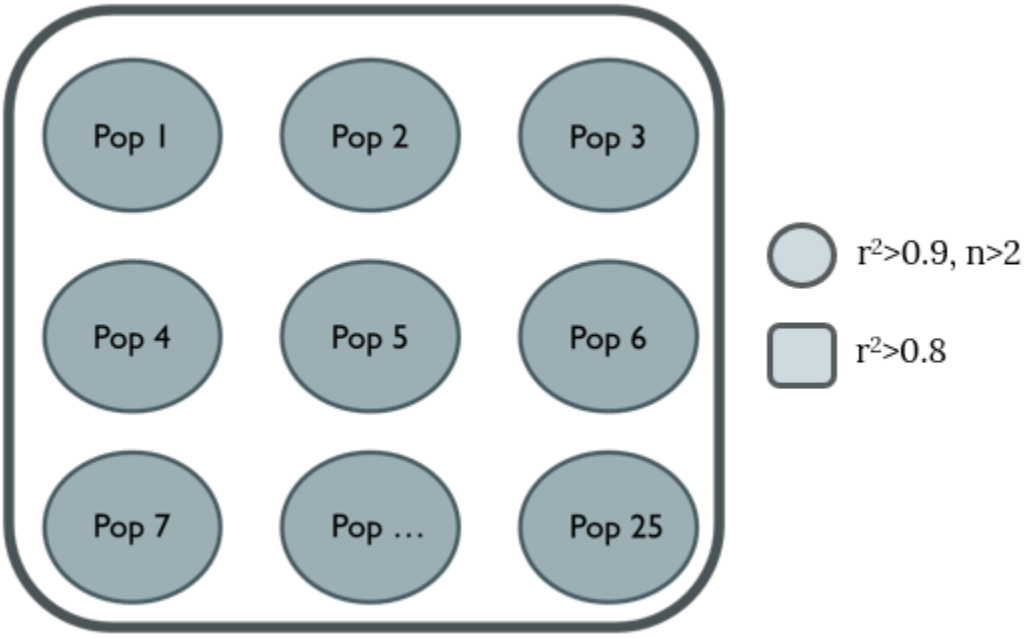

The Balancing Selection Nature of Sign Epistasis and Linkage Blocks

The hitchhiking of linked markers with alleles under balancing selection can generate haplotype blocks. Hence, if a sign epistatic interaction is under selection, besides the characteristic intrachromosomal haplotype block, an "interchromosomal block" is expected to be observed. To investigate this hypothesis in each candidate epistatic interaction, 40 markers flanking the candidate epistatic marker were used to run a linkage disequilibrium analysis using the combined data of the families. With intra and interchromosomal LD values for each interaction, heatmaps of 2D LD plots were constructed to visualize the potential existence of "interchromosomal LD blocks". Even though marker density is not uniform across the wheat genome and recombination hotspots could cause markers under selection to have no visible selection sweep, the presence of "interchromosomal linkage blocks" was examined.

Allele Frequencies

Selection for sign epistasis is expected to change allele frequencies differently than additive selection. Under selection for sign epistasis, the frequency of alleles is expected to be high in

contrasting allelic combinations and low in off-combinations, whereas for additive gene action, one single allelic combination is expected to be in very high allele frequency (Figure 2.2). To empirically test this hypothesis, we computed the allele frequencies for each of the candidate interactions. The two favorable allelic combinations in each candidate interaction were defined as the most frequent allelic combination and its respective opposite allelic combination, while the remaining off-combinations were classified as unfavorable. Since these families were genotyped in the F_6 generation using GBS, heterozygotes loci were still observed.

Figure 2.2 Expected allele frequencies of two genes under sign epistasis gene action (left) and additive gene action (right) in a hypothetical, ideal scenario.

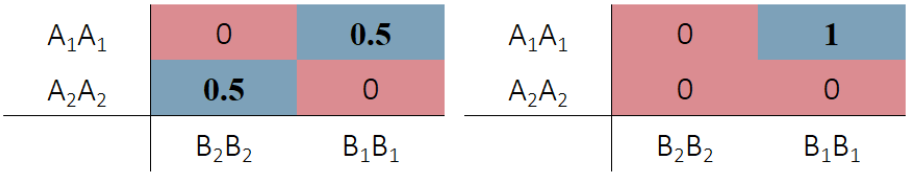

Independent Families and Breeding Program Validation

Conducting statistical inference on results that are not inherently independent from the criteria for selection, as defined by circular analysis, can compromise the validity of statistical tests and the resulting conclusions (Kriegeskorte et al., 2009). Thus, we subsequently utilized 15 distinct validation families to reanalyze the heatmaps of 2D LD plots and the distribution of allele frequencies for each candidate interactions. However, both the discovery and validation families were susceptible to the effects of genetic drift due to their limited effective size.

To disentangle the potential effects of genetic drift, we calculated the allele frequency of the candidate sign epistasis loci in the entire breeding program over a time span of 10 years, as random genetic drift is not expected to create consistent patterns of allelic associations across thousands of experimental lines from different breeding cycles. The breeding program dataset was divided by breeding stages: IPSR (individual plant selection row), PYN (preliminary yield nursery), AYN (advanced yield nursery) and EYN (elite yield nursery). This set of trials represents the sequential stages of yield testing, from the initial stage to elite yield trial in the program. Allele frequencies were calculated for each stage.

Under the influence of sign epistasis selection, we expect that the frequencies of the primary contrasting allelic combinations would progressively increase after each generation of selection, representing a dynamic response to the interaction between alleles. In contrast, for additive selection, we would expect one specific allelic combination to steadily increase in frequency over generations due to its direct additive effect.

Software and Packages

The linkage disequilibrium analysis was performed using the software PLINK (Purcell et al., 2007). The R software packages "factoextra" (Kassambara et al., 2017) and "circlize" (Gu and Gu, 2022), were utilized to perform the principal component analysis and to plot SNPs presenting strong interchromosomal LD, respectively. The package "ggplot2" and "cowplot" were used to plot the heatmap of 2D LD plots and the allele frequency counts (Wickham, 2016; Wilke et al., 2019). Built-in functions in R were used for data management and to calculate allele frequencies.

Results

Estimation of Magnitude Epistatic Variance

The estimated variance components of the parameters in the two models fitted were used to measure the contribution of epistatic variance to the total genetic variance and to contrast it to the additive genetic variance. The NOIA approach in both models led to genetic estimates that when summed with the residual variance are equal to the observed phenotypic variance (Figure 2.3). In the Additive Model the additive genetic variance explained 46% of the observed phenotypic variance. However, in the Additive plus Epistatic Model, additive variance only explains 18% of the observed phenotypic variance while the epistatic variance explains 39%.

The non-orthogonality between additive and epistatic effects complicates any biological interpretation of these variance component estimates. Additive plus Epistatic Model, however, reduces the residual variance and increases the total genetic variance by 28% compared to model 1, demonstrating that the epistatic term captures residual variance that the additive model cannot explain. The Deviance Information Criterion (DIC) for model 1 and 2 was 10455.7 and 10289.1, respectively. Model 2 was the best as lower DIC values indicate a better fit. This means that the inclusion of an epistatic term in the model improves the fit of the data.

Figure 2.3 Estimated posterior means and standard deviations of genetic variance components of the additive model (left) and the additive plus epistatic model (right) fitted. σ_A refers to additive variance, σ_I to additive-by-additive epistatic variance, σ_G to total genetic variance, and σ_R is the residual variance of the model.

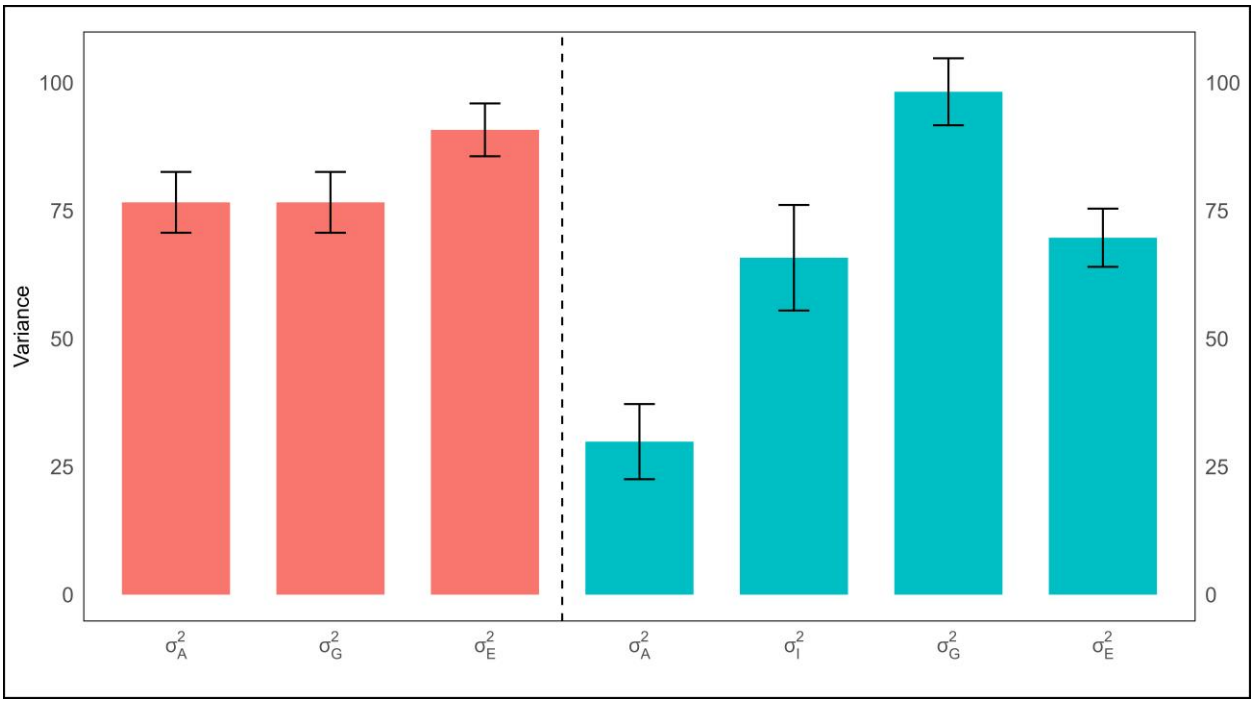

Detection of loci in strong interchromosomal linkage disequilibrium

The goal of the discovery stage was to pinpoint a manageable number of interactions in strong LD while minimizing the likelihood of being artifacts from population structure, genetic drift, or additive selection. By running the interchromosomal LD analysis within each families separately, we controlled the confounding effect of population structure that could arise should the families be analyzed altogether. A direct consequence of this approach is genetic drift, which occurs in any non-infinite population, but whose effects are especially predominant in smaller populations (Charlesworth et al., 2003; Charlesworth, 2009; Kliman et al., 2008; Rothammer et al. 2013). To counterbalance the forces of drift, we combined the data of the 25 families to increase the population size. This approach mitigates the influence of random genetic drift by averaging the strong LD that randomly arose between two markers in a given family with the weak or no LD that is observed between these same markers in the remaining families.

Figure 2.4 Candidate selection signatures of sign epistasis. The inner links represent regions (SNPs) in strong interchromosomal LD following the discovery approach previously described. The outer histogram plots represent the marker density in each chromosome. The outermost bar represents the 7 chromosomes and 3 subgenomes of wheat.

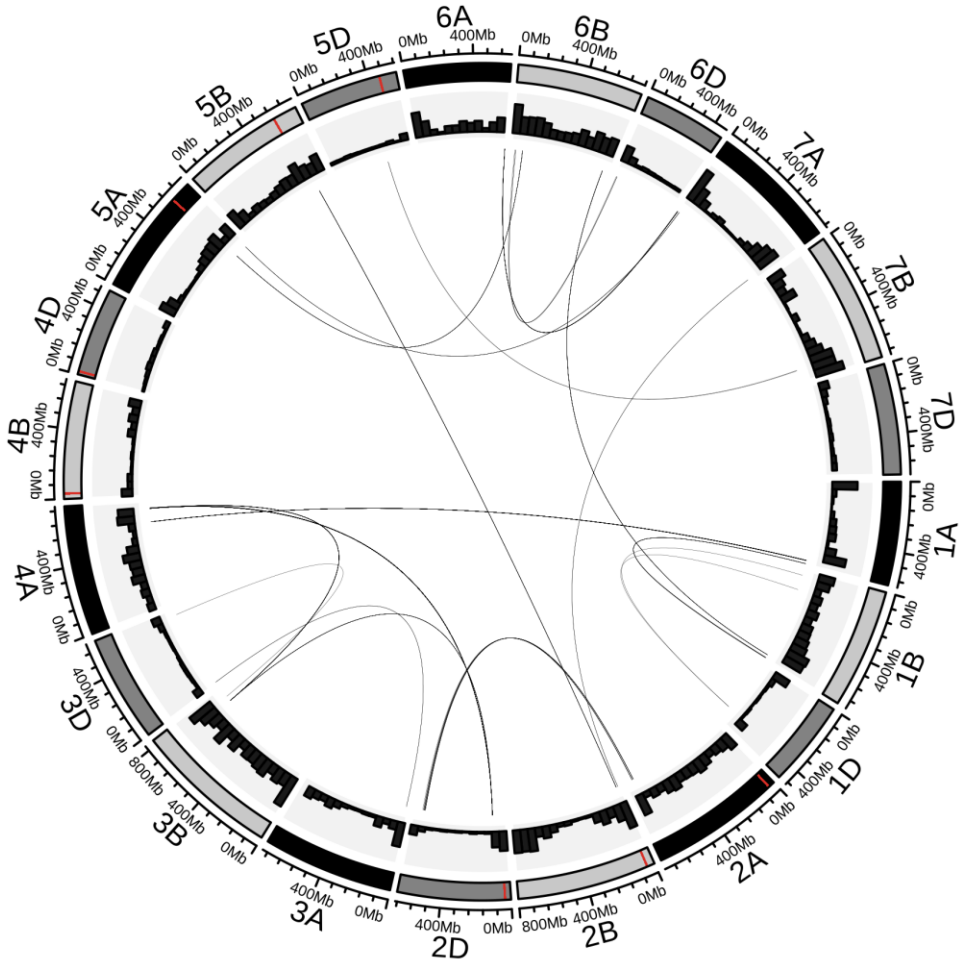

In total, 269 pairwise SNPs, which represents 19 interacting genomic regions, passed the set thresholds, and were considered candidate selection signatures (Figure 2.4). Wheat subgenome B had the most candidate interactions with 15, followed by A and D with 13 and 10, respectively. The chromosomes with the most candidate interactions were 1B and 6B, with four interactions each. In total, 14 out of the 19 interactions were intergenomic, and most involved subgenomes B and D. Subgenome A and B had candidate intragenomic interactions, which were absent in subgenome D.

The interchromosomal LD analysis measures the strength of association between pairs of markers, but three-way interactions can be identified through the combined analysis of three

markers and their mutual interactions. In this study, a candidate of a three-way selection signature was observed, which involves chromosomes 2D, 3B and 4A (Figure 2.4).

The candidate interactions segregated in at least four discovery families, which was crucial to distinguish it from population structure. Any true selection signatures fixed in opposed allelic combinations in different families, but not segregating in any, would not be captured in our analysis as it they would be confounded with population structure.

A total of seven candidate interactions had opposing allelic combinations fixed in different discovery families, suggesting that both combinations could be under equal selection pressure (Table 2.1). A total of 12 interactions were fixed for one candidate favorable allelic combination, yet the opposed allelic combination was observed in segregating families. This could indicate that one combination outperforms the other, potentially due to superior fitness compared to the alternative allelic combination or because it is part of a higher-order interaction that was not detected in our analysis. If both interactions contribute similarly to adaptation, these observations might also indicate unequal initial allele frequencies, where one allelic combination is prevalent in the breeding pool while the other was recently introduced.

Table 2-1 Summary of SNPs in strong interchromosomal linkage disequilibrium – candidate sign epistatic selection signatures.

Chr 1	SNP 1	Chr 2	SNP 2	Allelic Combinations*	Populations Segregating	# Populations fixed	
						Comb 1	Comb 2
1A	565519207	4A	598236311	A/T - C/C	15	8	2
6B	26204619	6Da⁺	14436093	C/A - T/G	17	1	7
5A	598520962	6B	81973027	C/A - G/G	8	1	16
3B	752546905	3D	567747632	C/T - T/A	12	3	10
2B	25458554	5B	600423012	A/A - G/G	15	9	1
2A	713142609	2D	572257428	A/C - G/G	12	1	12
1B	659660316	6B	669333749	A/T - G/C	4	20	1
5D	378314409	7B	661308545	T/A - A/G	4	21	0
2D	91221807	3B	713887174	C/C - A/T	10	15	0
2D	91221807	4A	693794455	C/C - A/T	12	13	0

3B	713887174	4A	693794455	C/C - T/T	10	15	0
5A	687959438	7A	17199897	T/C - C/T	12	13	0
6A	611814110	7A	4327054	T/G - CC	6	19	0
3A	17107524	3D	9881568	A/G - T/A	4	21	0
1A	589041708	1B	683324328	T/A - C/C	12	13	0
1B	146796395	1D	391069881	T/A - G/C	12	13	0
1B	39577562	1D	391069881	A/A - T/C	12	13	0
2B	12856952	7A	704484934	T/C - C/T	5	20	0
6B	33136603	6Db+	19567942	C/G - A/T	4	21	0

* The allelic combinations represents the two opposing allelic combinations under selection. For example, in the first interaction (1A-4A), SNP S1A_565519207 had the alleles A and C, while SNP S4A_598236311 had the alleles T and C. The four allelic combinations were: A/T, A/C, C/T, and C/C, and the two interactions presented in the table represent the candidate favorable interactions from a sign epistasis model of gene action.

+ Two interactions involved the chromosome 6BS and the same region on chromosome 6D. To distinguish between interactions, the letters a and b was added to each of them.

Putative Balancing Selection Associated with Sign Epistasis

The analysis of linkage drag was performed for each of the 19 candidate selection signatures of sign epistasis, and the results for the candidate interaction involving segments of chromosomes 1A and 4A is found in Figure 2.5-B. The depicted results reveal the presence of "interchromosomal linkage blocks" associated with the candidate selection signature. These blocks are primarily attributed to a sizable linkage block located on chromosome 1A and a smaller block situated on chromosome 4A. The control interaction involving segments of chromosomes 1D and 2B did not present any indication of interchromosomal LD blocks (Figure 2.5-B), even though there was strong intrachromosomal linkage disequilibrium in 2B.

The remaining interactions presented “interchromosomal linkage blocks” of variable sizes, as the number of flanking SNPs in strong LD with the candidate interaction was variable (Supplemental Figures A.1-18). For example, candidate interactions 5D-7B, 2D-3B, 1BS-1D and 1BL-1D were in intrachromosomal LD with a few SNPs, resulting in very small “interchromosomal LD blocks”.

Figure 2.5 Allele frequency count (staked bar plots – left column) and heatmaps of 2D LD plots (right column) of the candidate epistatic interaction involving segments of chromosomes **1A** and **4A**. **A** and **B** represents the data from the discovery populations. **C** and **D** displays data from the validation population. **E** and **F** consists of data from the last four stages of the breeding

pipeline. In all plots, the control interaction, randomly selected and involving segments of chromosomes **1B** and **2D**, contrasts the candidate interaction with the null hypothesis. Shades of blue indicate favorable allelic combinations, whereas shades of red indicate unfavorable interactions, as in Figure 2.2 left.

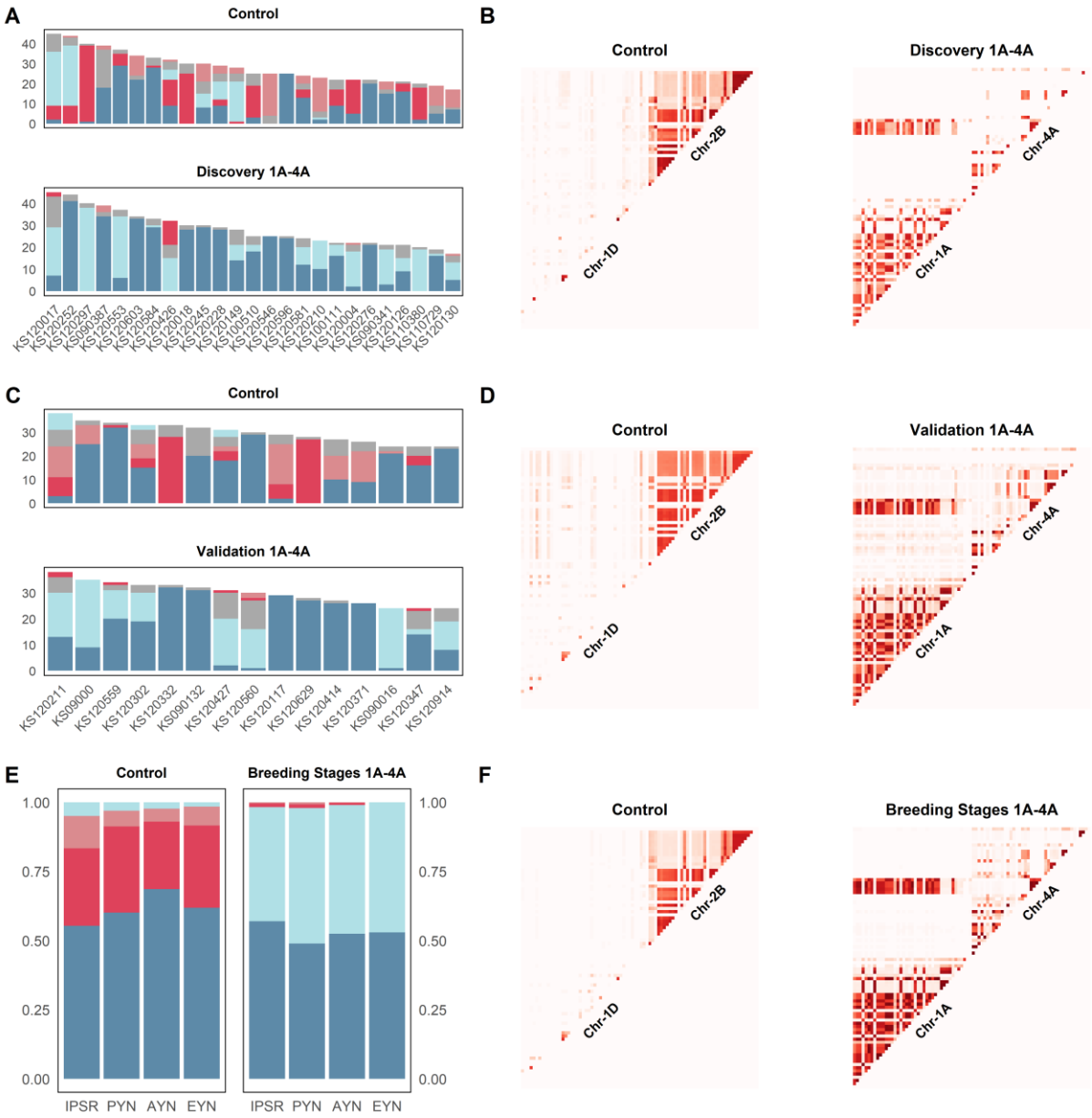

Allelic Frequencies Can Disentangle Epistasis from Genetic Artifacts

The results obtained from the linkage drag analysis align well with population genetics theory concerning balancing selection extended to interactions between two loci. However, two genomic regions under positive or additive selection with similar allelic frequencies can also give

rise to selective sweeps that are in strong interchromosomal linkage disequilibrium (Bamshad and Wooding, 2003). Allele frequencies are anticipated to reflect the adaptive contributions of the allele or allelic combination under selection. These expectations differ between scenarios of sign epistasis and additive gene action. To illustrate this, Figure 2.5-A visually presents the allele frequencies of the candidate loci 1A-4A across each discovery family. The frequency count reveals that many families are nearly fixed for the A/T and C/C allelic combinations (shades of blue). Families segregating for these two alleles exhibited a high frequency of opposing allelic combinations, suggesting that selection is actively favoring both the A/T and C/C allelic combinations. The off-combinations (shades of red) were consistently found at very low frequency in most segregating families. The absence of a predominant allelic combination in high frequency among segregating populations weakens the hypothesis of additive gene action. In contrast, the allele frequencies of the random interaction involving chromosomes 1D and 2B showed a variable predominance of allelic combinations in different families, which is suggestive of genetic drift in unselected loci (Figure 2.5-A).

The candidate interactions 6B-6Da, 3B-3D, 2B-5B had a similar distribution of opposing allelic combinations as interaction 1A-4A (Supplemental Figures A.1-A, A.3-A, A.4-A). Candidate interactions 2A-2D, 2D-3B, 2D-4A, 3B-4A and 5A-7A had a common pattern where one of the contrasting combinations predominated in most families, followed by the opposed combination as the second most frequent, and then by heterozygotes (Supplemental Figures A.5-A, A.8-10-A). However, for interactions 5A-6B, 1B-6B, 5D-7B, 6A-7A, 3A-3D, 1A-1B, 1BL-1D,1BS-1D, 2B-7A and 6B-6Db, the most common allelic combination was found at a very high frequency in most families, and the opposing combination was observed in only a few families (Supplemental Figures A.2-A, A.6-A, A.7-A, A.12-18-A). In all cases, the off-combinations were observed at very low frequencies or absent in many families.

Validation Families Support Sign Epistatic Hypothesis

The results from the discovery families did not provide conclusive evidence to refute the hypothesis that selection signatures of sign epistasis exist within the K-State wheat breeding pool. However, the circular nature of the analysis prevents reaching conclusions (Kriegeskorte et al., 2009). Thus, the heatmap of 2D LD plots and the allele frequency were reanalyzed in the validation families.

The patterns of LD in the validation families remained consistent with the discovery families for interaction 1A-4A, where a long linkage block on chromosome 1A and a small block on 4A created the characteristic "interchromosomal linkage block" (Figure 2.5-D). The frequency of the allelic combinations in the validation families indicates a similar pattern as in the discovery families (Figure 2.5-C). Six populations are fixed for the A/T combination, and the remaining 11 are segregating with both A/T and C/C as the most frequent combinations. The frequency of off-combinations was also very low. The random interaction (1D-2B) exhibited different allelic combinations dominating different families as in the discovery families, showing, once again, the contrast of a candidate sign epistatic interaction to the null hypothesis (random genetic drift).

Interaction 2B-5B (Supplemental Figure A.4-C) had a similar pattern of allelic combination as interaction 1A-4A, where the validation families had an allele frequency pattern similar to the discovery families. The interchromosomal linkage analysis for interactions 1B-6B, and 5D-7B did not present the characteristic "interchromosomal LD block" (Supplemental Figure A.6-D and A.7-D), which could be explained by the very small number of genotypes in only a few families that were not fixed with the major allelic combinations (Supplemental Figure A.6-C and A.7-C). The virtual absence of diversity at the interacting loci aligns with genetic drift predictions, which suggest that if one combination reaches a high frequency, it is possible that the opposing combination randomly fixes in some genotypes, giving rise to LD patterns and allelic configurations characteristic of balancing selection and sign epistasis. Consequently, these two interactions were classified as originating from genetic drift and were discarded.

On the allele frequency analysis, five candidate interactions (Supplemental Figures A.11-C, A.15-C-18C) had at least one family with an off-combination as the most frequent allelic combination. This suggests that these loci are not under selection, as negative selection is expected to reduce the frequency of off-combinations and implies that genetic drift led to the detection of these interactions in the discovery stage. As a consequence, the sign epistasis hypothesis was rejected in these candidate interactions.

The interaction 6B-6Da also had population KS120427 with off-combination as the most common combination, but the abnormal high frequency of heterozygotes, which could have a biological meaning or simply be the consequence of genotyping errors, prevents drawing any definitive conclusions about the interaction (Supplemental Figure A.1C).

Interaction 3B-3D had population KS090132 fixed for an off-combination but presented allelic frequencies matching the sign epistasis hypothesis for the remaining families (Supplemental Figure A.3-C). It is probable that the parental lines of population KS090132 were fixed for the off-combination, which prevents observing the favorable candidate combinations. Thus, this interaction was kept for further analysis.

For the remaining interactions, a consistent pattern emerged where one allelic combination predominated in the majority of families, either fixed or at a very high frequency, while the opposing allelic combination was observed in a few other families at varying frequencies (Supplemental Figures A.2-C, A.5-C, A.8:10-C, A.12:14-C).

Validation in Breeding Program Data Could Eliminate Drift Artifact

To further validate that the 12 non-falsified interactions are not merely the result of genetic drift affecting both discovery and validation families similarly, we extended our investigation of the sign epistasis hypothesis by analyzing the heatmap of 2D LD plots and the allele frequency of genotypes from the yield trial stages of the K-State wheat breeding program over a time span of 10 years. The results depicted in Figure 2.5-F show that the characteristic interchromosomal linkage block is still observed when considering the broader breeding program dataset. Figure 2.5-E reveals that off-combinations were present at low frequencies in the early stages of yield trials (IPSR). As artificial selection progressed across generations, it appeared to be working against the off-combinations, ultimately leading to their complete elimination in the elite yield trials (EYN). Notably, the two opposing allelic combinations, A/T and C/C, exhibited a balanced frequency across all breeding stages analyzed. Just as in the discovery and validation families, the random interaction exhibited allele frequencies that did not align with the predictions of the sign epistasis hypothesis. In summary, the null hypothesis showed that random genetic drift can lead to a high frequency of certain allelic combinations, but it rarely places the opposing allelic combinations as the second most frequent combination within the same families. Moreover, the most common interaction across families displayed substantial volatility. The combination of these two observations suggest that interaction 1A-4A could genuinely be under selection. Consequently, the sign epistasis hypothesis remains unfalsified for this interaction.

The same pattern was observed for interactions 6B-6Da, 5A-6B, and 6A-7A (Supplemental Figure A.1-E, A.2-E, and A.12-E), which exhibited no or very few off-combinations at the EYN

stage. However, the latter two candidate interactions had a very low frequency of the second most common favorable combination across the breeding stages, suggesting that the detection of these interactions may have arisen due to genetic drift. Consequently, the sign epistasis hypothesis for the 5A-6B and 6A-7A interactions was rejected. Similar allele frequencies were observed for interactions 3A-3D and 1A-1B, leading to the rejection of these combinations as well (Supplemental Figure A.13-E and A.14-E).

The six remaining interactions (3B-3D, 2B-5B, 2A-2D, 2D-3B, 2D-4A, and 3B-4A) displayed a high frequency of both opposing allelic combinations but showed minor variations in off-combinations across the breeding stages (Supplemental Figures A.3:5-E, A.8:10-E). Interactions 2B-3D, 2B-5B, and 2A-2D had an average of 94% of genotypes with the two favorable contrasting allelic combinations, at an average ratio of 4:1 between the most common allelic combination and its opposed combination. This may be indicative that the main allelic combination in these interactions either provides better adaptive advantages or is found at higher frequencies in the breeding program due to founder effects.

Discussion

Modeling Magnitude Epistasis Increases Total Genetic Variance

The NOIA parametrization of the variance components did not yield orthogonal partitioning of genetic effects, as reported by Vitezica et al. (2017) and Raffo et al. (2022). Although the estimation of variance components accounted for the covariance between markers (Lehermeier et al., 2017), linkage disequilibrium has been attributed as the cause of non-orthogonality of partitioned genetic effects (Hill and Mäki-Tanila 2015; Zeng et al. 2005). The existence of simultaneous weak mutual linkage disequilibrium between a QTL and two markers was shown to create epistatic variance in a purely additive system (de Los Campos et al., 2019; Schrauf et al. 2020), but this is not expected to be the underlying reason for overestimated epistatic effects, as strong LD is observed in wheat.

The expansion of the additive model to incorporate an epistatic term resulted in an increase in total genetic variance and a reduction in residual variance of the model. This suggests that the epistatic term captures variance that is not accounted for by the additive term, implying that magnitude epistasis may play a role in the genetic architecture of grain yield in wheat. Numerous

studies have lent support to this hypothesis by detecting epistatic gene action underlying agronomic traits in wheat as stem rust (Singh et al., 2013; Rouse et al., 2014), stripe rust (Vazquez et al., 2015), plant height (Zhang et al., 2008; Sannemann et al., 2018; Santantonio et al., 2019), photoperiod response (Shaw et al., 2020), vernalization (Kippes et al., 2014), and grain yield heterosis (Boeven et al., 2020; Jiang et al., 2017), among others. The significance of epistasis in wheat genetics has been long reported, with early studies employing classical mating designs to estimate the relationship between genotypes instead of molecular markers. These studies identified significant epistatic variance influencing important agronomic traits in wheat, including grain yield, heading date, kernels/spikelet, kernel weight, and plant height (Goldringer et al., 1997; Ketata et al., 1976a; Ketata et al., 1976b; Sun et al., 1972; Chapman and McNeal, 1971; Singh and Singh, 1976). Collectively, these findings underscore the importance of epistasis in wheat breeding and genetics.

Despite numerous recurrent studies indicating the presence of epistasis in wheat, the actual contribution of epistatic gene action in the genetic architecture of important agronomic traits is likely underestimated. Additive-by-additive gene action can be converted to additive variance depending on allele frequencies (Whitlock et al. 1995; Cheverud and Routman, 1995; Wade and Goodnight, 1998; Bernardo,2020; Technow et al., 2021), resulting in underestimated epistatic variance. As a consequence, establishing the true significance of epistasis in wheat breeding is virtually impossible. Forsberg and Carlborg (2017) introduced a classification of three types of pairwise epistatic gene actions. Two of these types result in marginal additive and genetic variance heterogeneity effects, and one, sign epistasis, does not yield any marginal additive or variance heterogeneity. This suggests that every study that estimated epistatic variance missed entirely the effects of sign epistasis, introducing an additional layer of complexity when evaluating the role of epistasis in wheat breeding.

Strong Interchromosomal LD Could be Created from Selection for Epistasis

One of the primary objectives of this study was to understand if the linkage disequilibrium that affects the orthogonal partitioning of genetic effects could have been partially created from selection for epistatic interactions. To ensure that lower recombination rates would not interfere with the random assortment of alleles when analyzing long-range LD in chromosomes, we focused on interchromosomal LD. However, other phenomena such as single locus selection driven by

additive gene effects, genetic drift, and population structure could potentially generate interchromosomal LD that are confounded with sign epistasis. To address this challenge, we analyzed interchromosomal LD patterns within and across 25 discovery breeding families, which led to the identification of 19 candidate selections signatures suggestive of sign epistasis. Subsequently, these candidate interactions underwent testing in both validation families and the broader context of the breeding program. This systematic approach was thoughtfully designed to prevent any circular analysis, safeguarding the robustness of our research (Kriegeskorte et al., 2009).

The effect of sign epistasis on the genome resembles balancing selection in each of the genes involved, which is expected to generate nearly complete LD around the selected sites with length varying based on the age of the advantageous polymorphism and the selection intensity (Kreitman and Rienzo, 2004; Tian et al., 2002). Thus, sign epistasis is anticipated to yield what we refer to as an "interchromosomal linkage block", whose dimensions depend on the length of intrachromosomal LD of each of the interacting loci. All interactions presented variable sizes of "interchromosomal LD blocks" in the discovery families, but some were nearly absent in the validation families as a consequence of quasi or completely fixed markers in favorable allelic configurations. The randomly selected pair of markers used as the null hypothesis showed that genetic drift could also create interchromosomal LD, but it vanished with larger population sizes. Interchromosomal LD patterns were also observed in tetraploid wheat (Laido et al 2014) and common beans (Rossi et al., 2009; Diniz et al., 2018), but no conclusions were made regarding the genetic mechanism leading to interchromosomal LD.

In contrast, positive selection of single-locus reduces the polymorphism of linked neutral sites, and results in selective sweeps (Bamshad and Wooding, 2003) characterized by strong linkage disequilibrium. When two such regions present similar allele frequencies, they can give rise to the distinctive "interchromosomal LD block" pattern. To rule out the additive gene action hypothesis, we analyzed the allele frequency of each pairwise interaction in all families. For all interactions analyzed, the pattern of two opposing allelic combinations in high frequencies, while off-combinations exhibited very low frequencies or, in some cases, were entirely absent, was observed in the discovery families. However, subsequent analysis in the validation families and the broader breeding program revealed that 11 out of 19 interactions exhibited clear or suggestive indications of genetic drift, as previously reported in simulation studies by Id-Lahoucine et al.

(2019) and Vilas et al. (2012). In general, the criteria to eliminate interactions that likely arose due to drift was conservative because the allele frequencies were not extremely high nor variable as observed in the null hypothesis interaction.

Strong evidence of genetic drift falsified the hypothesis of sign epistasis for eleven interactions. However, the hypothesis of sign epistasis could not be definitively rejected for the remaining eight interactions based on the current dataset and analysis. Interestingly, a potential three-way epistatic selection signature was identified in this dataset, which is composed of three pairwise interactions that were not individually falsified. Although eight allelic combinations could be expected in three-way interactions, two contrasting allelic configurations represented 98% of the breeding program, as the remaining 2% were off-combinations. We could not find enough evidence to falsify the sign epistasis hypothesis for the three-way interaction.

In this study, we detected candidate selection signatures of sign epistatic interactions in breeding families that underwent four generations of visual single-plant selection as part of the breeding pipeline. Considering the near-complete recovery of opposing allelic combinations, we speculate that artificial selection alone may not be the primary driver of changes in allele frequencies. Instead, it is possible that natural selection, through a nearly lethal response to off-combinations, is responsible for the recovering of opposing allelic combinations, similar to hybrid necrosis in wheat (Tsunewaki, 1960). In rapid cycling of breeding materials (single seed descent), the quantity of seed recovered after three generations of inbreeding is often significantly lower than expected based only on poor levels of germination. This anecdotal evidence aligns with the results of this study, assuming that varying numbers of sign epistatic interactions could be segregating in the SSD populations. As the random assortment of alleles leads off-combinations to fixation, it is possible that plants may experience a severe setback on performance, eventually leading to their premature death or reproductive incapability. Populations with a higher number of segregating epistatic interactions may consequently end up with fewer viable plants by the $F_{2:6}$ generation. As a consequence, the immediate effect of sign epistasis within breeding programs could be a reduction in the effective population size of breeding populations, as genotypes carrying off-combinations are swiftly eliminated. One alternative to overcome this challenge is to constrain the genetic diversity of the breeding program with the fixation of one of the interacting alleles (Hill et al., 2008; Technow et al., 2021). This ensures that the selection pressure is constant for the

alleles in the interacting locus and increases the probability of having one favorable combination fixed.

The presence of superior combinations in opposing allelic states implies that transitioning from one superior combination to another requires two allelic substitutions, passing through a transitional state of inferior performance (Wright, 1988). This suggests the existence of allelic combinations representing high and low adaptation, and, if extended to many gene interactions, it indicates the presence of hills and valleys of adaptation on the fitness landscape, as proposed by the shifting balance theory (Wright, 1932; Holland, 2001 – Figure 1.6). As highlighted by Technow et al. (2021), there are striking similarities between the assumptions of the shifting balance theory and the structure of commercial breeding programs.

In the shifting balance theory, we can assume that a base population ("star" shapes on Figure 1.6) is navigating on different adaptive peaks in the fitness landscape. Once a reduction in effective population size occurs, as through the creation of two hypothetical subpopulations, it maximizes the effects of random genetic drift within each subpopulation, which may lead to the random fixation of alleles. The randomness of genetic drift suggests that different subpopulations may fix different alleles. As a consequence, the subpopulations restrain the area explored in the fitness landscape (squares and circles in Figure 1.6) and will evolve based on these fixed allelic combinations (adaptive peaks). Since genetic drift reduces the genetic diversity by randomly fixing alleles, it also promotes the conversion of nonadditive variance to additive variance and increases the potential of adaptation of the two subpopulation to local environments (Wade and Goodnight, 1998), as less complex genetic systems have higher heritability and respond better to natural selection. By chance, subpopulation "square" was constrained at the base of the global optimum and is expected to evolve past the maximum fitness levels attainable by subpopulation "circles". Therefore, migration from subpopulations with higher fitness to subpopulations with lower fitness permits the transmission of superior allelic combinations to increase the overall adaptation of the species.

Considering the evolution of wheat analogous to the shifting balance theory, the founder wheat germplasm can be considered to be the "star" population. Breeding programs are usually formed from a few founder lines that represent a portion of the total genetic diversity of wheat, fitting the subpopulation definition. Ideally, these could be seen as the "square" and "circles" subpopulations. Genetic drift and selection for local adaptation diminish the genetic complexity to

manageable levels by converting epistatic variance to additive variance, increasing the genetic gain and adaptation. As superior lines or varieties are shared among breeding programs, superior alleles may be transmitted from one breeding pool to another (Wright, 1932; Technow et al., 2021), improving the overall performance of wheat varieties.

The potential presence of sign epistasis within the K-State wheat breeding program suggests that the program may not be limited to a single adaptive peak but could be navigating through various peaks, as in the "star" population (Figure 1.6). This implies the reintroduction of epistatic variance in crosses involving lines from different sub-pools, such as the "squares" and "circles" pools. Even with intense artificial selection applied to segregating populations, the random assortment of alleles will inevitably lead to the fixation of off-combinations in inbred lines. This could reduce the effectiveness of selection and the likelihood of developing superior lines within those populations. An additional issue relates to the utilization of genomic tools, especially genomic selection. The presence of different adaptive peaks can lead to significant variations in the estimation of allelic effects depending on the specific population and its genetic composition. Using the candidate interaction 1A-4A (Figure 2.5) as an example, if the training population has most genotypes with the A allele in locus 1A fixed, then most of the positive additive effects in locus 4A comes from allele T. But, if the validation population has the C allele fixed in locus 1A, then the effects in 4A would be flipped, and prediction of performance would be very poor. Thus, sign epistasis could be one of the underlying reasons, along with linkage phase, as to why relatedness is so crucial in genomic prediction models (Bernardo 2020; Liu et al., 2016; Kristensen et al. 2018)

The second issue concerning rugged fitness landscapes pertains to the more favorable scenario where a breeding program is navigating only one adaptive peak. In such cases, genetic complexity is reduced, heritability is increased, and genomic selection models should theoretically provide more accurate estimates of allelic effects. However, if selection is never counterbalanced, the program may become trapped in a local fitness peak and struggle to reach global peaks (Holland, 2001). Furthermore, introducing foreign germplasm into the breeding pool to enhance diversity can be challenging because it may introduce different epistatic frameworks, which will also reintroduce epistatic variance in the breeding population.

In conclusion, the evidence obtained with the scrutinization of candidate selection signatures of sign epistasis was not sufficient to reject the favorable hypothesis of this study.

Further studies to validate these candidate interactions and empirically test the existence of fitness landscapes in the wheat germplasm pool are underway.

Conclusion

In this study we aimed to extend our understanding of the importance of epistasis in wheat breeding. In our first study, we modeled the contribution of magnitude epistasis in wheat grain yield. The partitioning of genetic variance components into additive and epistatic effects was not orthogonal, but the inclusion of the epistatic term revealed an increase in total genetic variance and a decrease in residual variance. Although the variances estimates are not reliable, the reduction in residual variance may indicate the existence of additive-by-additive epistasis in the genetic architecture of grain yield in the K-State wheat breeding program. In our second study, we aimed to detect interchromosomal selection signatures of sign epistasis. The approach utilized in this study relied on linkage disequilibrium to narrow down the pool of interactions worth investigating and was designed to minimize the impact of population structure and random genetic drift. In total, 19 candidate interactions were identified. Subsequent tests in the validation population and the broader breeding program led to the rejection of the sign epistasis hypothesis for 11 of these interactions, as the patterns observed could be attributed to genetic drift. However, with the current dataset and analysis tested, the sign epistasis hypothesis could not be rejected in eight of the identified interactions. The potential existence of sign epistasis within the wheat germplasm pool has significant implications on breeding strategies.

References

Acosta-Pech, R., Crossa, J., de Los Campos, G., Teyssèdre, S., Claustres, B., Pérez-Elizalde, S., & Pérez-Rodríguez, P. (2017). Genomic models with genotype× environment interaction for predicting hybrid performance: an application in maize hybrids. Theoretical and Applied Genetics, 130, 1431-1440.

Alvarez-Castro JM, Carlborg O (2007) A unified model for functional and statistical epistasis and its application in quantitative trait Loci analysis. Genetics 176:1151–1167.

Bamshad, M., & Wooding, S. P. (2003). Signatures of natural selection in the human genome. Nature Reviews Genetics, 4(2), 99-110.

Bernardo, R. (2020). Breeding for quantitative traits in plants (Vol. 3, p. 422). Woodbury: Stemma press.

Boeven, P. H., Zhao, Y., Thorwarth, P., Liu, F., Maurer, H. P., Gils, M., ... & Würschum, T. (2020). Negative dominance and dominance-by-dominance epistatic effects reduce grain-yield heterosis in wide crosses in wheat. Science advances, 6(24), eaay4897.

Chao, S., Dubcovsky, J., Dvorak, J., Luo, M. C., Baenziger, S. P., Matnyazov, R., ... & Akhunov, E. D. (2010). Population-and genome-specific patterns of linkage disequilibrium and SNP variation in spring and winter wheat (Triticum aestivum L.). BMC genomics, 11(1), 1-17.

Chapman, S. R., & McNeal, F. H. (1971). Gene Action for Yield Components and Plant Height in a Spring Wheat Cross 1. Crop Science, 11(3), 384-386.

Charlesworth, B. (2009). Effective population size and patterns of molecular evolution and variation. Nature Reviews Genetics, 10(3), 195-205.

Charlesworth, B., Charlesworth, D., & Barton, N. H. (2003). The effects of genetic and geographic structure on neutral variation. Annual Review of Ecology, Evolution, and Systematics, 34(1), 99-125.

Charlesworth, B., Nordborg, M., & Charlesworth, D. (1997). The effects of local selection, balanced polymorphism and background selection on equilibrium patterns of genetic diversity in subdivided populations. Genetics Research, 70(2), 155-174.

Charlesworth, D. (2006). Balancing selection and its effects on sequences in nearby genome regions. PLoS genetics, 2(4), e64.

Cheverud, J. M., & Routman, E. J. (1996). Epistasis as a source of increased additive genetic variance at population bottlenecks. Evolution, 50(3), 1042-1051.

Cooper, M., Podlich, D. W., Micallef, K. P., Smith, O. S., Jensen, N. M., Chapman, S. C., & Kruger, N. L. (2002). Complexity, quantitative traits and plant breeding: a role for simulation modelling in the genetic improvement of crops. In Quantitative genetics, genomics and plant breeding (pp. 143-166). Wallingford UK: CABI Publishing.

de Los Campos, G., Sorensen, D. A., & Toro, M. A. (2019). Imperfect linkage disequilibrium generates phantom epistasis (& perils of big data). G3: Genes, Genomes, Genetics, 9(5), 1429-1436.

Diniz, A. L., Giordani, W., Costa, Z. P., Margarido, G. R., Perseguini, J. M. K., Benchimol-Reis, L. L., Chiorato, A.F., Garcia, A.A.F., & Vieira, M. L. C. (2018). Evidence for strong kinship influence on the extent of linkage disequilibrium in cultivated common beans. Genes, 10(1), 5.

Endelman, J. B. (2011). Ridge regression and other kernels for genomic selection with R package rrBLUP. The plant genome, 4(3).

Federer, W. T., & Raghavarao, D. (1975). On augmented designs. Biometrics, 29-35.

Fisher, R. A. (1918). XV.—The correlation between relatives on the supposition of Mendelian inheritance. Earth and Environmental Science Transactions of the Royal Society of Edinburgh, 52(2), 399-433.

Flint-Garcia, S. A., Thornsberry, J. M., & Buckler IV, E. S. (2003). Structure of linkage disequilibrium in plants. Annual review of plant biology, 54(1), 357-374.

Forsberg, S. K., & Carlborg, Ö. (2017). On the relationship between epistasis and genetic variance heterogeneity. Journal of experimental botany, 68(20), 5431-5438.

Goldringer, I., Brabant, P., & Gallais, A. (1997). Estimation of additive and epistatic genetic variances for agronomic traits in a population of doubled-haploid lines of wheat. Heredity, 79(1), 60-71.

Gu, Z., Gu, M. Z., & GlobalOptions, I. (2022). Package ‘circlize’.

He, S., Reif, J. C., Korzun, V., Bothe, R., Ebmeyer, E., & Jiang, Y. (2017). Genome-wide mapping and prediction suggests presence of local epistasis in a vast elite winter wheat populations adapted to Central Europe. Theoretical and Applied Genetics, 130, 635-647.

Hill, W. G., & Mäki-Tanila, A. (2015). Expected influence of linkage disequilibrium on genetic variance caused by dominance and epistasis on quantitative traits. Journal of animal breeding and genetics, 132(2), 176-186.

Holland, J. B. (2001). Epistasis and plant breeding. Plant breeding reviews, 21, 27-92.

Huang, W., & Mackay, T. F. (2016). The genetic architecture of quantitative traits cannot be inferred from variance component analysis. PLoS genetics, 12(11), e1006421.

Hudson, R. R., & Kaplan, N. L. (1988). The coalescent process in models with selection and recombination. Genetics, 120(3), 831-840.

Id-Lahoucine, S., Molina, A., Cánovas, A., & Casellas, J. (2019). Screening for epistatic selection signatures: A simulation study. Scientific reports, 9(1), 1-5.

Jarquín, D., Lemes da Silva, C., Gaynor, R. C., Poland, J., Fritz, A., Howard, R., ... & Crossa, J. (2017). Increasing genomic-enabled prediction accuracy by modeling genotype× environment interactions in Kansas wheat. The plant genome, 10(2), plantgenome2016-12.

Jiang Y, Reif JC (2015) Modeling epistasis in genomic selection. Genetics 201:759–768.

Jiang, Y., Schmidt, R. H., Zhao, Y., & Reif, J. C. (2017). A quantitative genetic framework highlights the role of epistatic effects for grain-yield heterosis in bread wheat. Nature genetics, 49(12), 1741-1746.

Joshi, R., Meuwissen, T. H., Woolliams, J. A., & Gjøen, H. M. (2020). Genomic dissection of maternal, additive and non-additive genetic effects for growth and carcass traits in Nile tilapia. Genetics Selection Evolution, 52(1), 1-13.

Joukhadar, R., Daetwyler, H. D., Gendall, A. R., & Hayden, M. J. (2019). Artificial selection causes significant linkage disequilibrium among multiple unlinked genes in Australian wheat. Evolutionary Applications, 12(8), 1610-1625.

Kassambara, A., & Mundt, F. (2017). Package 'factoextra'. Extract and visualize the results of multivariate data analyses, 76(2).

Ketata, H., Edwards, L. H., & Smith, E. L. (1976b). Inheritance of Eight Agronomic Characters in a Winter Wheat Cross 1. Crop Science, 16(1), 19-22.

Ketata, H., Smith, E. L., Edwards, L. H., & McNew, R. W. (1976a). Detection of Epistatic, Additive, and Dominance Variation in Winter Wheat (Triticum aestivum L. em Thell.) 1. Crop Science, 16(1), 1-4.

Kippes, N., Zhu, J., Chen, A., Vanzetti, L., Lukaszewski, A., Nishida, H., Kato, K., Dvorak, J., & Dubcovsky, J. (2014). Fine mapping and epistatic interactions of the vernalization gene VRN-D4 in hexaploid wheat. Molecular Genetics and Genomics, 289(1), 47-62.

Kliman, R., B. Sheehy & J. Schultz (2008) Genetic drift and effective population size. Nature Education 1(3).

Koch, E., Ristroph, M., & Kirkpatrick, M. (2013). Long range linkage disequilibrium across the human genome. PloS one, 8(12), e80754.

Kreitman, M., & Di Rienzo, A. (2004). Balancing claims for balancing selection. TRENDS in Genetics, 20(7), 300-304.

Kriegeskorte, N., Simmons, W. K., Bellgowan, P. S., & Baker, C. I. (2009). Circular analysis in systems neuroscience: the dangers of double dipping. Nature neuroscience, 12(5), 535-540.

Kristensen, P. S., Jahoor, A., Andersen, J. R., Cericola, F., Orabi, J., Janss, L. L., & Jensen, J. (2018). Genome-wide association studies and comparison of models and cross-validation strategies for genomic prediction of quality traits in advanced winter wheat breeding lines. Frontiers in plant science, 9, 69.

Laido, G., Marone, D., Russo, M. A., Colecchia, S. A., Mastrangelo, A. M., De Vita, P., & Papa, R. (2014). Linkage disequilibrium and genome-wide association mapping in tetraploid wheat (Triticum turgidum L.). PloS one, 9(4), e95211.

Lehermeier, C., de Los Campos, G., Wimmer, V., & Schön, C. C. (2017). Genomic variance estimates: With or without disequilibrium covariances?. Journal of Animal Breeding and Genetics, 134(3), 232-241.

Lewontin, R. C., & Hubby, J. L. (1966). A molecular approach to the study of genic heterozygosity in natural populations. II. Amount of variation and degree of heterozygosity in natural populations of Drosophila pseudoobscura. Genetics, 54(2), 595.

Lewontin, R. C., & Kojima, K. I. (1960). The evolutionary dynamics of complex polymorphisms. Evolution, 458-472.

Lin, C. S., & Poushinsky, G. R. E. G. (1985). A modified augmented design (type 2) for rectangular plots. Canadian journal of plant science, 65(3), 743-749.

Liu, G., Zhao, Y., Gowda, M., Longin, C. F. H., Reif, J. C., & Mette, M. F. (2016). Predicting hybrid performances for quality traits through genomic-assisted approaches in Central European wheat. PLoS One, 11(7), e0158635.

Maccaferri, M., Sanguineti, M. C., Noli, E., & Tuberosa, R. (2005). Population structure and long-range linkage disequilibrium in a durum wheat elite collection. Molecular Breeding, 15, 271-290.

Pérez, P., & de los Campos, G. (2014). BGLR: a statistical package for whole genome regression and prediction. Genetics, 198(2), 483-495.

Poelwijk, F. J., Kiviet, D. J., Weinreich, D. M., & Tans, S. J. (2007). Empirical fitness landscapes reveal accessible evolutionary paths. Nature, 445(7126), 383-386.

Poland JA, Brown PJ, Sorrells ME, Jannink J-L (2012) Development of high-density genetic maps for barley and wheat using a novel two-enzyme genotyping-by-sequencing approach. PLoS ONE 7.

Purcell, S., Neale, B., Todd-Brown, K., Thomas, L., Ferreira, M. A., Bender, D., ... & Sham, P. C. (2007). PLINK: a tool set for whole-genome association and population-based linkage analyses. The American journal of human genetics, 81(3), 559-575.

Raffo, M. A., Sarup, P., Guo, X., Liu, H., Andersen, J. R., Orabi, J., Jahoor, A., & Jensen, J. (2022). Improvement of genomic prediction in advanced wheat breeding lines by including additive-by-additive epistasis. Theoretical and Applied Genetics, 135(3), 965-978.

Rossi, M., Bitocchi, E., Bellucci, E., Nanni, L., Rau, D., Attene, G., & Papa, R. (2009). Linkage disequilibrium and population structure in wild and domesticated populations of Phaseolus vulgaris L. Evolutionary Applications, 2(4), 504-522.

Rothammer, S., Seichter, D., Förster, M., & Medugorac, I. (2013). A genome-wide scan for signatures of differential artificial selection in ten cattle breeds. BMC genomics, 14(1), 1-17.

Rouse, M. N., Talbert, L. E., Singh, D., & Sherman, J. D. (2014). Complementary epistasis involving Sr12 explains adult plant resistance to stem rust in Thatcher wheat (Triticum aestivum L.). Theoretical and Applied Genetics, 127(7), 1549-1559.

Sannemann, W., Lisker, A., Maurer, A., Léon, J., Kazman, E., Cöster, H., Holzapfel, J., Kempf, H., Korzun, V., Ebmeyer, E., & Pillen, K. (2018). Adaptive selection of founder segments and epistatic control of plant height in the MAGIC winter wheat population WM-800. BMC genomics, 19(1), 1-16.

Santantonio, N., Jannink, J. L., & Sorrells, M. (2019). Homeologous epistasis in wheat: the search for an immortal hybrid. Genetics, 211(3), 1105-1122.

Schrauf, M. F., Martini, J. W., Simianer, H., de Los Campos, G., Cantet, R., Freudenthal, J., Korte, A., Munilla, S. (2020). Phantom epistasis in genomic selection: on the predictive ability of epistatic models. G3: Genes, Genomes, Genetics, 10(9), 3137-3145.

Shaw, L. M., Li, C., Woods, D. P., Alvarez, M. A., Lin, H., Lau, M. Y., Chen, A., Dubcovsky, J. (2020). Epistatic interactions between PHOTOPERIOD1, CONSTANS1 and CONSTANS2 modulate the photoperiodic response in wheat. PLoS genetics, 16(7), e1008812.

Singh, A., Knox, R. E., DePauw, R. M., Singh, A. K., Cuthbert, R. D., Campbell, H. L., Singh, D., Bhavani, T., & Clarke, F. (2013). Identification and mapping in spring wheat of genetic factors controlling stem rust resistance and the study of their epistatic interactions across multiple environments. Theoretical and Applied Genetics, 126(8), 1951-1964.

Singh, S., & Singh, R. B. (1976). Triple test cross analysis in two wheat crosses. Heredity, 37(2), 173-177.

Sorensen, D., Fernando, R., & Gianola, D. (2001). Inferring the trajectory of genetic variance in the course of artificial selection. Genetical Research, 77, 83–94.

Sun, P. L. F., Shands, H. L., & Forsberg, R. A. (1972). Inheritance of kernel weight in six spring wheat crosses 1. Crop Science, 12(1), 1-5.

Takahata, N., & Satta, Y. (1998). Footprints of intragenic recombination at HLA loci. Immunogenetics, 47, 430-441.

Technow, F., Podlich, D., & Cooper, M. (2021). Back to the future: implications of genetic complexity for the structure of hybrid breeding programs. G3, 11(7), jkab153.

Tian, D., Araki, H., Stahl, E., Bergelson, J., & Kreitman, M. (2002). Signature of balancing selection in Arabidopsis. Proceedings of the National Academy of Sciences, 99(17), 11525-11530.

Tsunewaki K (1960) Monosomic and conventional analyses in common wheat. III. Lethality. Jpn J Genet 35:71–75

Turelli, M. (2017). Commentary: Fisher's infinitesimal model: A story for the ages. Theoretical population biology, 118, 46-49.

VanRaden, P. M. (2008). Efficient methods to compute genomic predictions. Journal of dairy science, 91(11), 4414-4423.

Vazquez, M. D., Zemetra, R., Peterson, C. J., Chen, X. M., Heesacker, A., & Mundt, C. C. (2015). Multi-location wheat stripe rust QTL analysis: genetic background and epistatic interactions. Theoretical and Applied Genetics, 128(7), 1307-1318.

Vilas, A., Pérez-Figueroa, A., & Caballero, A. (2012). A simulation study on the performance of differentiation-based methods to detect selected loci using linked neutral markers. Journal of Evolutionary Biology, 25(7), 1364-1376.

Vitezica ZG, Legarra A, Toro MA, Varona L (2017) Orthogonal estimates of variances for additive, dominance, and epistatic effects in populations. Genetics 206:1297–1307.

Wade, M. J., & Goodnight, C. J. (1998). Perspective: the theories of Fisher and Wright in the context of metapopulations: when nature does many small experiments. Evolution, 52(6), 1537-1553.

Weinreich, D. M., Watson, R. A., & Chao, L. (2005). Perspective: sign epistasis and genetic costraint on evolutionary trajectories. Evolution, 59(6), 1165-1174.

Whitlock, M. C., Phillips, P. C., Moore, F. B. G., & Tonsor, S. J. (1995). Multiple fitness peaks and epistasis. Annual review of ecology and systematics, 601-629.

Wickham H (2016). ggplot2: Elegant Graphics for Data Analysis. Springer-Verlag New York. ISBN 978-3-319-24277-4, https://ggplot2.tidyverse.org.

Wilke, C. O., Wickham, H., & Wilke, M. C. O. (2019). Package 'cowplot'. Streamlined plot theme and plot annotations for 'ggplot2, 1.

Wiuf, C., Zhao, K., Innan, H., & Nordborg, M. (2004). The probability and chromosomal extent of trans-specific polymorphism. Genetics, 168(4), 2363-2372.

Wright, S. (1932). The roles of mutation, inbreeding, crossbreeding, and selection in evolution.

Wright, S. (1988). Surfaces of selective value revisited. The American Naturalist, 131(1), 115-123.

Zeng, Z. B., Wang, T., & Zou, W. (2005). Modeling quantitative trait loci and interpretation of models. Genetics, 169(3), 1711-1725.

Zhang, K., Tian, J., Zhao, L., & Wang, S. (2008). Mapping QTLs with epistatic effects and QTL× environment interactions for plant height using a doubled haploid population in cultivated wheat. Journal of Genetics and Genomics, 35(2), 119-127.

Zhao, J., Zheng, X., Qiao, L., Yang, C., Wu, B., He, Z., ... & Qi, Z. (2022). Genome-wide association study reveals structural chromosome variations with phenotypic effects in wheat (Triticum aestivum L.). The Plant Journal, 112(6), 1447-1461.

Chapter 3 - Estimation of sub genome additive and epistatic effects in hexaploid wheat for genomic selection

Abstract

The goal of wheat breeding is to develop superior cultivars to the target population of environments. Determining the most promising crosses is an important step to the success of a breeding program. The breeding value of a wheat genotype has traditionally been used to establish its importance as a parental line. With the advent of molecular markers and genomic prediction, genomic estimated breeding values (GEBV) have been used to estimate the additive effects of candidate lines. Differently than the original purpose of breeding values, GEBV are applied to predict the performance of candidate lines instead of its parental value. One caveat is that non-additive genetic effects are ignored. In this study, we are modeling additive and additive-by-additive epistatic effects to better understand the genetic architecture of grain yield in wheat. The data set used is comprised of 3740 $F_{5:6}$ experimental lines tested in the K-State wheat breeding program between 2016 and 2018 that were genotyped using genotype-by-sequencing. We constructed relationship matrices based on the sub genomes marker data to estimate additive and epistatic effects, and contrasted the results with the traditional approach that uses whole genome covariance matrices. Using a natural and orthogonal interaction approach (NOIA) parameterization, we estimated the additive and epistatic variance using sub genome and whole genome models, but the epistatic models failed to achieve orthogonal partitioning of genetic effects. The sub genome additive effects were estimated with a fully additive model and showed that genotypes with the highest whole genome genetic effects usually had a combination of sub genomes with moderately high additive effects. Modeling epistasis only marginally improved the predictive accuracy of genomic selection models. We concluded that the utilization of models that estimate genetic effects by sub genomes holds potential for attributing biological importance to genetic effects, although further studies are required. This approach has the potential to amplify genetic variability across sub genomes and increase the rates of genetic gain.

Introduction

The main goal of wheat breeding is to continuously develop better adapted and more resilient cultivars for a specific target population of environments (Cooper et al,. 2002). A variety of breeding tools are employed to expedite the development of superior cultivars, one of which is genomic selection (GS - Meuwissen et al. 2001). Genomic selection is a method of whole genome prediction that has been applied to different crop species (Crossa et al., 2010; Crossa et al., 2013; Jarquín et al., 2014). The main feature of GS is the genomic estimated breeding values (GEBV) which is the estimated additive effects of an individual calculated using only molecular marker data. Falconer (1981) defined the breeding value of a genotype as the mean performance of its progeny. Hence, the value of GEBV lies in the ability to predict the breeding values of an individual before its progeny is even tested.

In wheat breeding, selection of experimental lines has historically been based on phenotypic selection, which comprises all forms of genetic effects. With the utilization of GS to predict the performance of candidate lines, the contribution of non-additive effects is ignored, and only additive effects are estimated. However, non-additive effects, especially epistasis, can play an important role in the genetic makeup of agronomic traits (Goldringer et al., 1997; Sun et al., 1972; Chapman and McNeal; Zhang et al., 2008; Jiang et al., 2017). Epistasis can be defined as the interaction between alleles of different genes and is normally classified into three categories of two-way interactions: additive-by-additive, additive-by-dominance, and dominance-be-dominance. Higher order interactions involving more than two genes are difficult to capture for being fit later in the model and are normally ignored. In inbred wheat, generations of self-pollination lead to highly homozygous lines where only additive and additive-by-additive genetic effects contributes to the total genetic variance.

Historically, complex mating designs had to be utilized to properly estimate the covariance between relatives and to be powerful enough to estimate epistatic effects, as the triple test cross proposed by Bauman (1959). In current breeding programs, there is an abundance of experimental lines genotyped with phenotypic records, which facilitates the estimation of different genetic effects. With large number of markers covering the genome and quantitative trait loci assumed to have a normal distribution, genome-wide markers can be used to estimate the additive covariance between individuals and used to predict the additive genetic value of individuals (Nejati-Javaremi et al. 1997; VanRaden 2008). To obtain an approximation of the additive -by-additive relationship

matrix between individuals, Henderson (1985) proposed the use of the Hadamard product of the additive covariance matrix based on pedigree information, which was later expanded to accommodate genomic-based additive relationship matrices (Su et al., 2012). Recently, Vitezica et al (2017) expanded the natural and orthogonal interactions approach (NOIA – Alvarez-Castro and Carlborg, 2007) to build genomic relationship matrices using genotypic (not allelic) frequencies and to include genome-wide epistasis, resulting in an orthogonal partitioning of genetic variance components, even if not in Hardy-Weinberg Equilibrium. Thus, it becomes possible utilizing already existing data to estimate and better understand the genetic architecture of important agronomic traits. However, obtaining orthogonal estimates of genetic variance components is challenging under the influence of linkage disequilibrium, as it creates dependency among loci and covariance among genetic effects (Zeng et al, 2005; Hill and Mäki-Tanila 2015).

Common wheat (*Triticum aestivum* spp *aestivum*) is a hexaploid species originated from the interspecific hybridization between tetraploid wheat, *Triticum turgidum* (Sax 1922; Kihara 1924), the source of the AABB genome, and *Aegilops tauschii* (Kihara 1944; McFadden and Sears, 1946), the source of the DD genome. Hexaploid in nature, the three sub genomes of common wheat undergo disomic segregation (Feldman and Levy, 2012) and are normally treated as diploids in breeding programs (Santantonio et al., 2019). For that reason, partitioning whole genome genetic effects into sub genomes opens up the possibility to attribute biological importance to whole genome genetic effects and variance estimates. Attributing additive effects to sub genomes A, B and D could be highly useful in designing breeding strategies that target improving all genomes simultaneously instead of relying on whole genome estimates, which may limit the potential gains. For instance, as the D sub genome in hexaploid wheat only captures a small fraction of the genetic diversity from *Aegilops tauschii* (Zhou et al., 2021), crosses that enhance variation in the D sub genome or that combine lines with high additive effects in A and B sub genomes with lines that present high additive effects in the D sub genome are promising. The success of this approach depends on the extent of intra and inter sub genome epistatic interactions.

The objectives of this study were to: (i) partition the total genetic variance of wheat grain yield into additive and epistatic effects; (ii) partition the whole genome genetic effects into sub genome effects; (iii) measure the improvement in prediction accuracy of genomic selection models when epistasis was modeled.

Material and Methods

Phenotypic Data

The phenotypic data utilized in this study consists of grain yield records for 3740 $F_{5:6}$ wheat lines grown in the early yield trail stage (IPSR) of the K-State hard red winter wheat breeding program between 2016 and 2018. The IPSR is the first stage of the breeding program where selection is based on grain yield data (previous stages consisted of visual single plant selection). This stage represents the core of the genetic diversity of each breeding cycle.

At the time, the experimental design employed in unreplicated trials was a modified augmented design (Federer and Raghavarao, 1975) type II with one replication of each experimental line. However, to minimize the special variability of these large experiments, we employed a two-stage analysis approach (Smith et al., 2001, Welham et al., 2010) and fitted a spatial model to account for patterns associated with environmental factors (Cullis and Gleeson, 1991; Cullis et al., 1998; Smith et al., 2001). Due to the limited number of replications in the trials, an extra step was added to the first-stage analysis. In the first step, the genotypes were fitted as random effects to provide an estimate of the spatial trend, which permits utilizing all genotypes to estimate the trend. In the second step, the genotypes were fitted as fixed effects to calculate the best linear unbiased estimates (BLUEs) necessary for the second-stage analysis (Smith et al., 2001). The statistical model used in both steps of the first-stage analysis was:

$$\boldsymbol{y_{ipq} = \mu + g_i + r_p + c_q + \varepsilon_{ipq}: AR1(R) \otimes AR1(C)}$$

Where $\boldsymbol{y_{ipq}}$ is the grain yield of genotype *i* in row *p* and column *q*; $\boldsymbol{\mu}$ is the intercept; $\boldsymbol{g_i}$ is the effect of genotype; $\boldsymbol{r_p}$ is the random effect of row *p*; $\boldsymbol{c_q}$ is the random effect of column *q*; and $\boldsymbol{\varepsilon_{ipq}}$ is the residual effect modeled using first-order autoregression (AR1) for row *q* and column *q*. As described in the previous paragraph, the initial phase of our analysis employed the first-step approach to calculate variance component estimates for the random spatial terms, while fitting the genotype as a random effect. In the second step, these variance component estimates were utilized to derive the BLUEs for the genotypes and their corresponding weights, where genotype was treated as a fixed effect. The weights were computed as the inverse of the residual variance for each field, multiplied by the replication count for each genotype, and the pooled residual variance across all fields (Cullis et al. 1996).

The second-stage analysis was conducted using the BLUEs and weights for genotypes in order to obtain the BLUPs according to the following statistical model:

$$Z_{ij} \odot w_{ij} = \boldsymbol{\mu} + \boldsymbol{g_i} + \boldsymbol{l_j} + \boldsymbol{gl_{ij}} + \boldsymbol{\varepsilon_{ij}}$$

Where $Z_{ij} \odot w_{ij}$ is the weighted BLUEs from the first-stage analysis for genotype *i* in location *j*; $\boldsymbol{l_j}$ is the effect of location *j*; $\boldsymbol{gl_{ij}}$ is the effect of genotype *i* in location *j*; and $\boldsymbol{\varepsilon_{ij}}$ is the residual. The BLUPs obtained from the second-stage analysis were used in the downstream analyses of this study. The two-stage analysis was conducted using the Echidna Mixed Model Software (Gilmour, 2018).

Genotypic Data

The lines analyzed were in the $F_{5:6}$ generation and underwent genotyping using genotype-by-sequencing (GBS) (Poland et al. 2012). To ensure data quality, markers with a minor allele frequency (MAF) lower than 0.01, more than 20% missing values, and more than 20% heterozygotes were filtered out. The marker imputation process was carried out using the 'rrBLUP' package (Endelman, 2011), resulting in a dataset containing a total of 55,148 single nucleotide polymorphisms (SNPs).

Statistical Models

To assess the contribution of additive and epistatic effects across subgenomes, we employed four models in this study. The first two models comprised of whole genome analysis while the last two partitioned the genetic effects by subgenome, including both additive and epistatic effects. In both sets of models, variance estimation was carried out using the natural and orthogonal interactions approach (NOIA) parametrization, as outlined by Alvarez-Castro and Carlborg (2007) and Vitezica et al. (2017).

Whole Genome Models (WG)

Model 1 – Additive Effects

The linear model for grain yield performance that includes an additive term is given by:

$$y = \mu + Zg + \varepsilon \quad (1)$$

where $\boldsymbol{y}$ is the response vector (adjusted phenotypic data), μ is the intercept, $\boldsymbol{\varepsilon}$ is a vector of random residuals with $\boldsymbol{\varepsilon} \sim N(0, \sigma_e^2)$, where σ_e^2 is the residual variance, $\boldsymbol{Z}$ is a design matrix of random effects and $\boldsymbol{g}$ is the vector of additive genomic breeding values with $\boldsymbol{g} \sim N(\boldsymbol{0}, \sigma_A^2 A)$, where σ_A^2 is the genomic additive genetic variance and the **A** is an additive genomic relationship constructed according to Vitezica et al. (2017) (see Raffo et al. 2022) as:

$$A = \frac{WW'}{tr(WW')/n}$$

where $\boldsymbol{W}$ is the centered and standardized matrix of markers calculated as $w_{ij} = (x_{ij} - 2p_j)$**,** where *i* denotes the genotypes and *j* the markers, and p_j is the allele frequency of the reference allele in the population, and the term $\frac{tr(WW')}{n}$ is the trace for the *WW'* matrix, which standardizes the **A** variance equal to one.

Model 2 - Additive and Epistatic Effects

Following Henderson (1985), the epistatic covariance of individuals can be determined by calculating the Hadamard product of the component covariance matrices. Given that, the second model, which extends the first by including an additive-by-additive epistatic term was defined as:

$$y = \mu + Zg + Zh + \varepsilon \quad (2)$$

where y, μ, Z, g and ε are the same as in the previous model, $\boldsymbol{h}$ is a vector of additive-by-additive epistatic genomic values with $h \sim N(0, \sigma_H^2 H)$, where σ_H^2 is the epistatic variance and H is the additive-by-additive relationship matrix given by:

$$H = \frac{K_G \odot K_G}{tr(K_G \odot K_G)/n}$$

where $tr(K_G \odot K_G)/n$ is the trace for the $K_G \odot K_G$ matrix, which standardizes the additive-by-additive relationship matrix to a variance of 1, and $\odot$ is the Hadamard product between the two matrices.

Sub Genome Models

Model 3 – Additive Effects

As described in Santantonio et al (2019), we can decompose G_j into individual additive effects for each subgenome, such that $G_j = A_j + B_j + D_j$. The following model is then obtained:

$$y = \mu + Z_A g_A + Z_B g_B + Z_D g_D + \varepsilon \quad (3)$$

The decomposition of the whole genome into subgenome permits each subgenome to have its own additive genetic variance and covariance among individuals, such that $\boldsymbol{g}_A \sim N(0, \sigma_A^2 A)$, $\boldsymbol{g}_B \sim N(0, \sigma_B^2 B)$ and $\boldsymbol{g}_D \sim N(0, \sigma_D^2 D)$. The matrices A, B, and D are the realized additive genetic variance-covariance for each subgenome and are calculated following the previously described approach for the whole genome additive variance-covariance matrix.

Model 4 – Additive and Epistatic Effects

As for the whole genome additive term, the whole genome epistatic term, H, can also be decomposed into intra and inter subgenome epistatic interactions, such that $H_i = AA_i + BB_i + DD_i + AB_i + AD_i + BD_i$. The new additive plus epistatic subgenome model is given by:

$$y = \mu + Z_A g_A + Z_B g_B + Z_D g_D + Z_{AA} g_{AA} + Z_{BB} g_{BB} + Z_{DD} g_{DD} + Z_{AB} g_{AB} + Z_{AD} g_{AD} + Z_{BD} g_{BD} + \varepsilon \quad (4)$$

The decomposition of the whole genome epistatic term into subgenome terms permits each pair of subgenome to have their own additive-by-additive genetic variance-covariance among

individuals, such that $\boldsymbol{g_{AA}} \sim N(0, \sigma^2_{AA} AA)$, $\boldsymbol{g_{BB}} \sim N(0, \sigma^2_{BB} BB)$ *and* $\boldsymbol{g_{DD}} \sim N(0, \sigma^2_{DD} DD)$, and $\boldsymbol{g_{AB}} \sim N(0, \sigma^2_{AB} AB)$, $\boldsymbol{g_{AD}} \sim N(0, \sigma^2_{AD} AD)$ and $\boldsymbol{g_{BD}} \sim N(0, \sigma^2_{BD} BD)$. The matrices AA, BB, and DD, and AB, AD, and BD, are the realized intra and inter subgenome epistatic variance-covariance matrices and are calculated following the previously described approach for the whole genome additive-by-additive variance-covariance matrix.

Variance Components and Heritability

The estimation of variance components was conducted using a Bayesian approach implemented in the BGLR R-package (Pérez and de los Campos, 2014). To enhance computational efficiency, we employed the eigenvalue decomposition of the variance-covariance matrices following the method described by Acosta-Pech et al. (2017) and modeled it as Bayesian Ridge Regression (BRR). For each model, a total of 50,000 iterations were performed, with the first 5,000 iterations discarded as burn-in. Subsequently, the remaining iterations were thinned by selecting one out of every ten samples, resulting in 4,500 samples used for estimating the variance components. In a Bayesian Markov Chain Monte Carlo (MCMC) framework, the genetic variance components were calculated based on the genetic values derived from each MCMC sample, as proposed by Sorensen, Fernando, and Gianola (2001) (refer to Lehermeier et al., 2017 for details).

The broad-sense heritability was calculated according to the following equation:

$$H^2 = \frac{\sigma_g}{\sigma_p}$$

where σ_g is the total genetic variance and σ_p is the phenotypic variance. For the fully additive models (1 and 3), the broad-sense heritability only utilizes additive variance, so it is actually the narrow-sense heritability.

Genomic prediction

In order to test the predictive ability of models and the variation in prediction accuracy, a five-fold cross validation approach with 10 replicates was utilized. In each replicate, the set of 3740 lines was randomly divided into five groups, in which four were used to train the model and the remaining was used to predict genetic values. With that structure, all four models were fitted, and the predicted genetic values of each line was recorded. The prediction of the five folds was correlated with the phenotypic value, and the resulting value was the prediction accuracy of the

model. The correlation of the predicted genetic values to phenotypic values permitted the comparison in accuracy of the different models fitted.

Prediction Accuracy Comparison Between Models

To test if statistical significance was observed between the prediction accuracy of the different models fitted, we utilized Tukey's honestly significant difference test implemented in the 'agricolae' package on R (de Mendiburu, 2019).

Results

Variance Components and Heritability

Whole Genome Models

The estimated posterior means of Model 1 had additive genetic effects accounting for 26.7% of the observed phenotypic variance for wheat grain yield (Figure 3.1). However, in Model 2, the contribution of additive variance decreased to only 11%, while the influence of epistatic variance became prominent, explaining 28.9% of the observed phenotypic variance. This substantial reduction in additive variance upon the inclusion of the epistatic term suggests a lack of orthogonality between these two genetic effects. Similar results were also obtained by Raffo et al. (2022), where the inclusion of an epistatic term captured much of the estimated line and additive variance.

By incorporating an epistatic term into Model 2, the total genetic variance increased, and the residual variance decreased when compared to Model 1. This suggests that the epistatic term, although not orthogonal, captures variance that the additive term alone cannot explain. Consequently, the broad-sense heritability of Model 2 (0.39) exceeded that of the fully additive model (0.27 – see Supplemental Table B.1). Although Raffo et al. (2022) also observed a lack of orthogonality between the genetic effects, their model with an epistatic term did not lead to an improvement in broad-sense heritability. Interestingly, although the addition of the epistatic term did not yield orthogonal partitioning of genetic effects, the correlation between additive and epistatic terms was virtually zero (Supplemental Table B.5).

The deviance information criteria value was smaller for Model 2 than for Model 1 (Supplemental Table B.1), suggesting that the incorporation of an epistatic term capture epistatic interactions present in the dataset and provide a better fit of data.

Figure 3.1 Estimated posterior means and standard deviations of genetic variance components of Model 1 (left of vertical dotted line) and Model 2 (right of vertical dotted line). σ_A refers to additive variance, σ_I to additive-by-additive epistatic variance, σ_G to total genetic variance, and σ_E is the residual variance of the model.

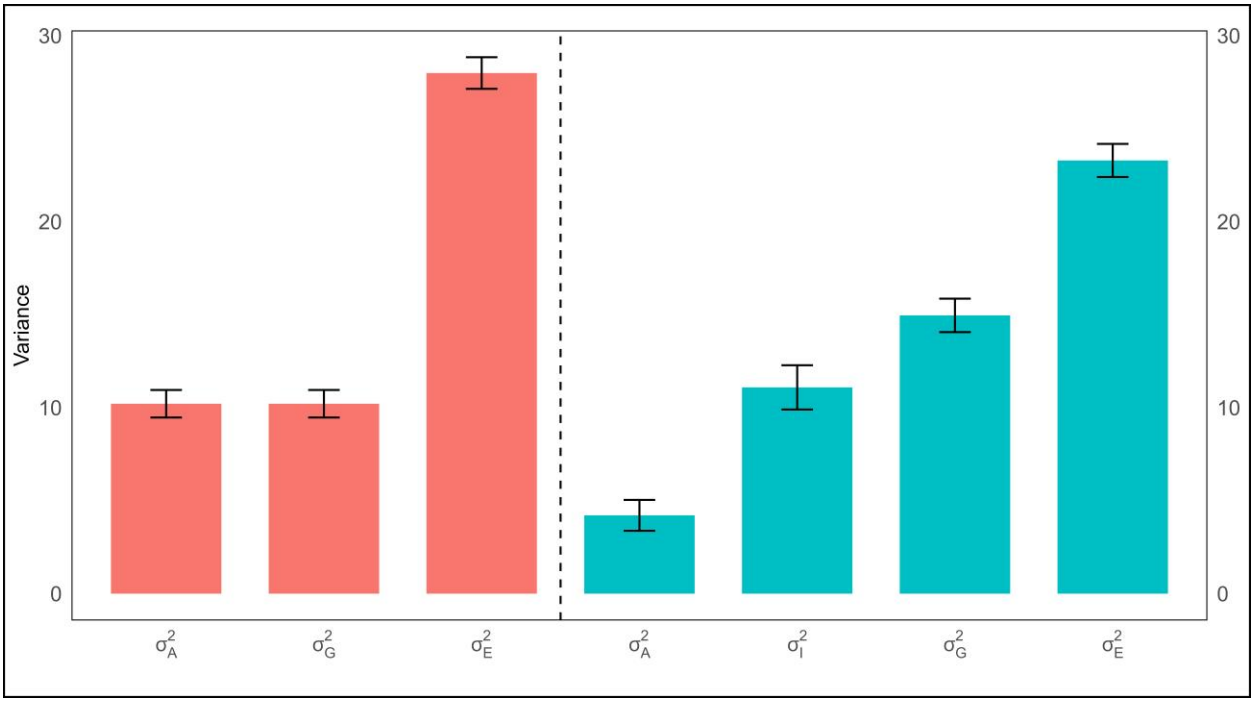

Sub Genome Models

The sum of additive genetic variance from the additive subgenome Model 3 was similar to the additive whole genome Model 1, which was expected since breaking the genome into subgenomes should not imply different additive effects (Figure 3.1 and 3.2). For the sub genome additive plus epistatic Model 4, the sum of the additive variance in the sub genome epistatic model added to 4.58 and the epistatic variance was 12.74, indicating a slight increase in epistatic variance while roughly maintaining the additive variance compared to Model 2. The sum of the additive and epistatic variance did not match the observed total genotypic variance because of a negative covariance of 0.99 between the terms in the Model 4. A negative correlation of 0.98 was also observed between the additive terms in Model 3.

In the additive subgenome Model 3, the A subgenome had the greatest amount of additive variance, followed by the D and B subgenomes (Figure 3.2). Upon introducing intra and inter subgenome interaction terms, the amount of additive variance associated with each subgenome decreased, and the D subgenome displayed the highest additive effects among the three subgenomes. The amount of additive variance generally decreased in epistatic models compared to strictly additive models in the study conducted by Santantonio et al. (2019). In their study, the D sub genome presented very small additive variance for grain yield in the epistatic model and the epistatic variance from interactions between sub genomes was very close to zero, which greatly differed from our findings.

As with Model 2, the addition of intra and inter subgenome epistatic terms resulted in non-orthogonal partitioning of genetic effects. Likewise, the correlation within and between additive and epistatic terms was nearly zero in all instances (Supplemental Table B.6).

Figure 3.2 Estimated posterior means and standard deviations of genetic variance components of Model 3 (left of vertical dotted line) and Model 4 (right of vertical dotted line). σ_A refers to additive variance in subgenome A, σ_B to subgenome B and σ_D to D. Intra and inter subgenomes additive-by-additive epistatic variance are depicted by σ_{AA}, σ_{BB}, σ_{DD}, and σ_{AB}, σ_{AD}, σ_{BD}, respectively. σ_G to total genetic variance, and σ_E is the residual variance of the model.

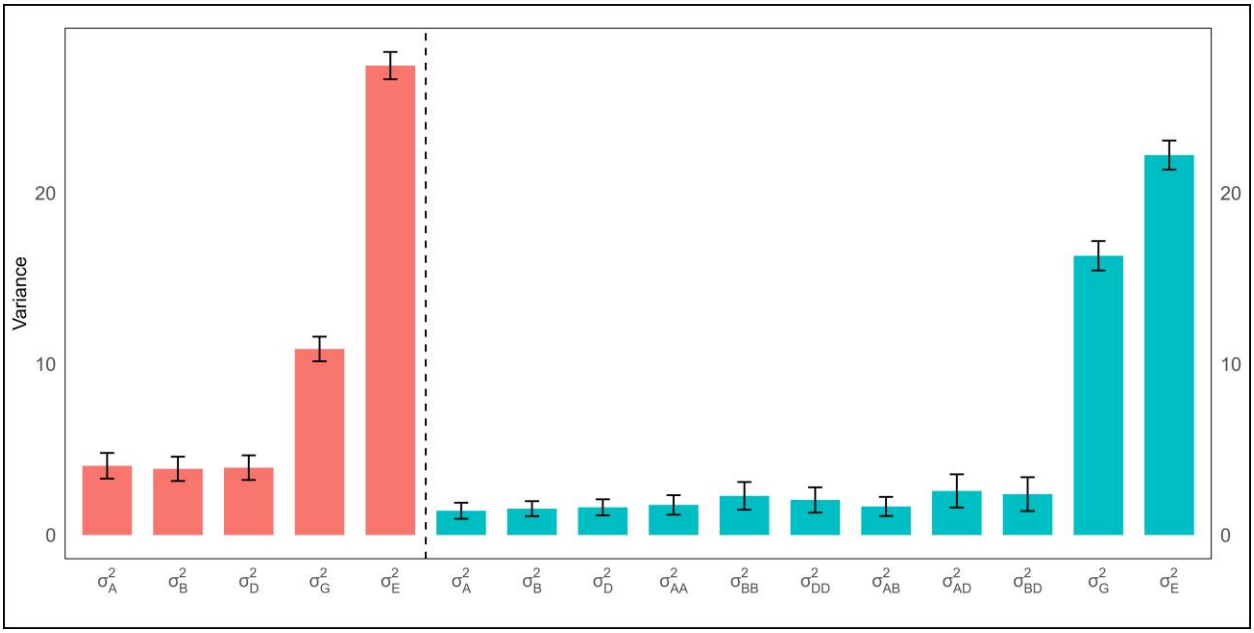

The higher total genetic variance associated with the Model 4 increased the broad sense heritability compared to whole genome models (Models 1 and 2 - Supplemental Table B.2). In

addition, the deviance information criteria values were smaller than the whole genome models, indicating a better fit of data with partitioned sub genomes. Santantonio et al. (2019) used the Akaike's Information Criterion (AIC) to compare whole genome and sub genome models and found that whole genome models tended to have the lowest values for most traits studied.

Sub Genome Additive Effects

The correlation between whole genome and subgenomes additive effects is found in Figure 3.3. The smallest correlation was observed between the effects of sub genome D and the whole genome effects (0.61 – Supplemental Table B.3), while the correlation for sub genome A and B with the whole genome were higher (0.72 and 0.69, respectively). The correlation between sub genomes was very low. Interestingly, when analyzing the sub genome additive effects from Model 4, which models epistasis, the correlation between sub genome and the whole genome as well as between sub genomes decreased, except for the correlation between sub genomes B and D. Although the correlation between sub genomes and whole genome varied, all three subgenomes presented similar maximum and minimum additive effects, and standard deviations (Supplemental Table B.4).

In total, 98 lines were found above the 95-percentile threshold for both whole and sub genome A additive effects (black dots). Of those, 28 and 22 genotypes were also above the 95-percentile threshold for sub genomes B and D, respectively. In sub genome B and D, 75 and 57 lines were found above the 95-percentile threshold for both sub genomes and whole genome additive effects, with 22 lines above this threshold in both sub genomes B and D. In total, 11 genotypes were above the 95-percentile for all sub genomes, 9 of which were sister lines. Hence, in general, the genotypes with the highest whole genome effects did not present the highest additive effects in more than one sub genome.

Of the top-100 genotypes with highest whole genome additive effects, 48 were advanced to the preliminary yield trials (PYT). Among these, 6 were selected for the advanced yield trials (AYT), but none of these genotypes made it to the elite trials (EYT). The possible reason to discard genotypes with high whole genome additive effects could be linked to other traits not considered in this prediction model, like disease resistance, cycle, and lodging. For instance, from this pool of 3740 genotypes evaluated in three breeding cycles, only eight reached the EYT stage, five of which were above the top-90 percentile.

Figure 3.3 Plot of whole genome additive effects by sub genome additive effects for grain yield in wheat. The dotted lines indicates the 95 percentile for whole or subgenome additive effects. The solid black lines is the correlation between whole genome and sub genome effects.

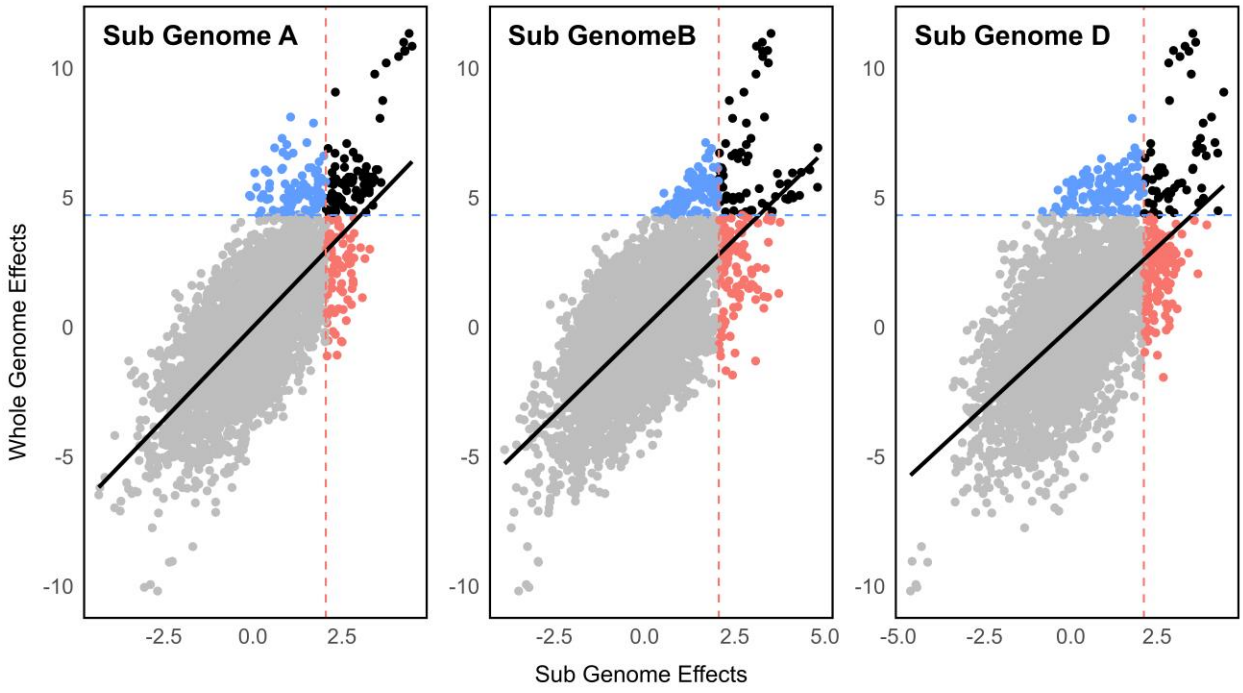

Genomic Predictive Ability

The prediction accuracy between the genomic estimated breeding values and the phenotypic values was evaluated using the five-fold cross validation method (Figure 3.4). For both whole and sub genome models, the inclusion of epistatic genetic effects marginally improved the prediction accuracy compared to fully additive models. On the other hand, partitioning the whole genome effects into sub genomes did not improve the accuracy of predictions. No significant difference was observed among the different models in predictive ability.

The correlation between the genetic values of the four models fitted showed very high correlations (Supplemental Table B.7), possibly because of the marginal contribution of epistasis to increase prediction accuracy. Similarly, the correlation between the genomic estimated breeding values (additive effects only) indicated a smaller correlation between the purely additive and the additive plus epistatic models. Yet, all the correlations were very high (Supplemental Table B.7).

Figure 3.4 Bar plot of predictive abilities of additive whole (left) and sub (right) genome models with the inclusion of an epistatic term or not using a five-fold cross validation approach with 10 replications. Same letters indicate no statistical difference with the Tukey honestly significant difference analysis.

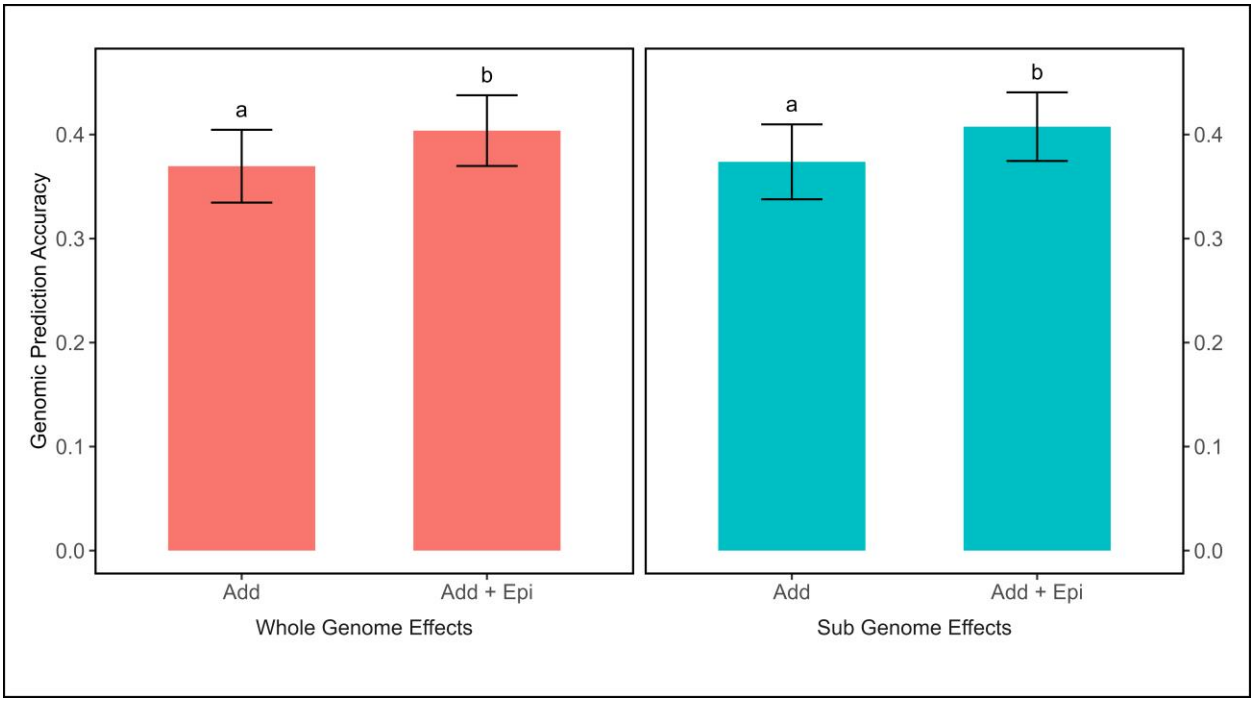

Discussion

Modeling Epistasis Improves Total Genetic Variance and Broad Sense Heritability

The partitioning of genetic variance using the NOIA parameterization resulted in non-orthogonal estimates of genetic effects in both whole and sub genome models, as the additive variance in Model 1 and 3 diminished when epistasis was modeled (Models 2 and 4). In the whole genome model, the inclusion of epistatic effects reduced the additive variance by 58% while for the sub genome model the reduction was in the order of 61%. Raffo et al (2022) also reported non-orthogonality of genetic effects for wheat grain yield, as the inclusion of epistatic effects led to a reduction in 58% of the additive variance in the fully additive model. The non-orthogonal partitioning of genetic effects could be attributed to linkage disequilibrium, which introduces nonindependence between loci (Vitezica et al. 2017). Under the presence of linkage disequilibrium, covariance between genetic effects can be introduced and the partitioning of genetic effects is not possible (Hill and Mäki-Tanila 2015; Zeng et al. 2005). In the simulated and

experimental studies of Vitezica et al. (2017) and Raffo et al (2022), the lack of orthogonality was evidenced through a high correlation between additive and epistatic variance component estimates. To our surprise, near zero correlations was observed between additive and epistatic variance estimates in either whole genome or sub genome models (Supplemental Table B.5 and B.6).

An alternative explanation for the high epistatic variance relative to additive variance could relate to phantom epistasis, a phenomenon that creates epistatic variance from a purely additive gene effect as a consequence of weak linkage disequilibrium between an additive QTL and two markers (de Los Campos et al., 2019; Schrauf et al. 2020). This scenario, however, is not expected to overestimate epistatic effects in this study because strong LD is commonly observed in wheat and in breeding crops in general.

Sub Genome Additive Effects as a Tool for Designing Promising Crosses

The partitioning of additive and epistatic effects was not orthogonal and did not allow disentangling the underlying genetic architecture of grain yield in wheat. However, the estimation of additive effects in each subgenome is a potential approach to attribute biological importance to genetic effects normally assigned to the whole genome (Santantonio et al 2019). For instance, the most common approach in selecting parental lines to develop breeding populations relies on breeding values or phenotypic data, which are based on whole genome effects. In this dataset, the genotypes with the highest amount of whole genome additive effects generally did not have the highest additive effect for more than one sub genome. Similar results were reported in Santantonio et al (2019), which, due to the low correlation between all subgenomes, suggested the possibility of making breeding crosses targeting genotypes with the highest additive effects in each sub genome. In that sense, assuming that the partitioning of additive effects is accurate, this approach opens up the opportunity to design crosses that combine genotypes with the best additive effects on each sub genome, producing a theoretical maximum whole genome effects of 13.71, which is 21% higher than the observed highest whole genome effect (11.34).

The success of this approach will be tightly linked to the interplay within and between subgenomes, that is, the underlying epistatic genetic effects. The potential existence of epistasis observed in this study suggests that it could play a role in determining whole genome genetic effects, but we cannot assert the extent of that influence because of the lack of orthogonality. However, other studies have shown the existence of epistasis in wheat affecting different traits,

such as stem rust (Singh et al., 2013; Rouse et al., 2014), stripe rust (Vazquez et al., 2015), plant height (Zhang et al., 2008; Sannemann et al., 2018), photoperiod response (Shaw et al., 2020), vernalization (Kippes et al., 2014), and grain yield heterosis (Boeven et al., 2020; Jiang et al., 2017). In this study, the low correlation between sub genome additive effects could suggest some level of independence between sub genomes. However, the reduction in the correlation between sub genome additive effects in Model 4 and whole genome effects could indicate that epistasis may be important. If epistasis is an important type of gene action underlying grain yield, we might not be able to exploit the full potential of estimating sub genome additive effects, although this strategy could still be applied at the expenses of having diminished success. For a better understanding of its application and usefulness in breeding programs, more studies are needed.

In this panel, all the sub genomes presented similar additive effects for grain yield in wheat, which is surprising for sub genome D. The D sub genome in wheat is known for having limited genetic variability due to the restricted gene flow during the hybridization event that created hexaploid wheat. However, the high additive effect and variance observed in this panel could be attributed to major QTLs conferring resistance to wheat streak mosaic virus (WSM). In 2017, there was a severe WSM infection in the experimental farm, but a considerable proportion of the genotypes evaluated had in their pedigree parental lines that carried the *Wsm1* and *Wsm2* genes. *Wsm1* is a translocation from *Agropyron intermedium* (Gill et al., 1995; Friebe et al., 1996) and is located on chromosome 4D, while *Wsm2* was discovered in a wheat breeding line CO960293-2 (Haley et al., 2002) and is located on chromosome 3B (Lu et al., 2011), and both confer resistance to WSM. Hence, the yield variance from the 2017 data is confounded with WSM resistance, which cannot be disentangled and justifies the higher-than-expected additive effects from the D sub genome.

Prediction Accuracy Improves When Epistasis is Modeled

The prediction accuracy modeling epistasis with the whole or sub genome models was only marginally improved. This result is consistent with the findings of Santantonio et al (2019), where no improvement in prediction accuracy was observed for grain yield, even though it improved other traits. Jiang and Reif (2015) observed an average improvement of 6% in prediction accuracy when modeling additive-by-additive epistatic interactions, while He et al (2017) found a 5% increase in prediction accuracy. The consistent small improvement in prediction accuracy when

modeling epistasis confronts the expectation that epistasis is an important type of gene action in wheat given the allopolyploid nature of the species. From a molecular biology perspective, the existence of homeologous genes could create positive or negative epistasis through subfunctionalization (Lynch and Force, 2000) or via competition for the same substrate (Qian et al., 2010), besides affecting the patterns of gene expression (Leach et al., 2014; Akhunova et al., 2010), which could directly influence the expression of phenotypic traits, like grain yield. In addition, homeologous interactions could be just a small portion of the total epistatic genetic effect in wheat, since epistasis has been reported in diploid wheat, *Triticum monococcum* (Tranquilli and Dubcovsky, 2000), and also within sub genomes in hexaploid wheat (Reif et al., 2011; Sehgal et al., 2020).

One potential reason for the marginal contribution of prediction accuracy when modeling epistasis lies in the highly quantitative genetic architecture of grain yield. Every stage of crop development is influenced by environmental stresses, and all of it adds up at the end of the cycle to determine grain yield. As different genetic interactions could be triggered during crop development, their contribution to grain yield may be so small that capturing epistatic effects would be virtually impossible.

Conclusion

In this research, we partitioned the whole genome additive and epistatic effects by sub genome and their respective interactions. The partitioning of genetic variance components into additive and epistatic effect was not orthogonal, although the estimated phenotypic variance matched the observed phenotypic variance. Using a fully additive model, we estimated the additive effect in each sub genome and showed that the genotypes that present the highest whole genome additive effects generally only had one sub genome above the top-95 percentile for additive effects. If the interaction between subgenomes is not of paramount importance to whole genome genetic effects, breeding programs could make crosses that combine parental lines with the highest additive effects in each sub genome. Further study must be conducted to into the role of sub genome interactions to validate this potential approach. Modeling epistasis in genomic selection models only marginally improved the prediction accuracy of genomic selection using either whole or sub genome models.

References

Acosta-Pech, R., Crossa, J., de Los Campos, G., Teyssèdre, S., Claustres, B., Pérez-Elizalde, S., & Pérez-Rodríguez, P. (2017). Genomic models with genotype x environment interaction for predicting hybrid performance: an application in maize hybrids. Theoretical and Applied Genetics, 130, 1431-1440.

Akhunova, A. R., Matniyazov, R. T., Liang, H., & Akhunov, E. D. (2010). Homoeolog-specific transcriptional bias in allopolyploid wheat. BMC genomics, 11(1), 1-16.

Alvarez-Castro JM, Carlborg O (2007) A unified model for functional and statistical epistasis and its application in quantitative trait Loci analysis. Genetics 176:1151–1167.

Bauman, L. F. (1959). Evidence of Non-Allelic Gene Interaction in Determining Yield, Ear Height, and Kernel Row Number in Corn 1. Agronomy Journal, 51(9), 531-534.

Boeven, P. H., Zhao, Y., Thorwarth, P., Liu, F., Maurer, H. P., Gils, M., ... & Würschum, T. (2020). Negative dominance and dominance-by-dominance epistatic effects reduce grain-yield heterosis in wide crosses in wheat. Science advances, 6(24), eaay4897.

Chapman, S. R., & McNeal, F. H. (1971). Gene Action for Yield Components and Plant Height in a Spring Wheat Cross 1. Crop Science, 11(3), 384-386.

Cooper, M., Podlich, D. W., Micallef, K. P., Smith, O. S., Jensen, N. M., Chapman, S. C., & Kruger, N. L. (2002). Complexity, quantitative traits and plant breeding: a role for simulation modelling in the genetic improvement of crops. In Quantitative genetics, genomics and plant breeding (pp. 143-166). Wallingford UK: CABI Publishing.

Crossa, J., Beyene, Y., Kassa, S., Pérez, P., Hickey, J. M., Chen, C., ... & Babu, R. (2013). Genomic prediction in maize breeding populations with genotyping-by-sequencing. G3: Genes, genomes, genetics, 3(11), 1903-1926.

Crossa, J., Campos, G. D. L., Pérez, P., Gianola, D., Burgueno, J., Araus, J. L., ... & Braun, H. J. (2010). Prediction of genetic values of quantitative traits in plant breeding using pedigree and molecular markers. Genetics, 186(2), 713-724.

Cullis, B. R., & Gleeson, A. C. (1991). Spatial analysis of field experiments-an extension to two dimensions. Biometrics, 1449-1460.

Cullis, B. R., Thomson, F. M., Fisher, J. A., Gilmour, A. R., & Thompson, R. (1996). The analysis of the NSW wheat variety database. II. Variance component estimation. Theoretical and Applied Genetics, 92, 28-39.

Cullis, B., Gogel, B., Verbyla, A., & Thompson, R. (1998). Spatial analysis of multi-environment early generation variety trials. Biometrics, 1-18.

de Los Campos, G., Sorensen, D. A., & Toro, M. A. (2019). Imperfect linkage disequilibrium generates phantom epistasis (& perils of big data). G3: Genes, Genomes, Genetics, 9(5), 1429-1436.

Endelman, J. B. (2011). Ridge regression and other kernels for genomic selection with R package rrBLUP. The plant genome, 4(3).

Falconer, D. S. (1981). Introduction to Quantitative Genetics, 2nd Edn. New York, NY: Longman Inc.

Federer, W. T., & Raghavarao, D. (1975). On augmented designs. Biometrics, 29-35.

Feldman, M., & Levy, A. A. (2012). Genome evolution due to allopolyploidization in wheat. Genetics, 192(3), 763-774.

Friebe, B., Gill, K. S., Tuleen, N. A., & Gill, B. S. (1996). Transfer of wheat streak mosaic virus resistance from Agropyron intermedium into wheat. Crop Science, 36(4), 857-861.

Gill, B. S., Friebe, B., Wilson, D. L., Martin, T. J., & Cox, T. S. (1995). Registration of KS93WGRC27 wheat streak mosaic virus resistant T4DL-4Ai# 2S wheat germplasm. Crop Science, 35(4), 1236-1237.

Gilmour, A. R. (2018). Echidna mixed model software. Proceedings of the World Congress Applied to Livestock Genetics, p. 995.

Goldringer, I., Brabant, P., & Gallais, A. (1997). Estimation of additive and epistatic genetic variances for agronomic traits in a population of doubled-haploid lines of wheat. Heredity, 79(1), 60-71.

Haley, S. D., Martin, T. J., Quick, J. S., Seifers, D. L., Stromberger, J. A., Clayshulte, S. R., ... & Friebe, B. (2002). Registration of CO960293-2 wheat germplasm resistant to Wheat streak mosaic virus and Russian wheat aphid.(Registrations Of Germplasm). Crop science, 42(4), 1381-1383.

He, S., Schulthess, A. W., Mirdita, V., Zhao, Y., Korzun, V., Bothe, R., ... & Jiang, Y. (2016). Genomic selection in a commercial winter wheat population. Theoretical and Applied Genetics, 129, 641-651.

Henderson C (1985) Best linear unbiased prediction of nonadditive genetic merits in noninbred populations. J Anim Sci 60:111–117.

Hill, W. G., & Mäki-Tanila, A. (2015). Expected influence of linkage disequilibrium on genetic variance caused by dominance and epistasis on quantitative traits. Journal of animal breeding and genetics, 132(2), 176-186.

Jarquín, D., Kocak, K., Posadas, L., Hyma, K., Jedlicka, J., Graef, G., & Lorenz, A. (2014). Genotyping by sequencing for genomic prediction in a soybean breeding population. BMC genomics, 15(1), 1-10.

Jiang Y, Reif JC (2015) Modeling epistasis in genomic selection. Genetics 201:759–768.

Jiang, Y., Schmidt, R. H., Zhao, Y., & Reif, J. C. (2017). A quantitative genetic framework highlights the role of epistatic effects for grain-yield heterosis in bread wheat. Nature genetics, 49(12), 1741-1746.

Kihara, H. (1924). Cytologische und genetische Studien bei wichtigen Getreidearten mit besonderer Rücksicht auf das Verhalten der Chromosomen und die Sterilität in den Bastarden. Memoirs of the College of Science, Kyoto Imperial University. Ser. B, 1(1), 1-200.

Kihara, H. (1944). Discovery of the DD-analyser, one of the ancestors of Triticum vulgare. Agric. Hort., 19, 13-14.

Kippes, N., Zhu, J., Chen, A., Vanzetti, L., Lukaszewski, A., Nishida, H., Kato, K., Dvorak, J., & Dubcovsky, J. (2014). Fine mapping and epistatic interactions of the vernalization gene VRN-D4 in hexaploid wheat. Molecular Genetics and Genomics, 289(1), 47-62.

Leach, L. J., Belfield, E. J., Jiang, C., Brown, C., Mithani, A., & Harberd, N. P. (2014). Patterns of homoeologous gene expression shown by RNA sequencing in hexaploid bread wheat. BMC genomics, 15(1), 1-19.

Lehermeier, C., de Los Campos, G., Wimmer, V., & Schön, C. C. (2017). Genomic variance estimates: With or without disequilibrium covariances?. Journal of Animal Breeding and Genetics, 134(3), 232-241.

Lu, H., Price, J., Devkota, R., Rush, C., & Rudd, J. (2011). A dominant gene for resistance to wheat streak mosaic virus in winter wheat line CO960293-2. Crop science, 51(1), 5-12.

Lynch, M., & Force, A. (2000). The probability of duplicate gene preservation by subfunctionalization. Genetics, 154(1), 459-473.

McFadden, E. S., & Sears, E. R. (1946). The origin of Triticum spelta and its free-threshing hexaploid relatives. Journal of heredity, 37(3), 81-89.

Mendiburu, F. D. (2019). Agricolae: statistical procedures for agricultural research.R package version 1.4.0.

Meuwissen, T. H., Hayes, B. J., & Goddard, M. (2001). Prediction of total genetic value using genome-wide dense marker maps. genetics, 157(4), 1819-1829.

Nejati-Javaremi, A., Smith, C., & Gibson, J. P. (1997). Effect of total allelic relationship on accuracy of evaluation and response to selection. Journal of animal science, 75(7), 1738-1745.

Pérez, Paulino, and Gustavo de Los Campos. "Genome-wide regression and prediction with the BGLR statistical package." Genetics 198, no. 2 (2014): 483-495.

Poland JA, Brown PJ, Sorrells ME, Jannink J-L (2012) Development of high-density genetic maps for barley and wheat using a novel two-enzyme genotyping-by-sequencing approach. PLoS ONE 7.

Qian, W., Liao, B. Y., Chang, A. Y. F., & Zhang, J. (2010). Maintenance of duplicate genes and their functional redundancy by reduced expression. Trends in Genetics, 26(10), 425-430.

Raffo, M. A., Sarup, P., Guo, X., Liu, H., Andersen, J. R., Orabi, J., Jahoor, A., & Jensen, J. (2022). Improvement of genomic prediction in advanced wheat breeding lines by including additive-by-additive epistasis. Theoretical and Applied Genetics, 135(3), 965-978.

Reif, J. C., Maurer, H. P., Korzun, V., Ebmeyer, E., Miedaner, T., & Würschum, T. (2011). Mapping QTLs with main and epistatic effects underlying grain yield and heading time in soft winter wheat. Theoretical and Applied genetics, 123, 283-292.

Rouse, M. N., Talbert, L. E., Singh, D., & Sherman, J. D. (2014). Complementary epistasis involving Sr12 explains adult plant resistance to stem rust in Thatcher wheat (Triticum aestivum L.). Theoretical and Applied Genetics, 127(7), 1549-1559.

Sannemann, W., Lisker, A., Maurer, A., Léon, J., Kazman, E., Cöster, H., Holzapfel, J., Kempf, H., Korzun, V., Ebmeyer, E., & Pillen, K. (2018). Adaptive selection of founder segments and epistatic control of plant height in the MAGIC winter wheat population WM-800. BMC genomics, 19(1), 1-16.

Santantonio, N., Jannink, J. L., & Sorrells, M. (2019). Prediction of subgenome additive and interaction effects in allohexaploid wheat. G3: Genes, Genomes, Genetics, 9(3), 685-698.

Sax, K. (1922). Sterility in wheat hybrids. II. Chromosome behavior in partially sterile hybrids. Genetics, 7(6), 513.

Schrauf, M. F., Martini, J. W., Simianer, H., de Los Campos, G., Cantet, R., Freudenthal, J., Korte, A., Munilla, S. (2020). Phantom epistasis in genomic selection: on the predictive ability of epistatic models. G3: Genes, Genomes, Genetics, 10(9), 3137-3145.

Sehgal, D., Rosyara, U., Mondal, S., Singh, R., Poland, J., & Dreisigacker, S. (2020). Incorporating genome-wide association mapping results into genomic prediction models for grain yield and yield stability in CIMMYT spring bread wheat. Frontiers in plant science, 11, 197.

Shaw, L. M., Li, C., Woods, D. P., Alvarez, M. A., Lin, H., Lau, M. Y., Chen, A., Dubcovsky, J. (2020). Epistatic interactions between PHOTOPERIOD1, CONSTANS1 and CONSTANS2 modulate the photoperiodic response in wheat. PLoS genetics, 16(7), e1008812.

Singh, A., Knox, R. E., DePauw, R. M., Singh, A. K., Cuthbert, R. D., Campbell, H. L., Singh, D., Bhavani, T., & Clarke, F. (2013). Identification and mapping in spring wheat of genetic factors controlling stem rust resistance and the study of their epistatic interactions across multiple environments. Theoretical and Applied Genetics, 126(8), 1951-1964.

Singh, R. P., Burnett, P. A., Albarran, M., & Rajaram, S. (1993). Bdv1: a gene for tolerance to barley yellow dwarf virus in bread wheats. Crop Science, 33(2), 231-234.

Smith, A., Cullis, B., & Thompson, R. (2001). Analyzing variety by environment data using multiplicative mixed models and adjustments for spatial field trend. Biometrics, 57(4), 1138-1147.

Sorensen, D., Fernando, R., & Gianola, D. (2001). Inferring the trajectory of genetic variance in the course of artificial selection. Genetical Research, 77, 83–94.

Su G, Christensen OF, Ostersen T, Henryon M, Lund MS (2012) Estimating additive and non-additive genetic variances and predicting genetic merits using genome-wide dense single nucleotide polymorphism markers. PLoS One 7:e45293.

Sun, P. L. F., Shands, H. L., & Forsberg, R. A. (1972). Inheritance of kernel weight in six spring wheat crosses 1. Crop Science, 12(1), 1-5.

Tranquilli, G., & Dubcovsky, J. (2000). Epistatic interaction between vernalization genes Vrn-Am1 and Vrn-Am2 in diploid wheat. Journal of Heredity, 91(4), 304-306.

VanRaden, P. M. (2008). Efficient methods to compute genomic predictions. Journal of dairy science, 91(11), 4414-4423.

Vazquez, M. D., Zemetra, R., Peterson, C. J., Chen, X. M., Heesacker, A., & Mundt, C. C. (2015). Multi-location wheat stripe rust QTL analysis: genetic background and epistatic interactions. Theoretical and Applied Genetics, 128(7), 1307-1318.

Vitezica ZG, Legarra A, Toro MA, Varona L (2017) Orthogonal estimates of variances for additive, dominance, and epistatic effects in populations. Genetics 206:1297–1307.

Welham, S. J., Gogel, B. J., Smith, A. B., Thompson, R., & Cullis, B. R. (2010). A comparison of analysis methods for late-stage variety evaluation trials. Australian & New Zealand Journal of Statistics, 52(2), 125-149.

Zeng, Z. B., Wang, T., & Zou, W. (2005). Modeling quantitative trait loci and interpretation of models. Genetics, 169(3), 1711-1725.

Zhang, K., Tian, J., Zhao, L., & Wang, S. (2008). Mapping QTLs with epistatic effects and QTL× environment interactions for plant height using a doubled haploid population in cultivated wheat. Journal of Genetics and Genomics, 35(2), 119-127.

Zhou, Y., Bai, S., Li, H., Sun, G., Zhang, D., Ma, F., ... & Song, C. P. (2021). Introgressing the *Aegilops tauschii* genome into wheat as a basis for cereal improvement. Nature Plants, 7(6), 774-786.

Appendix A - Chapter 2

Figure A.1 Allele frequency count (staked bar plots – left column) and heatmaps of 2D LD plots (right column) of the candidate epistatic interaction involving segments of chromosomes **6B** (S6B_27057995) and **6D** (S6D_14436093). **A** and **B** represents the data from the discovery populations. **C** and **D** displays data from the validation population. **E** and **F** consists of data from the last four stages of the breeding pipeline. In all plots, the control interaction, randomly selected and involving segments of chromosomes 1B and 2D, contrasts the candidate interaction with the null hypothesis.

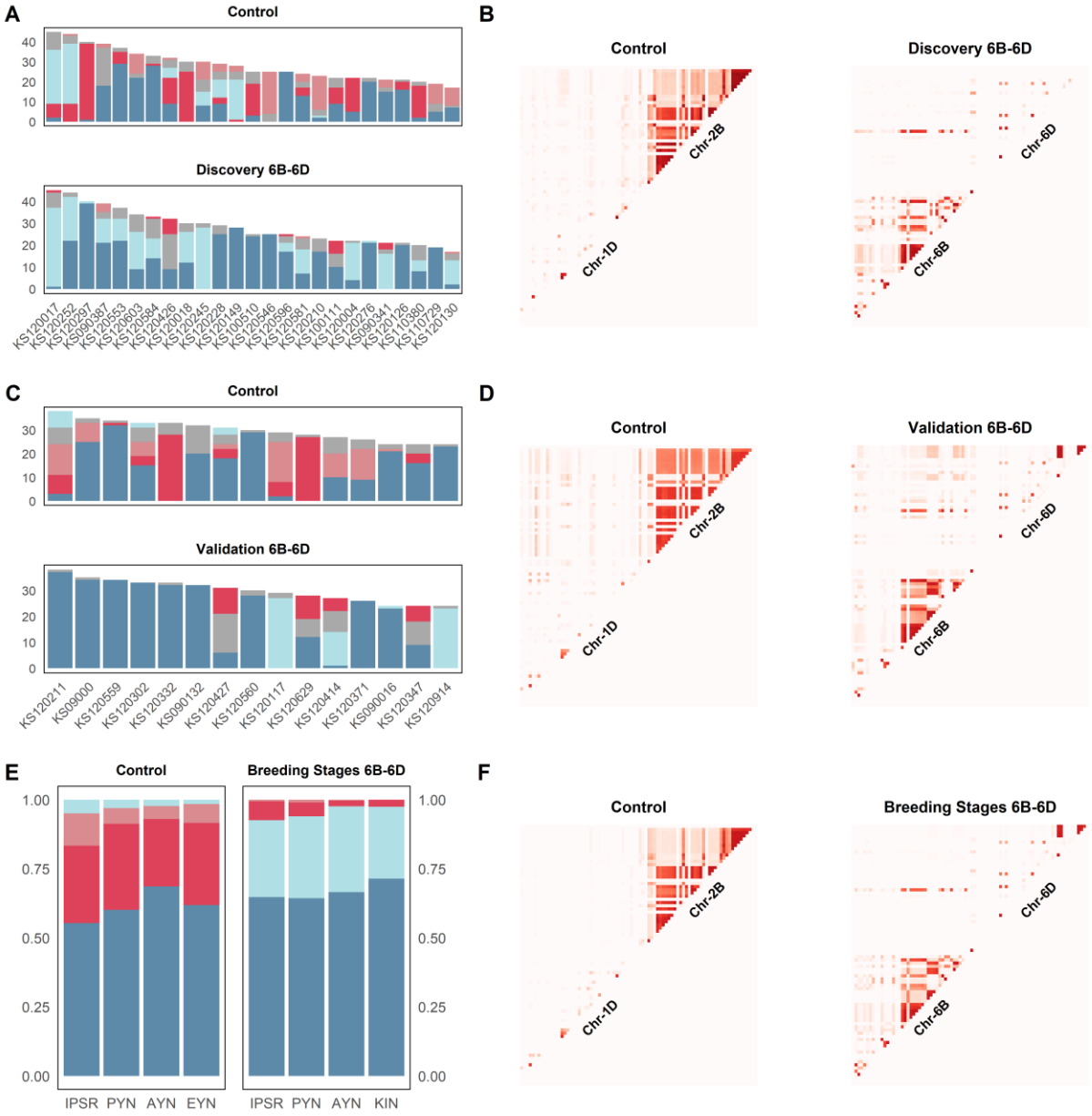

Figure A.2 Allele frequency count (staked bar plots – left column) and heatmaps of 2D LD plots (right column) of the candidate epistatic interaction involving segments of chromosomes **5A** and **6B**. **A** and **B** represents the data from the discovery populations. **C** and **D** displays data from the validation population. **E** and **F** consists of data from the last four stages of the breeding pipeline. In all plots, the control interaction, randomly selected and involving segments of chromosomes 1B and 2D, contrasts the candidate interaction with the null hypothesis.

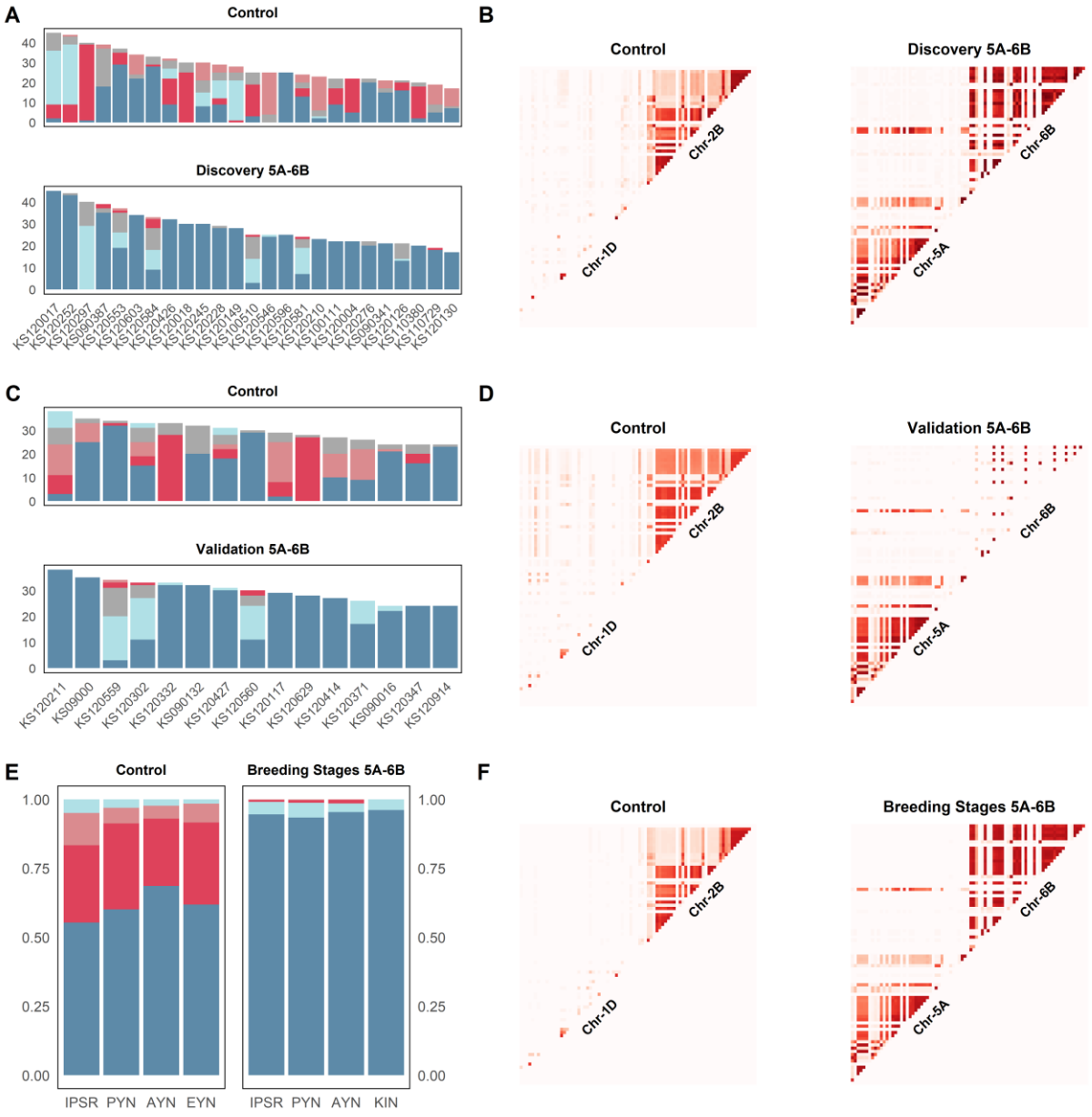

Figure A.3 Allele frequency count (staked bar plots – left column) and heatmaps of 2D LD plots (right column) of the candidate epistatic interaction involving segments of chromosomes **3B** and **3D**. **A** and **B** represents the data from the discovery populations. **C** and **D** displays data from the validation population. **E** and **F** consists of data from the last four stages of the breeding

pipeline. In all plots, the control interaction, randomly selected and involving segments of chromosomes 1B and 2D, contrasts the candidate interaction with the null hypothesis.

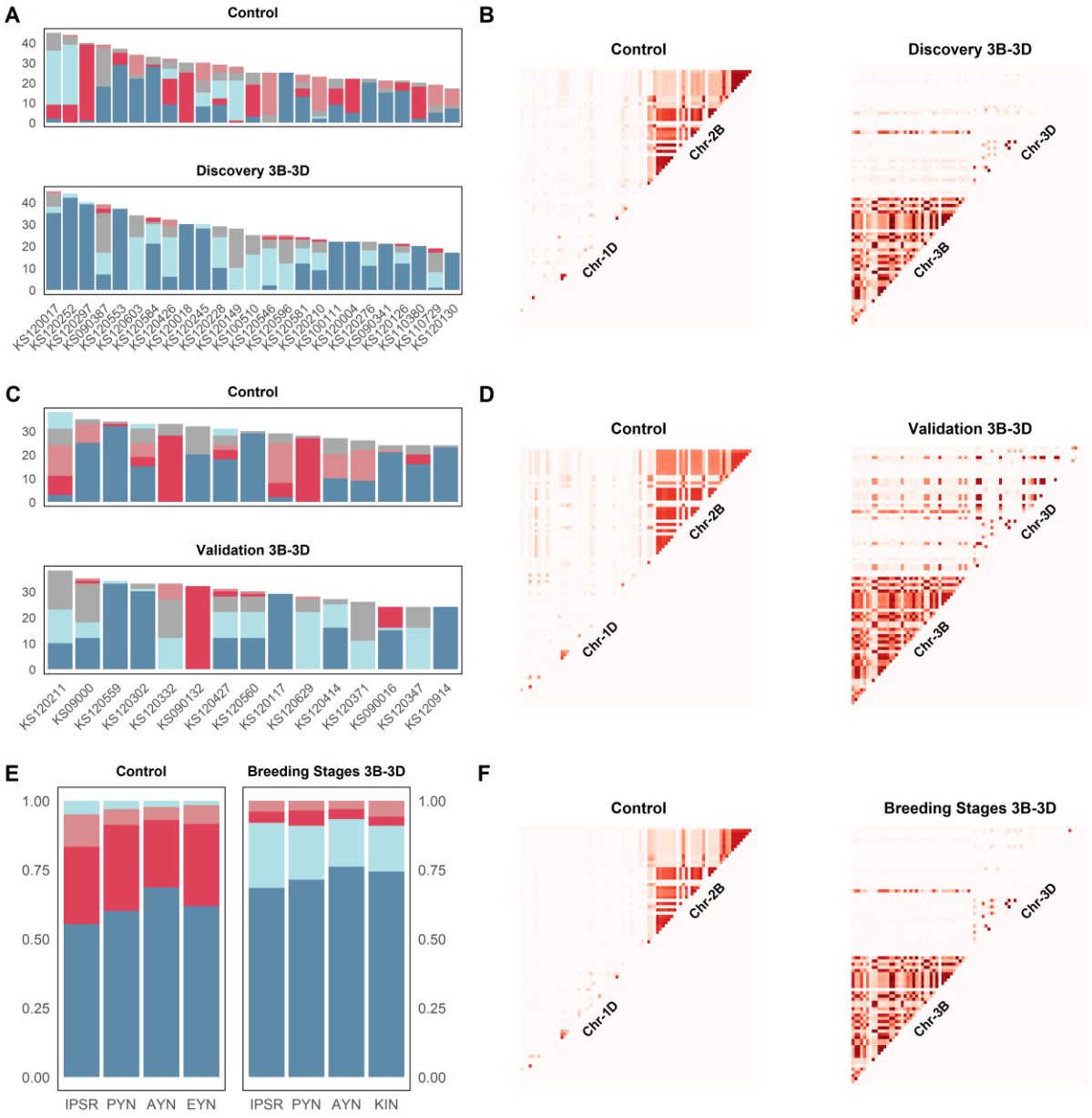

Figure A.4 Allele frequency count (staked bar plots – left column) and heatmaps of 2D LD plots (right column) of the candidate epistatic interaction involving segments of chromosomes **2B** and **5B**. **A** and **B** represents the data from the discovery populations. **C** and **D** displays data from the validation population. **E** and **F** consists of data from the last four stages of the breeding

pipeline. In all plots, the control interaction, randomly selected and involving segments of chromosomes 1B and 2D, contrasts the candidate interaction with the null hypothesis.

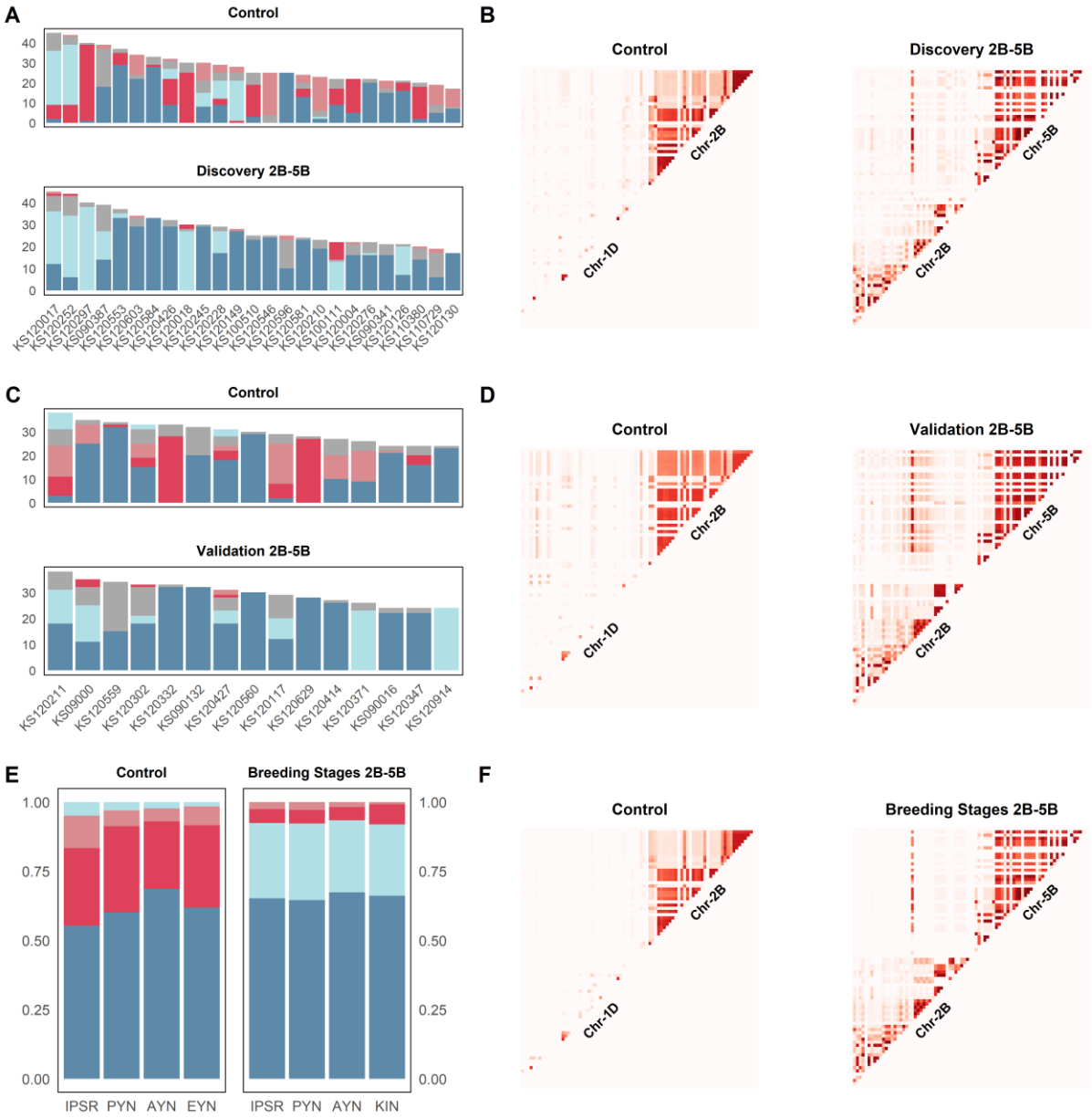

Figure A.5 Allele frequency count (staked bar plots – left column) and heatmaps of 2D LD plots (right column) of the candidate epistatic interaction involving segments of chromosomes **2A** and **2D**. **A** and **B** represents the data from the discovery populations. **C** and **D** displays data from the validation population. **E** and **F** consists of data from the last four stages of the breeding

pipeline. In all plots, the control interaction, randomly selected and involving segments of chromosomes 1B and 2D, contrasts the candidate interaction with the null hypothesis.

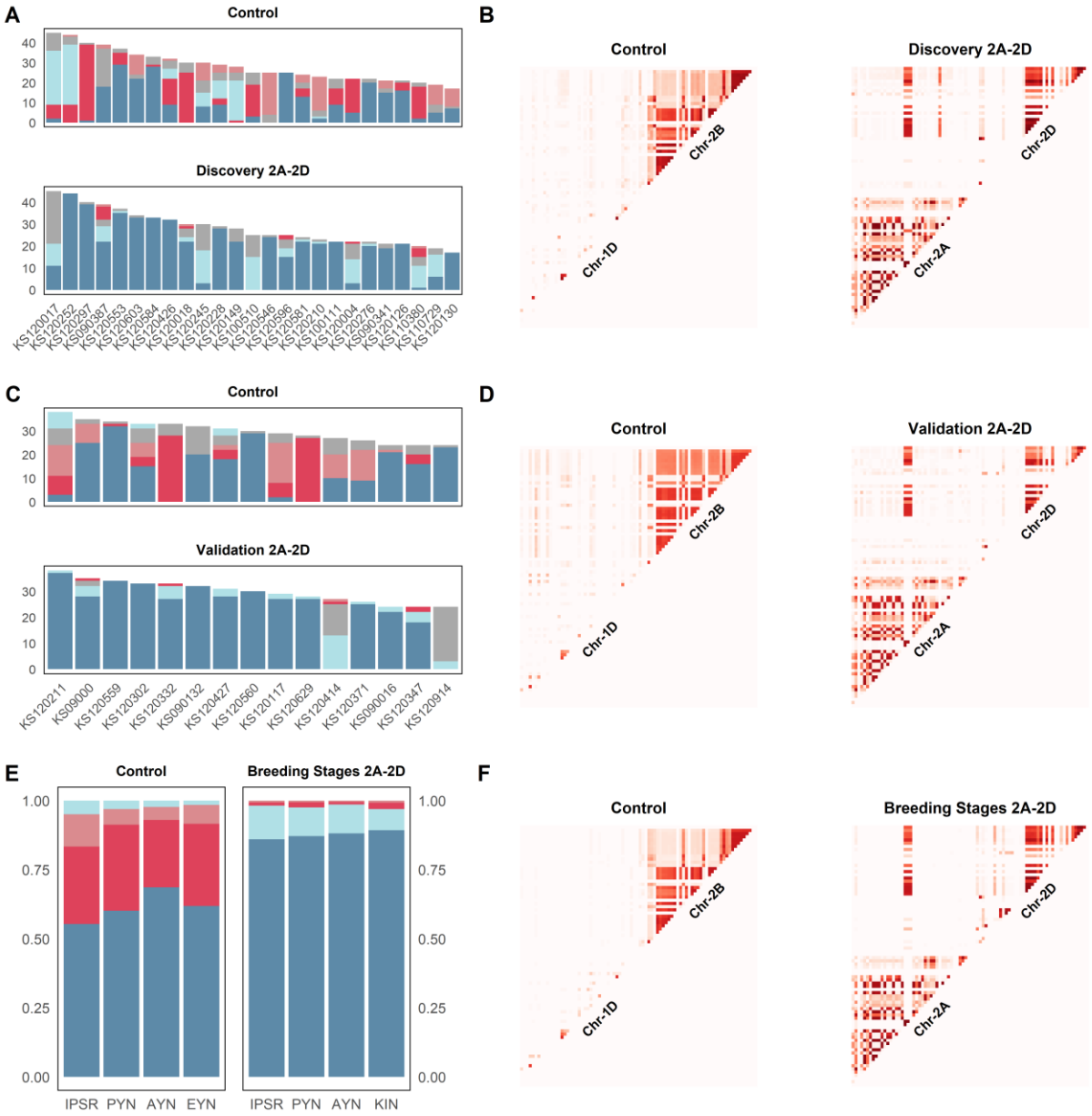

Figure A.6 Allele frequency count (staked bar plots – left column) and heatmaps of 2D LD plots (right column) of the candidate epistatic interaction involving segments of chromosomes **1B** and **6B**. **A** and **B** represents the data from the discovery populations. **C** and **D** displays data from the validation population. **E** and **F** consists of data from the last four stages of the breeding

pipeline. In all plots, the control interaction, randomly selected and involving segments of chromosomes 1B and 2D, contrasts the candidate interaction with the null hypothesis.

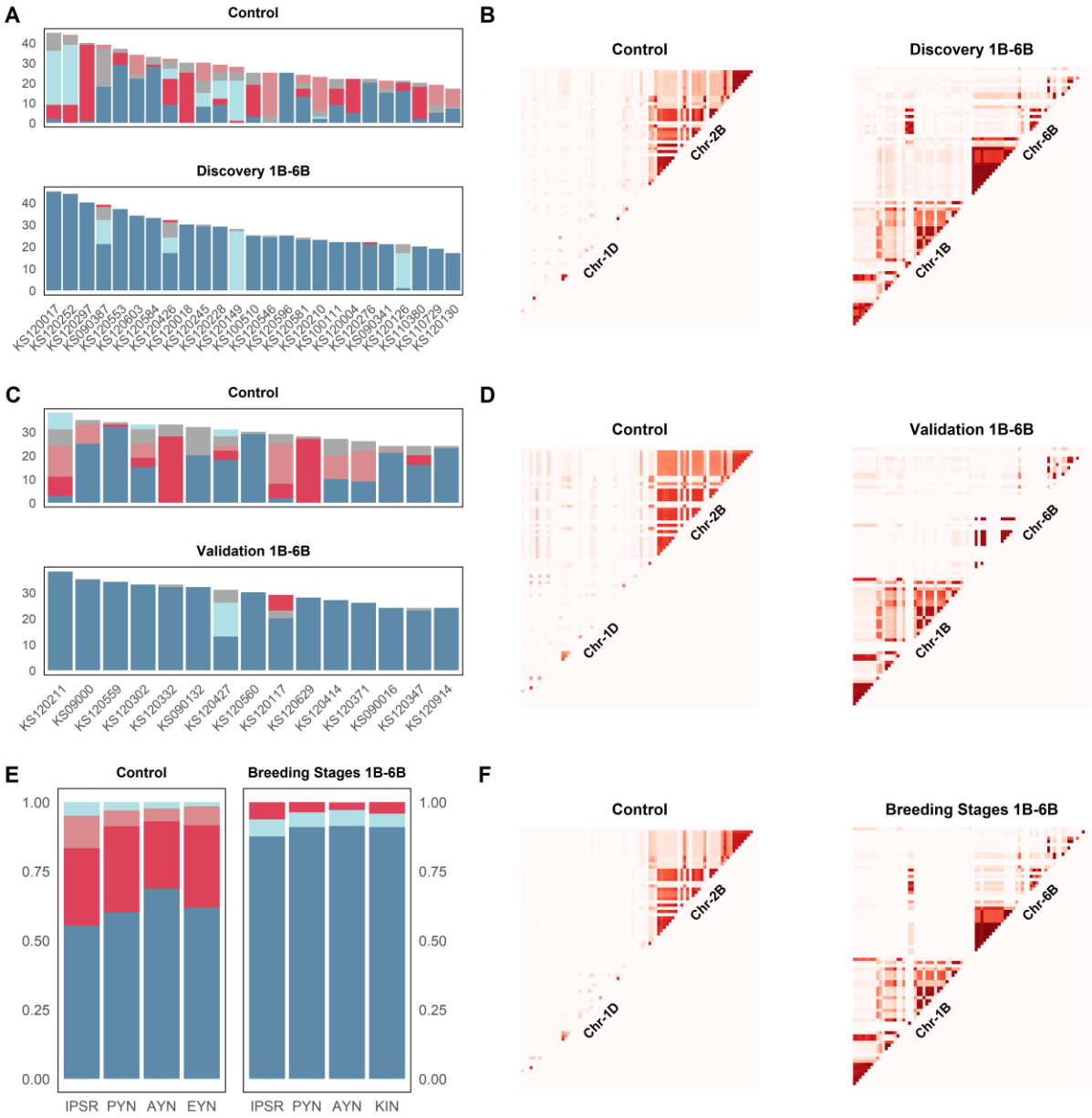

Figure A.7 Allele frequency count (staked bar plots – left column) and heatmaps of 2D LD plots (right column) of the candidate epistatic interaction involving segments of chromosomes **5D** and **7B**. **A** and **B** represents the data from the discovery populations. **C** and **D** displays data from the validation population. **E** and **F** consists of data from the last four stages of the breeding

pipeline. In all plots, the control interaction, randomly selected and involving segments of chromosomes 1B and 2D, contrasts the candidate interaction with the null hypothesis.

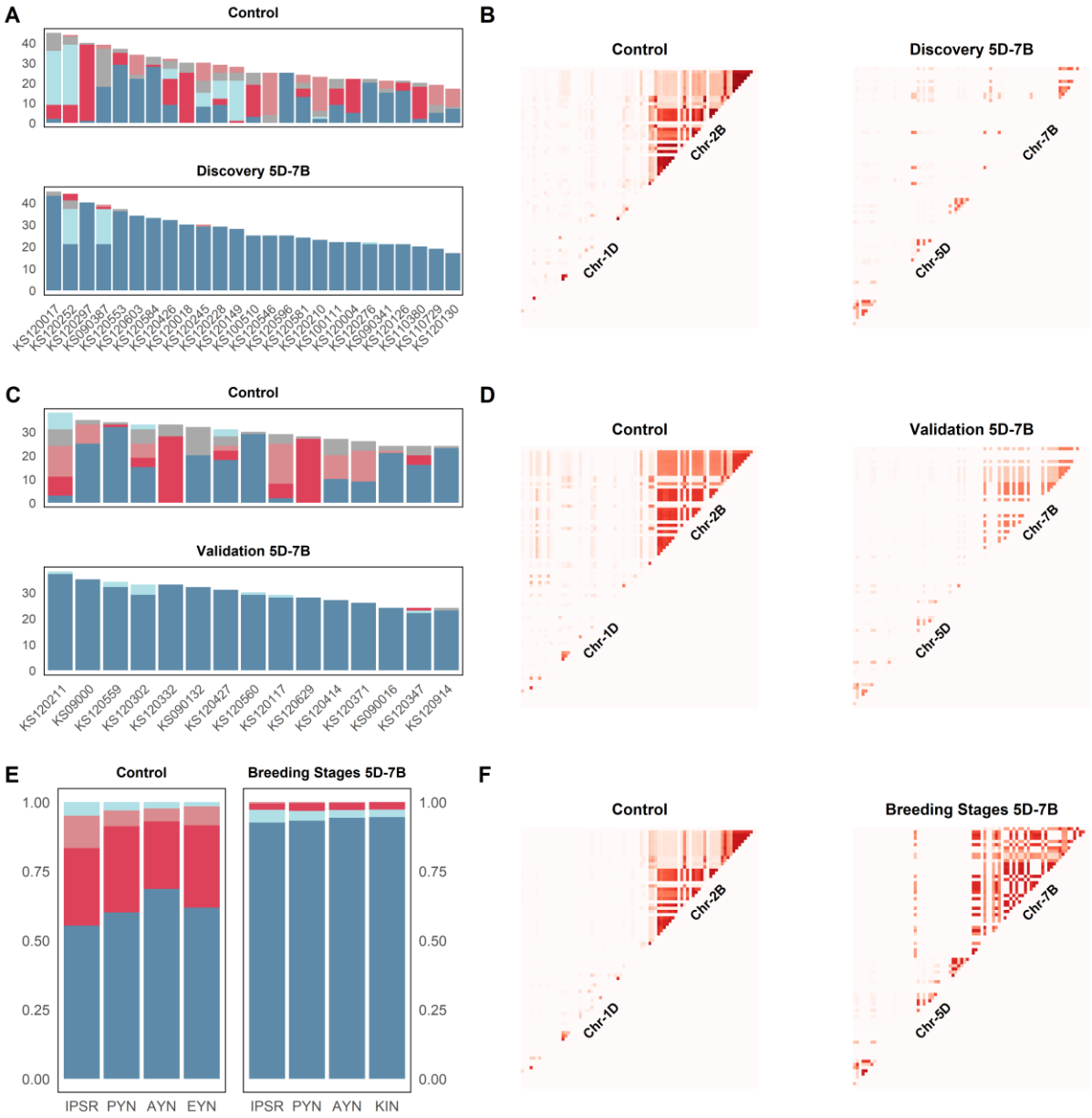

Figure A.8 Allele frequency count (staked bar plots – left column) and heatmaps of 2D LD plots (right column) of the candidate epistatic interaction involving segments of chromosomes **2D** and **3B**. **A** and **B** represents the data from the discovery populations. **C** and **D** displays data from the validation population. **E** and **F** consists of data from the last four stages of the breeding

pipeline. In all plots, the control interaction, randomly selected and involving segments of chromosomes 1B and 2D, contrasts the candidate interaction with the null hypothesis.

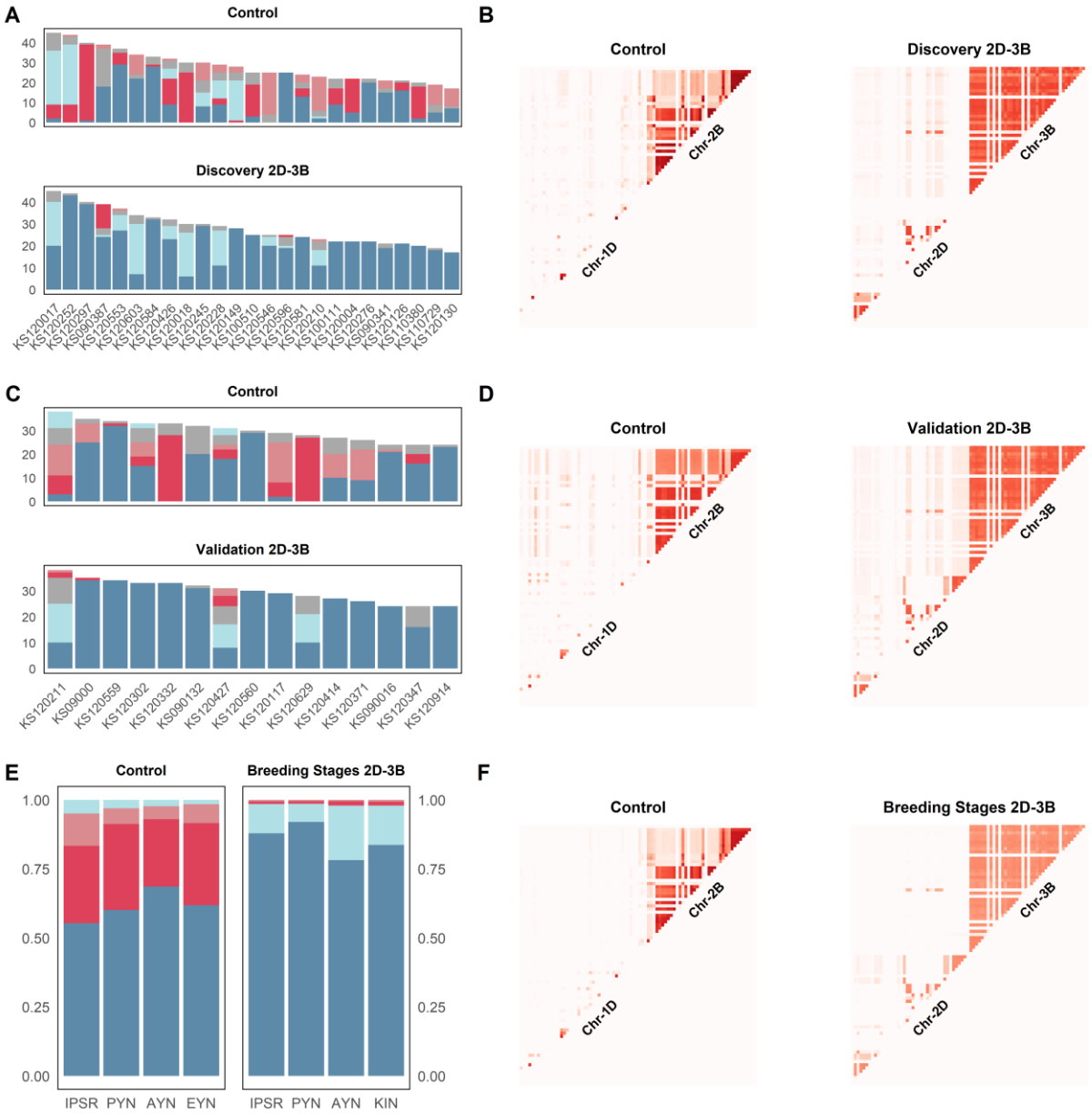

Figure A.9 Allele frequency count (staked bar plots – left column) and heatmaps of 2D LD plots (right column) of the candidate epistatic interaction involving segments of chromosomes **2D** and **4A**. **A** and **B** represents the data from the discovery populations. **C** and **D** displays data from the validation population. **E** and **F** consists of data from the last four stages of the breeding

pipeline. In all plots, the control interaction, randomly selected and involving segments of chromosomes 1B and 2D, contrasts the candidate interaction with the null hypothesis.

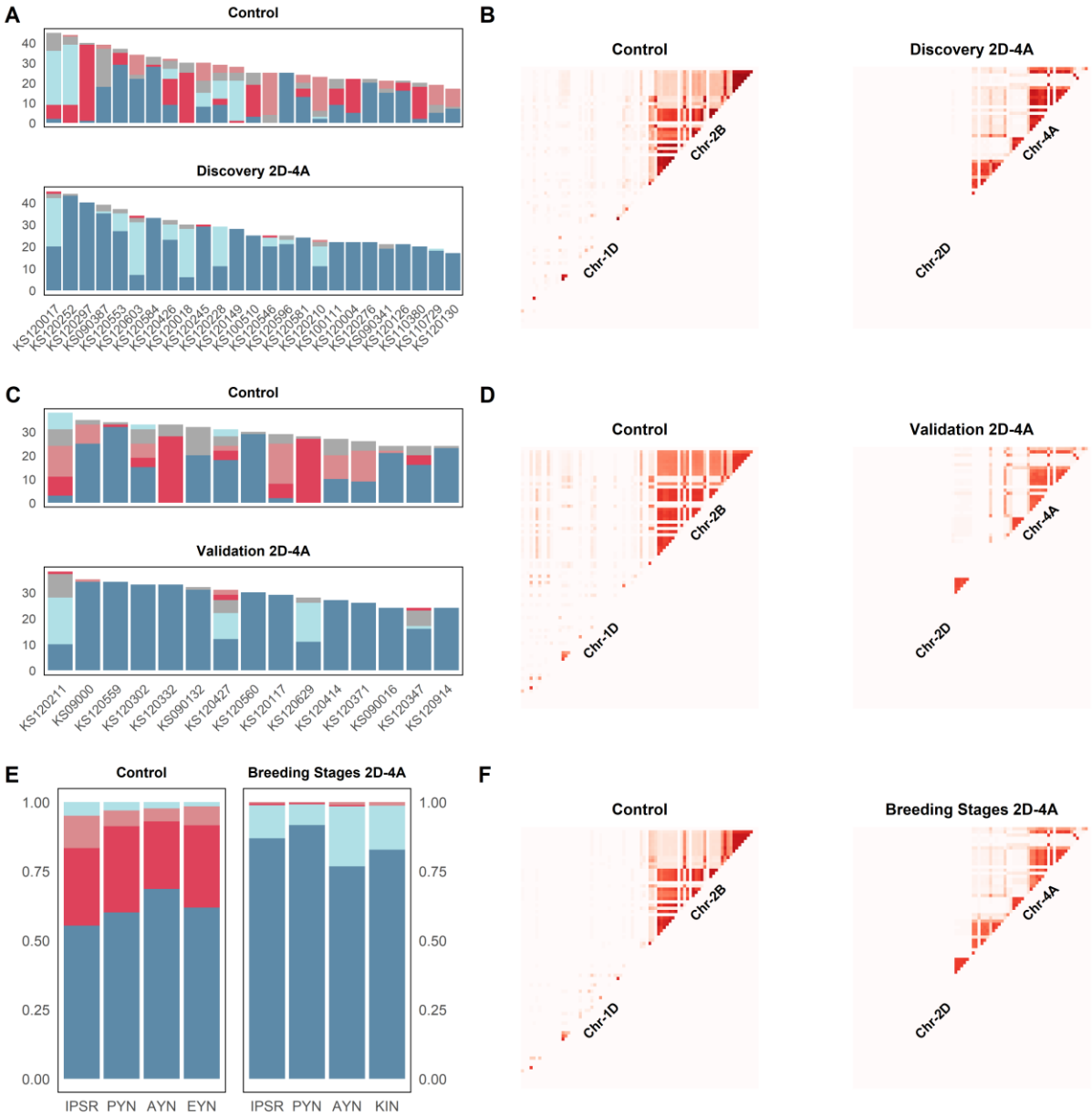

Figure A.10 Allele frequency count (staked bar plots – left column) and heatmaps of 2D LD plots (right column) of the candidate epistatic interaction involving segments of chromosomes **3B** and **4A**. **A** and **B** represents the data from the discovery populations. **C** and **D** displays data from the validation population. **E** and **F** consists of data from the last four stages of the breeding

pipeline. In all plots, the control interaction, randomly selected and involving segments of chromosomes 1B and 2D, contrasts the candidate interaction with the null hypothesis.

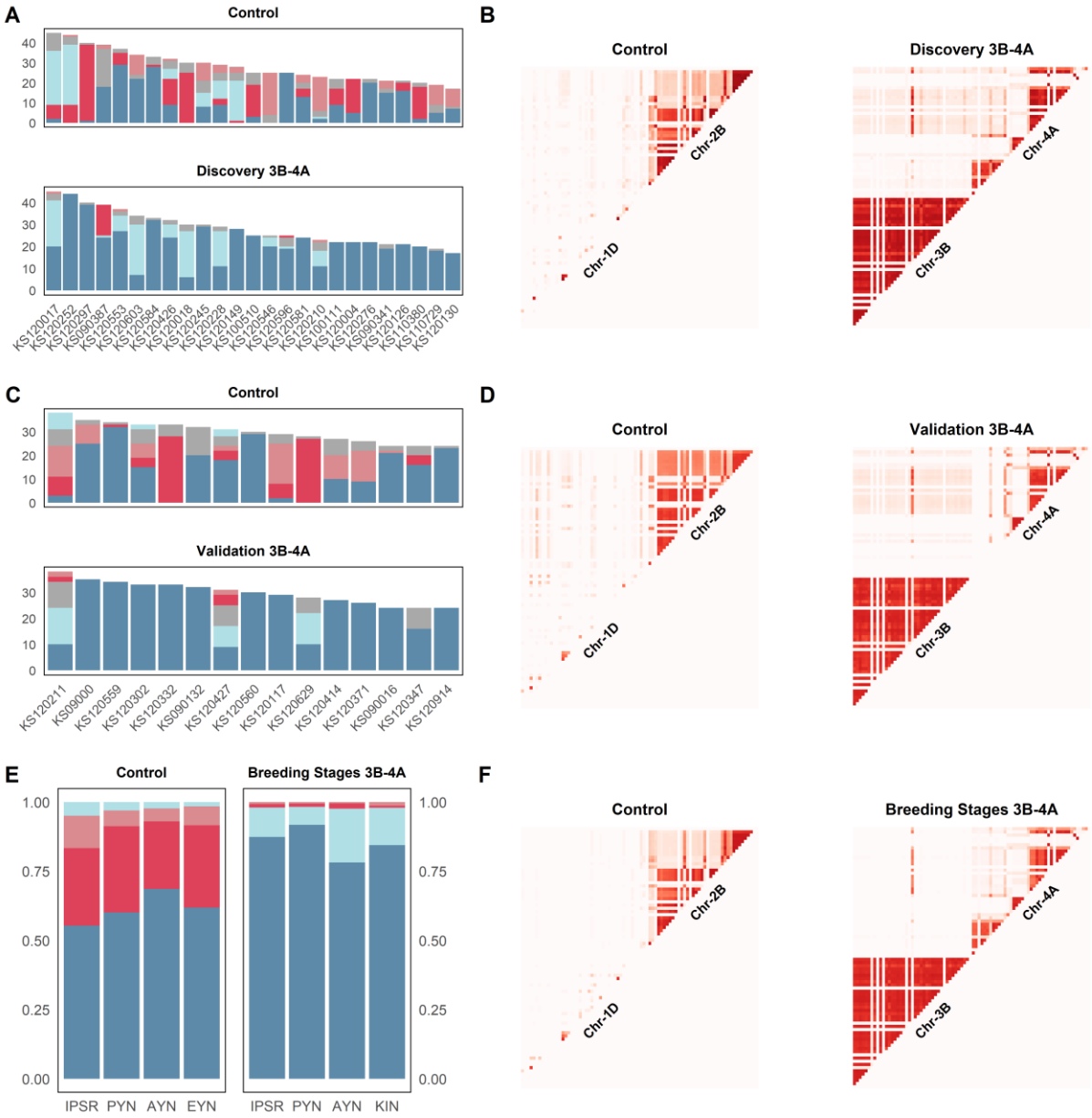

Figure A.11 Allele frequency count (staked bar plots – left column) and heatmaps of 2D LD plots (right column) of the candidate epistatic interaction involving segments of chromosomes **5A** and **7A**. **A** and **B** represents the data from the discovery populations. **C** and **D** displays data from the validation population. **E** and **F** consists of data from the last four stages of the breeding

pipeline. In all plots, the control interaction, randomly selected and involving segments of chromosomes 1B and 2D, contrasts the candidate interaction with the null hypothesis.

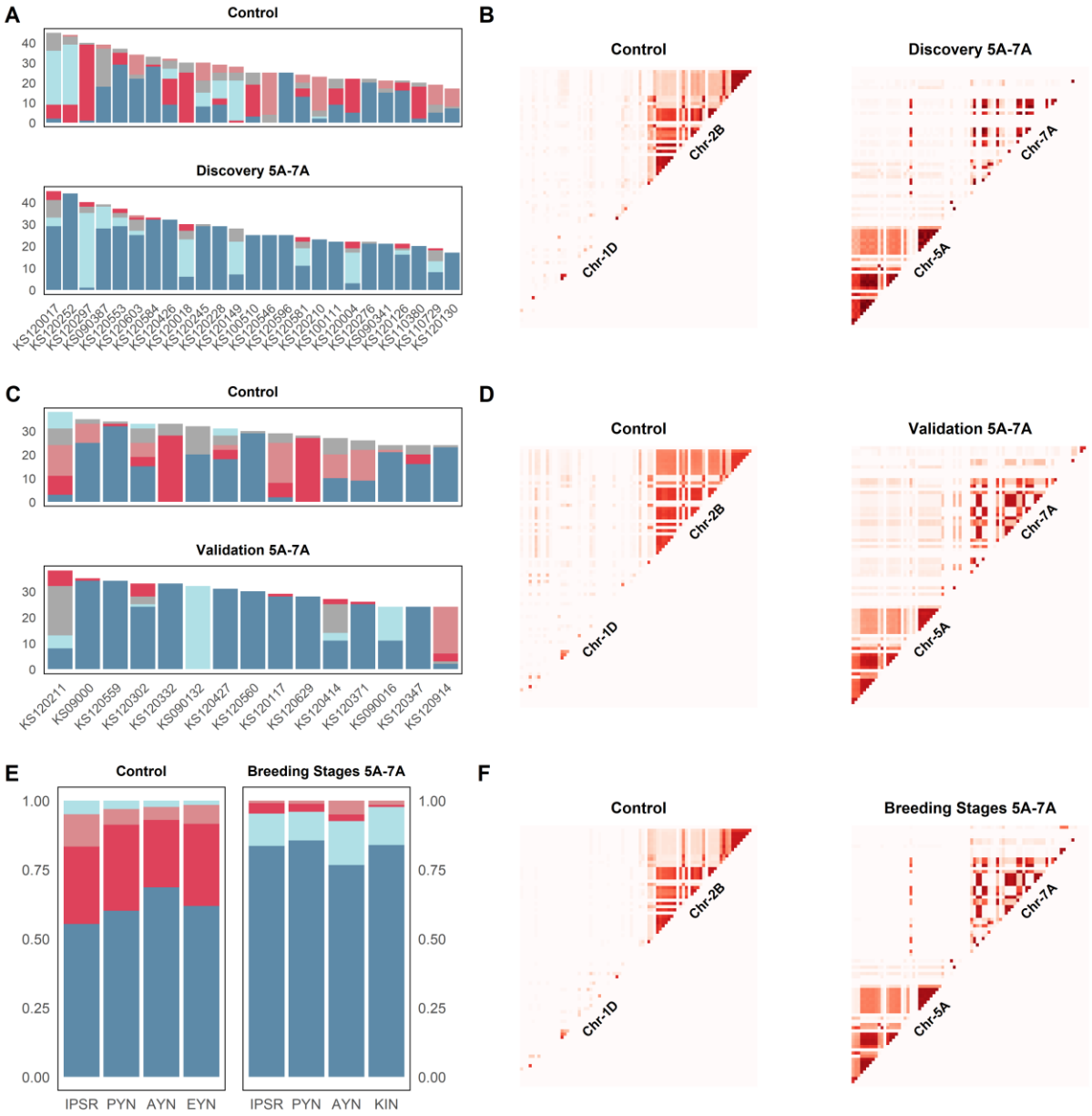

Figure A.12 Allele frequency count (staked bar plots – left column) and heatmaps of 2D LD plots (right column) of the candidate epistatic interaction involving segments of chromosomes **6A** and **7A**. **A** and **B** represents the data from the discovery populations. **C** and **D** displays data from the validation population. **E** and **F** consists of data from the last four stages of the breeding

pipeline. In all plots, the control interaction, randomly selected and involving segments of chromosomes 1B and 2D, contrasts the candidate interaction with the null hypothesis.

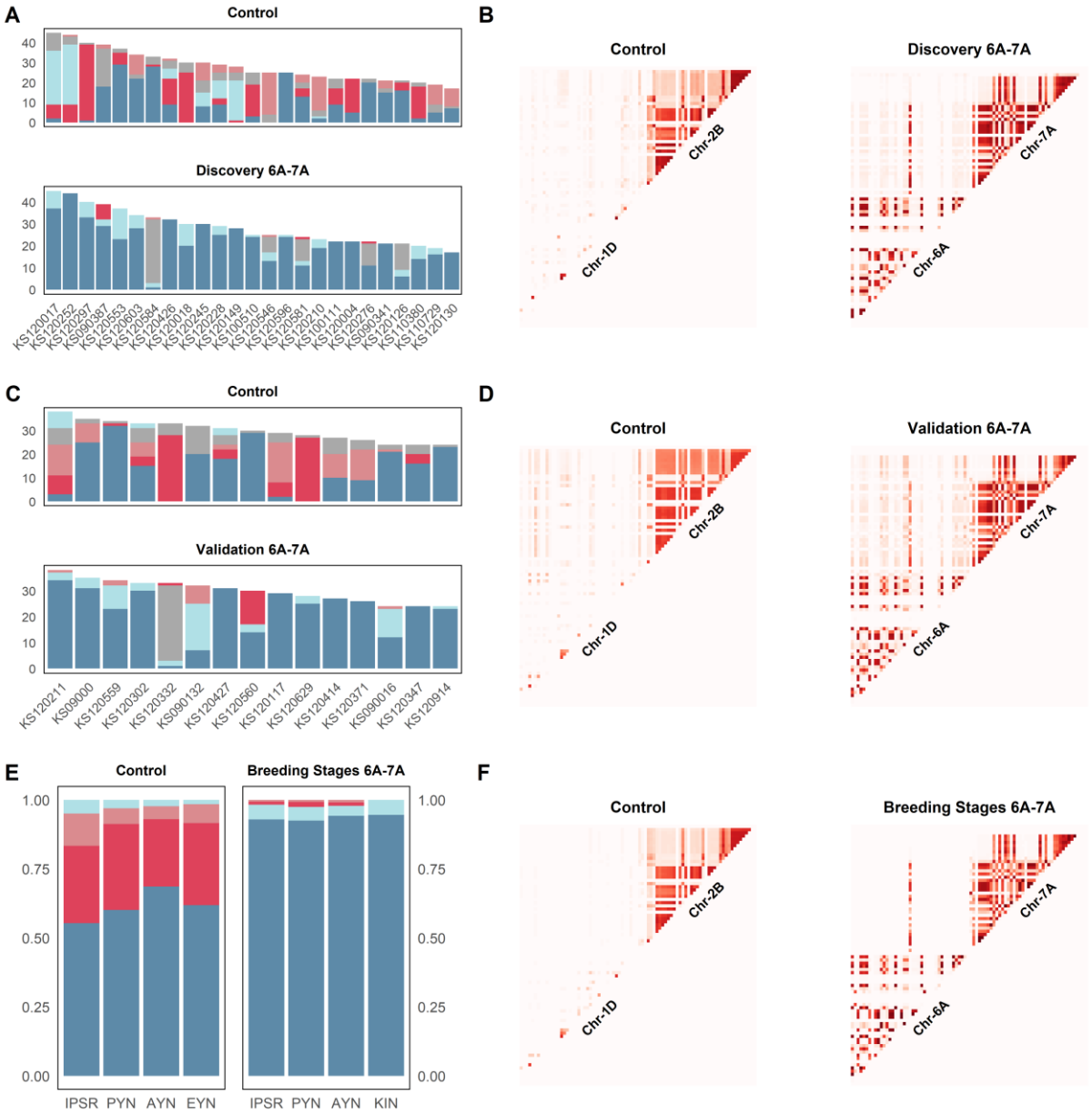

Figure A.13 Allele frequency count (staked bar plots – left column) and heatmaps of 2D LD plots (right column) of the candidate epistatic interaction involving segments of chromosomes **3A** and **3D**. **A** and **B** represents the data from the discovery populations. **C** and **D** displays data from the validation population. **E** and **F** consists of data from the last four stages of the breeding

pipeline. In all plots, the control interaction, randomly selected and involving segments of chromosomes 1B and 2D, contrasts the candidate interaction with the null hypothesis.

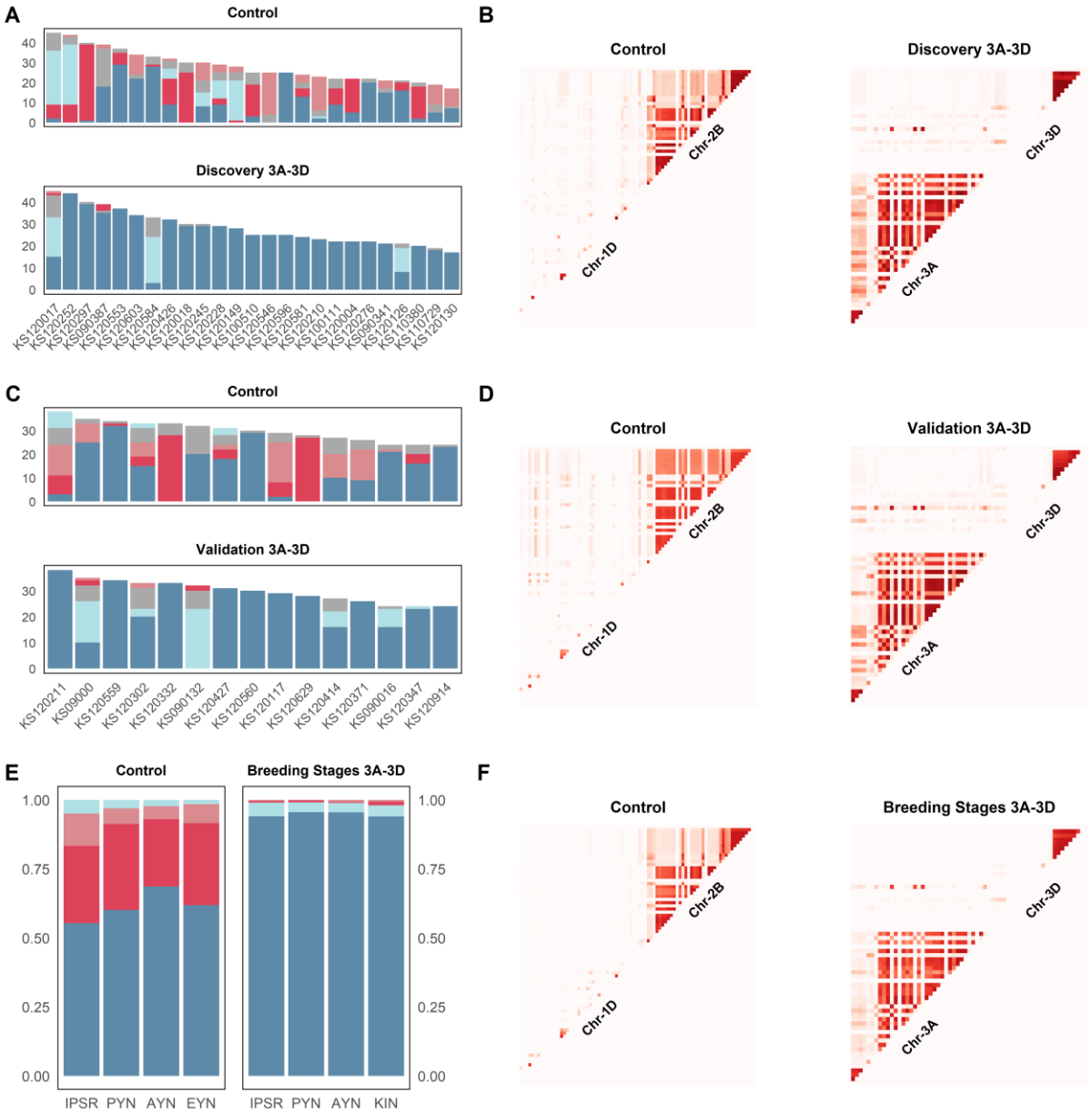

Figure A.14 Allele frequency count (staked bar plots – left column) and heatmaps of 2D LD plots (right column) of the candidate epistatic interaction involving segments of chromosomes **1A** and **1B**. **A** and **B** represents the data from the discovery populations. **C** and **D** displays data from the validation population. **E** and **F** consists of data from the last four stages of the breeding

pipeline. In all plots, the control interaction, randomly selected and involving segments of chromosomes 1B and 2D, contrasts the candidate interaction with the null hypothesis.

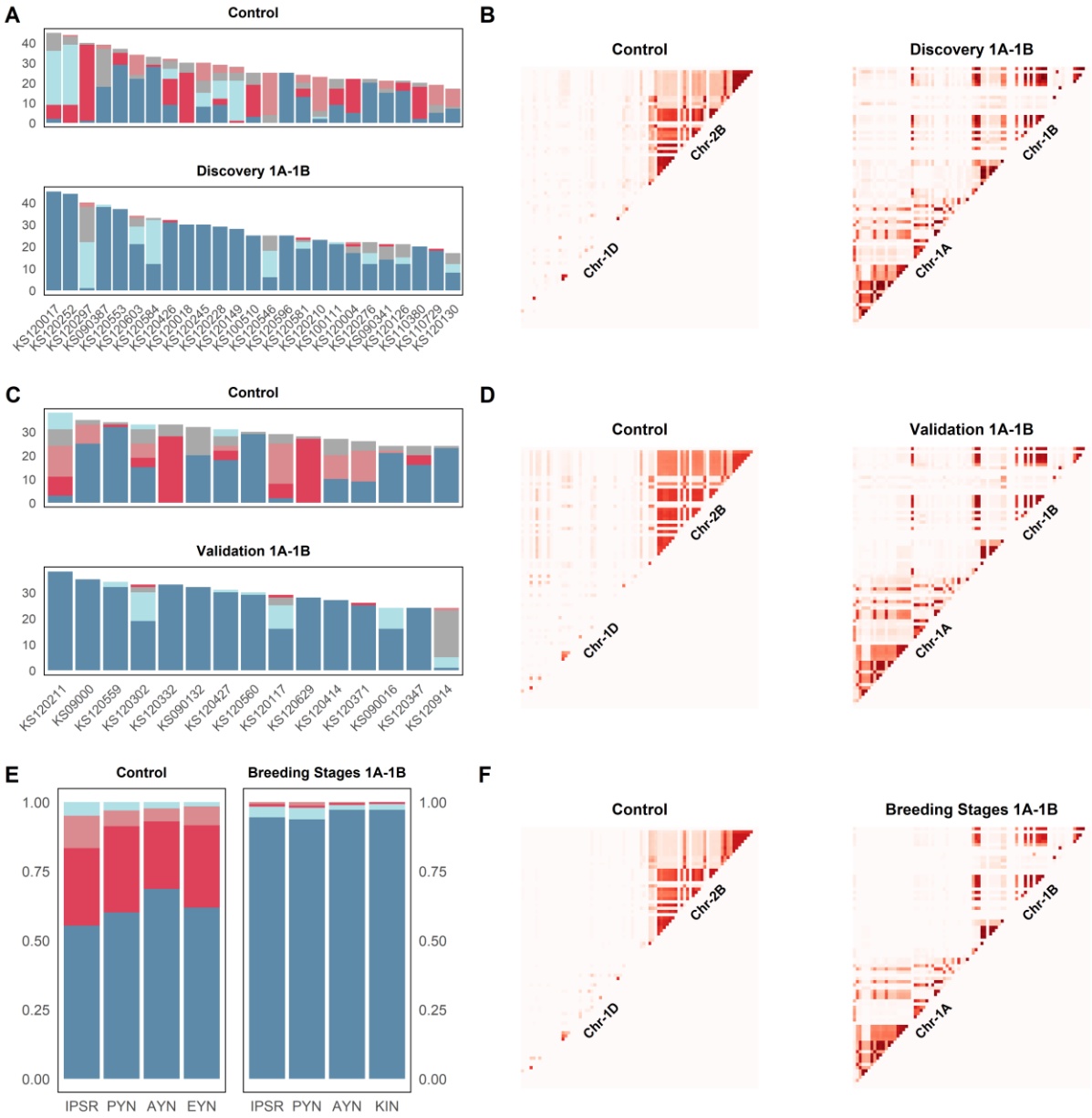

Figure A.15 Allele frequency count (staked bar plots – left column) and heatmaps of 2D LD plots (right column) of the candidate epistatic interaction involving segments of chromosomes **1BL** and **1D**. **A** and **B** represents the data from the discovery populations. **C** and **D** displays data from the validation population. **E** and **F** consists of data from the last four stages of the breeding

pipeline. In all plots, the control interaction, randomly selected and involving segments of chromosomes 1B and 2D, contrasts the candidate interaction with the null hypothesis.

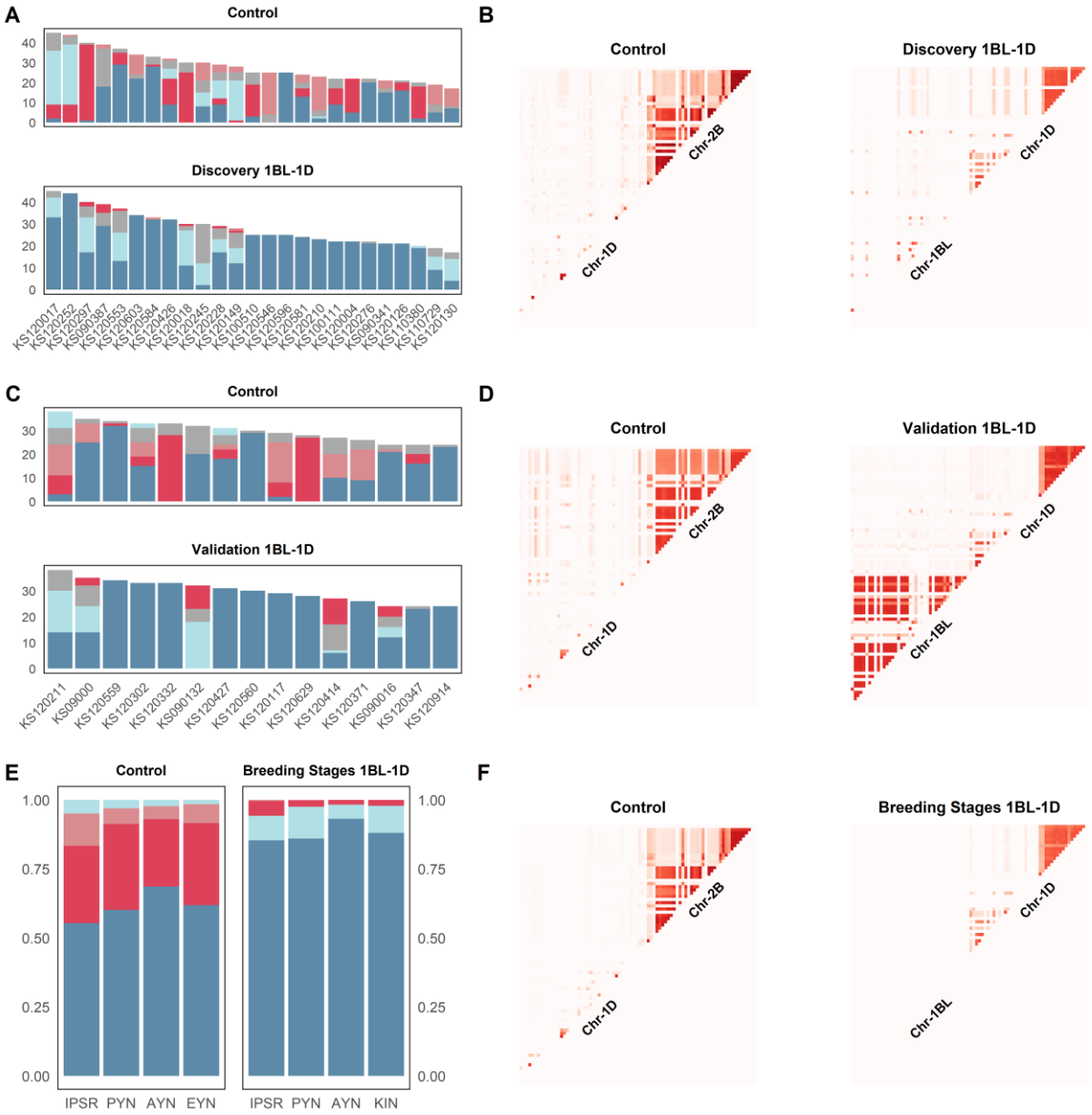

Figure A.16 Allele frequency count (staked bar plots – left column) and heatmaps of 2D LD plots (right column) of the candidate epistatic interaction involving segments of chromosomes **1BS** and **1D**. **A** and **B** represents the data from the discovery populations. **C** and **D** displays data from the validation population. **E** and **F** consists of data from the last four stages of the breeding

pipeline. In all plots, the control interaction, randomly selected and involving segments of chromosomes 1B and 2D, contrasts the candidate interaction with the null hypothesis.

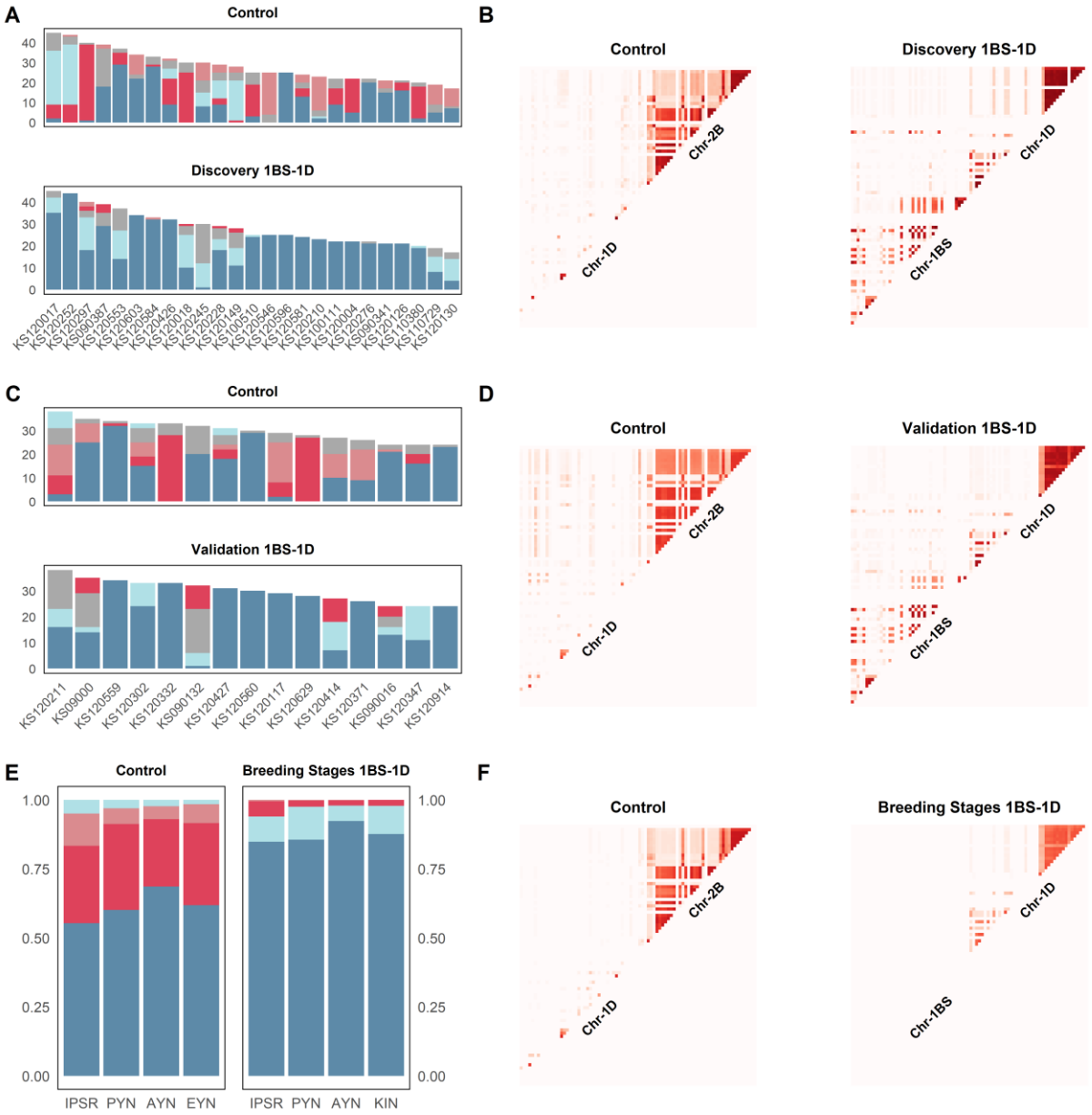

Figure A.17 Allele frequency count (staked bar plots – left column) and heatmaps of 2D LD plots (right column) of the candidate epistatic interaction involving segments of chromosomes **2B** and **7A**. **A** and **B** represents the data from the discovery populations. **C** and **D** displays data from the validation population. **E** and **F** consists of data from the last four stages of the breeding

pipeline. In all plots, the control interaction, randomly selected and involving segments of chromosomes 1B and 2D, contrasts the candidate interaction with the null hypothesis.

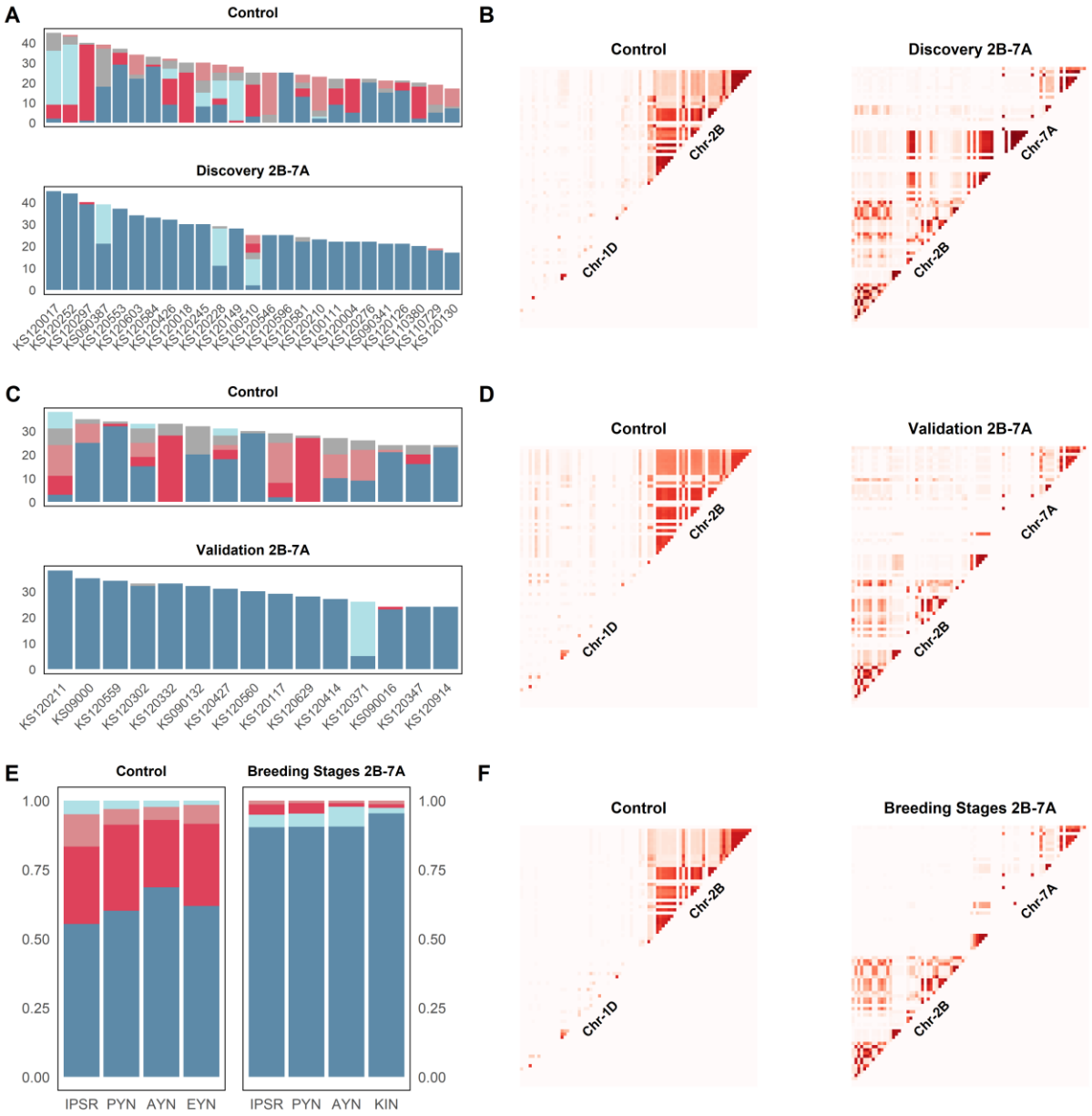

Figure A.18 Allele frequency count (staked bar plots – left column) and heatmaps of 2D LD plots (right column) of the candidate epistatic interaction involving segments of chromosomes **6B** (S6B_33136603) and **6D** (S6D_19567942). **A** and **B** represents the data from the discovery populations. **C** and **D** displays data from the validation population. **E** and **F** consists of data from the last four stages of the breeding pipeline. In all plots, the control interaction, randomly selected

and involving segments of chromosomes 1B and 2D, contrasts the candidate interaction with the null hypothesis.

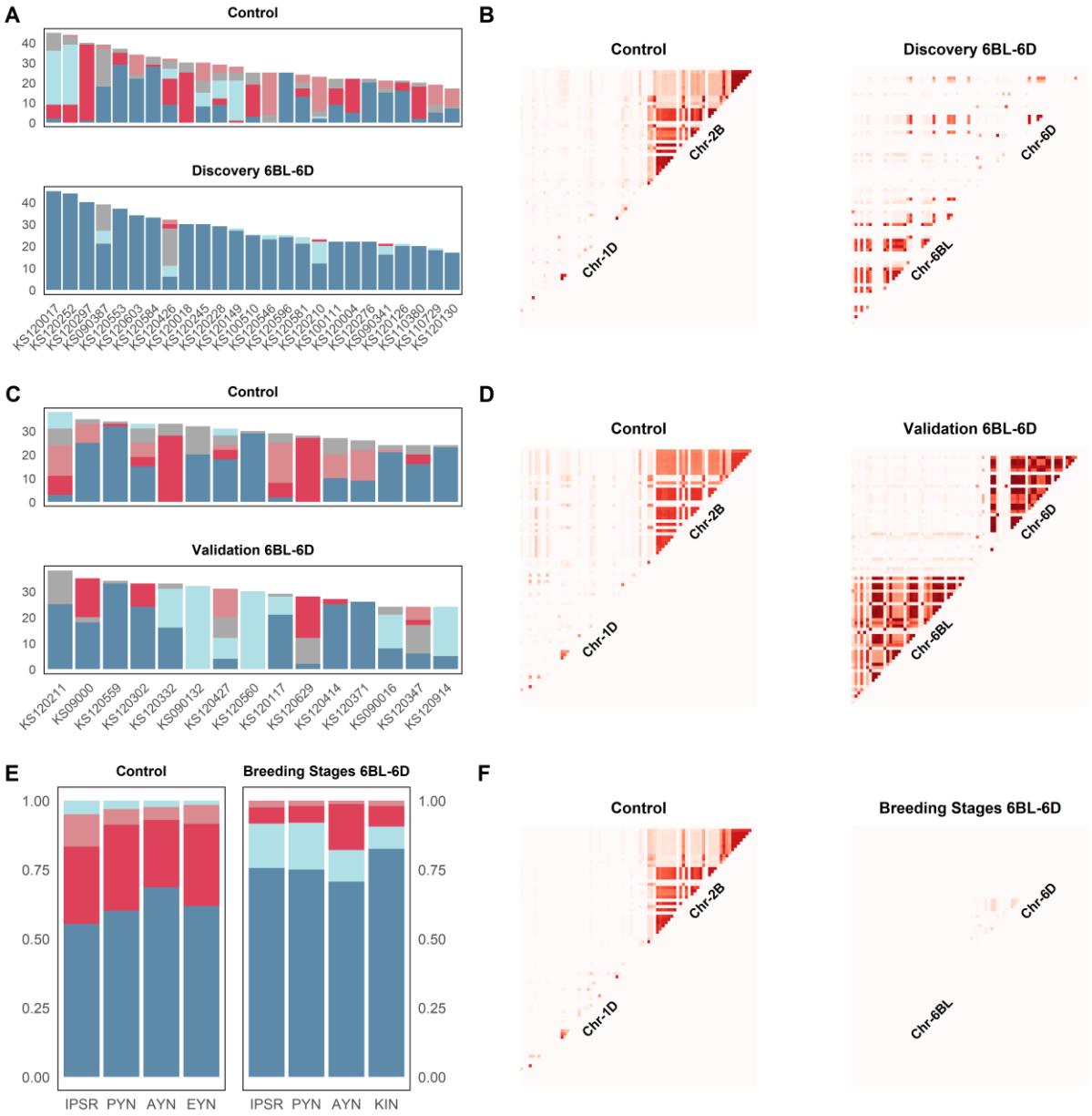

Appendix B - Chapter 3

Table B-1 Posterior means (± posterior standard deviation) of additive variance (V_A), epistatic variance (V_I), total genetic variance (V_G), residual variance (V_E), phenotypic variance (V_P), genomic broad sense heritability (H^2) and deviance information criteria (DIC) estimated with models WG-A (whole genome additive) and WG-AE (whole genome additive plus epistatic).

Model	V_A	V_I	V_G	V_E	V_P	H^2	DIC
1	10.21 ± 0.74	-	10.21 ± 0.74	27.99 ± 0.85	38.19 ± 0.85	0.27 ± 0.02	23592.16
2	4.21 ± 0.83	11.09 ± 1.19	14.96 ± 0.9	23.29 ± 0.89	38.26 ± 0.81	0.39 ± 0.02	23346.74

Table B-2 Posterior means (± posterior standard deviation) of additive variance in subgenome A (V_A), B (V_B) and D (V_D), intra genomic epistatic variance in subgenomes A (V_{AA}), B (V_{BB}) and D (V_{DD}), inter genomic epistatic variance in subgenomes AB (V_{AB}), AD (V_{AD}) and BD (V_{BD}), total genetic variance (V_{TG}), residual variance (V_E), phenotypic variance (V_P), genomic broad sense heritability (H^2) and deviance information criteria (DIC) estimated with models SG-A (sub genome additive) and SG-AE (sub genome additive plus epistatic).

Model	V_A	V_B	V_D	V_{AA}	V_{BB}	V_{DD}	V_{AB}	V_{AD}	V_{BD}	V_G	V_E	V_P	H^2	DIC
3	4.05 ± 0.75	3.87 ± 0.71	3.94 ± 0.72	-	-	-	-	-	-	10.88 ± 0.72	27.45 ± 0.8	38.33 ± 0.84	0.28 ± 0.02	23569.99
4	1.42 ± 0.47	1.54 ± 0.44	1.62 ± 0.47	1.76 ± 0.57	2.29 ± 0.81	2.05 ± 0.74	1.67 ± 0.56	2.58 ± 0.97	2.39 ± 0.99	16.33 ± 0.86	22.22 ± 0.85	38.55 ± 0.8	0.42 ± 0.02	23289.3

Table B-3 Correlation between whole genome and sub genome additive effects. Above diagonal is the correlation of sub genome additive effects from Model 3 (purely additive) and below the diagonal from Model 4 (additive plus epistatic).

	A	B	D	Whole
A	-	0.18	0.27	0.72
B	0.14	-	0.14	0.69
D	0.29	0.10	-	0.61
Whole	0.63	0.63	0.54	-

Table B-4 Mean (standard deviation), maximum and minimum additive effects associated with sub genome A, B and D (Model 3) and the whole genome (Model 1).

	A	B	D	Whole
Mean	0 ± 1.27	0 ± 1.27	0 ± 1.25	0 ± 2.51
Maximum	4.47	4.81	4.43	11.34
Minimum	-4.33	-3.88	-4.64	-10.19

Table B-5 Variance (diagonal), covariance (below diagonal) and correlation (above diagonal) of additive and epistatic effects from Model 2 (whole genome additive and epistatic).

	Additive	Epistatic
Additive	4.21	0.00
Epistatic	-0.17	11.09

Table B-6 Variance (diagonal), covariance (below diagonal) and correlation (above diagonal) between additive and epistatic effects from Model 4 (sub genome additive and epistatic).

	V_A	V_B	V_D	V_{AA}	V_{BB}	V_{DD}	V_{AB}	V_{AD}	V_{BD}
V_A	1.42	0	0	0	0	0	0	0	0
V_B	-0.05	1.54	0	0	0	0	0	0	0
V_D	0.02	-0.06	1.62	0	0	0	0	0	0
V_{AA}	-0.04	-0.01	-0.01	1.76	0	0	0	0	0
V_{BB}	-0.01	-0.02	-0.01	-0.01	2.29	0	0	0	0
V_{DD}	-0.01	-0.01	-0.03	-0.01	-0.01	2.05	0	0	0
V_{AB}	0.00	0.00	-0.01	-0.02	-0.01	-0.01	1.67	0	0
V_{AD}	-0.01	-0.01	-0.02	-0.02	-0.01	-0.01	-0.01	2.58	0
V_{BD}	-0.01	-0.01	-0.02	-0.01	-0.02	-0.01	-0.01	0.00	2.39

Table B-7 Correlation between Models 1-4 for genotypic values (above diagonal) and Genomic Estimated Breeding Values (below the diagonal).

	Model 1	**Model 2**	**Model 3**	**Model 4**
Model 1	-	0.92	0.98	0.90
Model 2	0.91	-	0.91	0.99
Model 3	0.99	0.89	-	0.91
Model 4	0.89	0.97	0.90	-